1996

Electroweak interactions and exchange currents in nuclei

Sergei M. Ananyan

College of William & Mary - Arts & Sciences

INFORMATION TO USERS

This manuscript has been reproduced from the microfilm master. UMI films the text directly from the original or copy submitted. Thus, some thesis and dissertation copies are in typewriter face, while others may be from any type of computer printer.

The quality of this reproduction is dependent upon the quality of the copy submitted. Broken or indistinct print, colored or poor quality illustrations and photographs, print bleedthrough, substandard margins, and improper alignment can adversely affect reproduction.

In the unlikely event that the author did not send UMI a complete manuscript and there are missing pages, these will be noted. Also, if unauthorized copyright material had to be removed, a note will indicate the deletion.

Oversize materials (e.g., maps, drawings, charts) are reproduced by sectioning the original, beginning at the upper left-hand corner and continuing from left to right in equal sections with small overlaps. Each original is also photographed in one exposure and is included in reduced form at the back of the book.

Photographs included in the original manuscript have been reproduced xerographically in this copy. Higher quality 6" x 9" black and white photographic prints are available for any photographs or illustrations appearing in this copy for an additional charge. Contact UMI directly to order.

UMI

A Bell & Howell Information Company
300 North Zeeb Road, Ann Arbor MI 48106-1346 USA
313/761-4700   800/521-0600

Electroweak Interactions and Exchange Currents in Nuclei

A Dissertation

Presented to The Faculty of the Department of Physics

The College of William and Mary

In Partial Fulfillment

Of the Requirements for the Degree of

Doctor of Philosophy

By

Sergei M. Ananyan

December 1996

UMI Number: 9805156

UMI

300 North Zeeb Road
Ann Arbor, MI 48103

APPROVAL SHEET

This dissertation is submitted in partial fulfillment
of the requirements for the degree of

Doctor of Philosophy.

Sergei Ananyan

Sergei M. Ananyan

Approved, December 1996

J.D. Walecka

F.L. Gross

J.M. Finn

D.S. Armstrong

C.R. Berquist

To my parents and grandparents

Contents

clei 89

v

Acknowledgments

I would like to extend my deepest thanks to my advisor, J.D. Walecka, the best teacher of physics I have ever seen, whose personality will be a standard for me for the rest of my life. Dirk taught me to see and enjoy the beauty of physics, and patiently guided me through the years of my graduate program, never getting tired of my numerous questions and mistakes.

Also I would like to acknowledge the constant moral support from my parents, which allowed me to never feel isolated from home and work productively during these years. I wish to thank them for showing me the wonderful world around, and for working from the very beginning of my life on developing my curiosity and creativity.

And I am very grateful to all my American friends who have made this country the second home for me.

List of Tables

List of Figures

ix

Abstract

In the first part of the dissertation, a consistent model for the long-range part of the weak meson exchange currents (MEC) preserving basic symmetries of the strong interactions is developed within the framework of an hadronic field theory of nuclear structure (QHD). A model which builds the nucleon-nucleon interaction out of σ, ω and π meson exchange is used to describe strong interactions in a nucleus. The scalar-pseudoscalar part of the problem coincides with the σ-model. In the linear realization of the sigma-model one obtains spatial axial exchange currents of order $(1/M)$ in a non-relativistic decomposition in nucleon mass due to ω-exchange. Consistency with the nuclear physics phenomenology requires the use of a very large m_{scalar}, and the low-mass σ cannot be introduced simply without breaking chiral invariance in this approach. A chiral transformation to the non-linear realization of the sigma-model is shown to be the natural way of treating the problem. PCAC is then satisfied identically for a one-body axial current even for a nucleon inside the nucleus. In this approach, the phenomenological low-mass σ can be incorporated in the model as a chiral singlet, still necessitating no additional exchange currents of order $(1/M)$ to be present. Here the first appearance of the axial MEC is in the familiar π-exchange term of order $(1/M^2)$ in the axial charge density. At the same time, there is now an additional relativistic one-body correction of order $(1/M)$ in the spatial part of the weak axial current that is required to satisfy PCAC. These correction terms are included in a unified analysis of weak and electromagnetic processes with some selected light nuclei where transition densities have been previously determined from available electromagnetic data.

In the second part of the dissertation, a potential use of electroweak experiments with excited $(J^\pi T) = (0^+0)$ nuclear states in addition to the ground state with the same quantum numbers is discussed. Existing low momentum transfer q^2 data on the inelastic charge form factor for the $(0^+0)_{gnd} \rightarrow (0^+0)^*$ transition in ^{4}He are fit within simple nuclear models, and predictions are made for higher q^2.

x

Chapter 1

Introduction

This dissertation is composed of two parts, the second of which is published, included as Part II, and briefly summarized at the end of this Introduction.

The objective of the first, and major, part of the present work is to develop a model including mesonic degrees of freedom into a description of weak interactions with nuclei in a consistent manner. There are three main reasons for pursuing this task. First, is the need for precise analyses of electroweak experiments with nuclear probes. Second, is the necessity for a detailed understanding of the nuclear structure in the language of the degrees of freedom relevant for the low-energy processes. Third, is the possibility of tying together results of more heuristic approaches, thus providing solid theoretical background for such calculations.

Two major sources of theoretical uncertainties in electroweak nuclear measurements are the lack of consistency in the treatment of the nuclear axial exchange currents involved in the interaction, and the lack of knowledge of reliable wave functions for the nuclei considered [1]. Both these issues are addressed in the present work.

It is well known that there exist good reasons to describe low-energy nuclear

1

processes in terms of mesons and nucleons instead of quarks and gluons, which are the basic degrees of freedom of Quantum Chromodynamics (QCD) [2]. Despite the many successes of the underlying theory of strong interactions - QCD - it provides little help in calculating low energy nuclear processes which correspond to the strong coupling limit of the theory. For the low-energy regime of the strong interaction physics, the relevant degrees of freedom are hadrons: mesons and nucleons. These effective low-energy degrees of freedom must be incorporated into any consistent theory describing low-energy nuclear physics processes. At the same time such a theory must, of course, preserve the basic symmetries of the underlying QCD.

Semileptonic electromagnetic and weak interactions with nuclei, of interest here, are among such low-energy processes. For a long time, only nucleonic degrees of freedom had been included in the analysis of these processes, despite the knowledge that meson fields are present in nuclei and should influence the result. In most cases such calculations were at least in the right ballpark for the lowest-energy processes, deviating from experimental results more at larger transferred momentum. The importance of considering mesonic degrees of freedom when calculating electromagnetic processes with nuclei was first demonstrated unequivocally by Riska and Brown [3]. A detailed theory of electromagnetic meson exchange currents (EXC) has been developed since then (for a review see [4–6]). It successfully accounted for discrepancies between the results of the nucleons-only model for the electromagnetic current and experiment in the medium-energy region.

The present work is devoted to building a consistent model of weak exchange currents (WXC) in nuclei and to calculating their effects in some selected nuclear electroweak processes. It is well known that weak currents consist of vector and axial vector parts [7]. In accordance with the conserved vector current (CVC) theory, the vector part of the weak current can be obtained by an isospin rotation of the isovector part of the corresponding electromagnetic current. Thus the vector part of WXC is

2

derived from the isovector part of the respective EXC, which have been determined accurately over the last two decades. The part of the weak current that still needs to be modeled on firm theoretical grounds is the axial exchange current (AXC).

There have been numerous attempts to describe the weak interaction effects of mesonic degrees of freedom in nuclei. They started with the work of Chemtob and Rho [8]. Probably the most important early treatment of the subject of AXC was made by Kubodera, Delorme and Rho [9], who predicted the dominant long-range piece of the AXC, performing power counting in the inverse nucleon mass parameter, while utilizing current algebra techniques and an assumption of pion-exchange dominance in the long-range effects. This work eventually lead to the "chiral filtering" hypothesis that states that only those degrees of freedom appear in the AXC whose presence is required by the Partial Conservation of the Axial Current (PCAC) theorem, while contributions of other fields are masked in nuclei [10]. Many different ideas had been developed to explain various particular results concerning weak interactions with nuclei [11–15]. The most interesting recent approaches to modeling AXC include: 1) A description of exchange currents in terms of all the degrees of freedom drawn from the phenomenological N-N potential [16–18]; 2) The hard-pion model calculations [19–21]; and 3) Application of chiral perturbation theory (χPT) [22–25].

Any model describing meson exchange currents (MEC) has to incorporate the following two features to become consistent with our present understanding of the low-energy nuclear physics:

1) it must contain the same degrees of freedom that are necessary to explain other important nuclear physics results, such as the phenomenological N-N potential, nuclear excitation spectra, various nuclear scattering results, the nuclear matter equation of state, etc.;

2) it has to incorporate the symmetries of the underlying theory of strong

3

interactions, QCD (slightly broken chiral symmetry realized in the Goldstone mode, is the most important symmetry in the present context).

The most consistent approach making the full use of the first condition is that of Riska and coworkers [16, 26]. It is well known that the phenomenological N-N potential can be split into different components that are ascribed to π, σ, ω and ρ meson exchange [27]. These effective low-energy degrees of freedom must be incorporated correspondingly in a theory describing weak interactions with nuclei. There have been many calculations of corrections to nuclear processes due to these additional non-nucleonic degrees of freedom [4]. Instead of investigating separate effects of different mesons, Riska and coworkers [16] take as a basis for the model the N-N phenomenological potential description that accounts for all the details of the interaction in terms of various meson exchanges. They write out the relativistic N-N interaction amplitude as a combination of five Fermi invariants with arbitrary coefficients. Comparing the non-relativistic limit of this expression with the phenomenological N-N potential, they determine the corresponding momentum-dependent coefficients of the various terms in the relativistic amplitude. To obtain the corresponding contributions to the AXC, they consider relativistic two-nucleon diagrams that include, in addition to the potential interaction, an extra axial current interaction attached to one of the nucleon legs of the interaction diagram. As customary, they take the non-relativistic limit of these diagrams, with only antinucleon components kept in the fermion propagator, to represent the nuclear AXC. This treatment allows one to be certain that no relevant mesonic degrees of freedom have been left out. It provides an elegant explanation of several nuclear puzzles [17, 28]. Nevertheless, this approach is bound to be phenomenological and incomplete. First, one has no means to account for the AXC that arise from the direct interaction of the exchanged mesons with the axial current. Second, this model does not incorporate chiral symmetry, which is one of the most important features that must be inherited by the low-energy effective the-

4

ories from the underlying QCD. And third, the model does not permit a lagrangian formulation, which would allow utilization of the full power of modern quantum field theory in the problem.

Another widely used phenomenological approach to calculating AXC is the "hard pion" model formulated by Ivanov and Truhlik [19]. This phenomenological lagrangian model was devised in an attempt to incorporate, in addition to the pion field, the ρ-meson, which is known to have some important nuclear effects, while preserving the correct chiral symmetry of the underlying theory of QCD. In this approach the formula for AXC reproduces earlier results [9] in the limit of soft pions, when the produced pion mass and momentum both approach zero. The AXC obtained in this calculation has been used to calculate the ratio of the axial-charge matrix element in the first-forbidden beta-decay to its impulse-approximation value [20]. The results are observed to be strongly dependent on the short-range correlation function of the nuclear wave function. The hard pion model in general has some drawbacks. Important ω and σ fields, which are known to contribute significantly to nuclear properties, have been left out in this treatment. In addition, consideration of the ρ-meson entailed inclusion of its chiral partner, a heavy A_1-meson, which is of little importance in traditional nuclear physics.

On the other end of the spectrum lies the χPT approach, which represents an attempt to find a link between the treatment of low-energy processes and the underlying theory of QCD. Here one performs an interaction amplitude decomposition with q/M and m_π/M - the transferred momentum and pion mass compared to the nucleon mass - as small expansion parameters. If the chiral symmetry of the underlying theory of QCD is preserved, then the zeroth-order term is identified unambiguously [29]. The lowest order effective lagrangian including nucleons was given by Weinberg [30, 31]. It coincides with the non-linear realization of the σ-model (in the large scalar-meson mass limit). Calculation of AXC to the first loop order in χPT combined with the

5

heavy-fermion formalism, has been performed in [23, 24]. Chiral symmetry is the cornerstone of the χPT approach. This approach elucidates the relation of the low-energy physics with the basic theory of QCD. However, it remains predominantly a theoretical tool. In the χPT approach one hopes to build all other known important low-energy phenomenological degrees of freedom from the multi-pion processes beyond the tree level. Calculations of MEC in this approach are complicated, and they do not utilize the power of the fact that the phenomenological N-N interactions can be expressed conveniently in the one-meson-exchange framework.

In the present work a lagrangian-based model for the axial meson-exchange currents is built, that incorporates both important features mentioned above: it contains the set of mesons required to explain major nuclear physics results, and it preserves the basic symmetries of the theory of strong interactions - gauge and partial chiral invariance. This model allows one to write down chiral-invariant sets of tree diagrams for the electroweak processes to the lowest order in the interaction constant. Chiral invariance combined with the pion-pole dominance hypothesis singles out the way to renormalize all the axial current vertices in the full theory. The covariant weak axial exchange nuclear currents due to exchange of various mesons are then identified. To make a connection with traditional nuclear physics calculations, the non-relativistic reduction of these currents is performed. Resulting non-relativistic nuclear currents satisfy the PCAC equation in coordinate space when corresponding N-N potential terms calculated in the same framework are taken into account. Thus various MEC due to exchange of different mesons are all tied together, since they now originate from the same underlying theory. The present approach follows closely, and is an extension of, the treatment of electromagnetic MEC by Dubach, Koch and Donnelly [6].

The model that incorporates π, σ and ω meson fields is developed here starting from an underlying hadronic field-theory lagrangian. It is important to include in the model σ and ω fields, as in the QHD I model of Walecka [32], because these two fields

6

model the most prominent features of the N-N potential: the σ-field is responsible for an intermediate-range attraction, while the ω-meson generates the short-range repulsion. The QHD I model provides explanation of many important nuclear physics results. The σ and ω fields play the most significant role in the treatment of nuclear matter, as well as finite nuclei, on the mean field theory (MFT) level. The QHD I calculations, involving extensions of MFT, that require fitting only four nuclear physics results (chosen usually [33] to be $(E/B)_{\text{n.m.}}, (k_F)_{\text{n.m.}}, (a_4)_{\text{n.m.}}$ - the binding energy per nucleon, density, and symmetry energy of the nuclear matter, and one finite nucleus result: $\sqrt{\langle r^2 \rangle_{^{40}\text{Ca}}}$), had many successes.
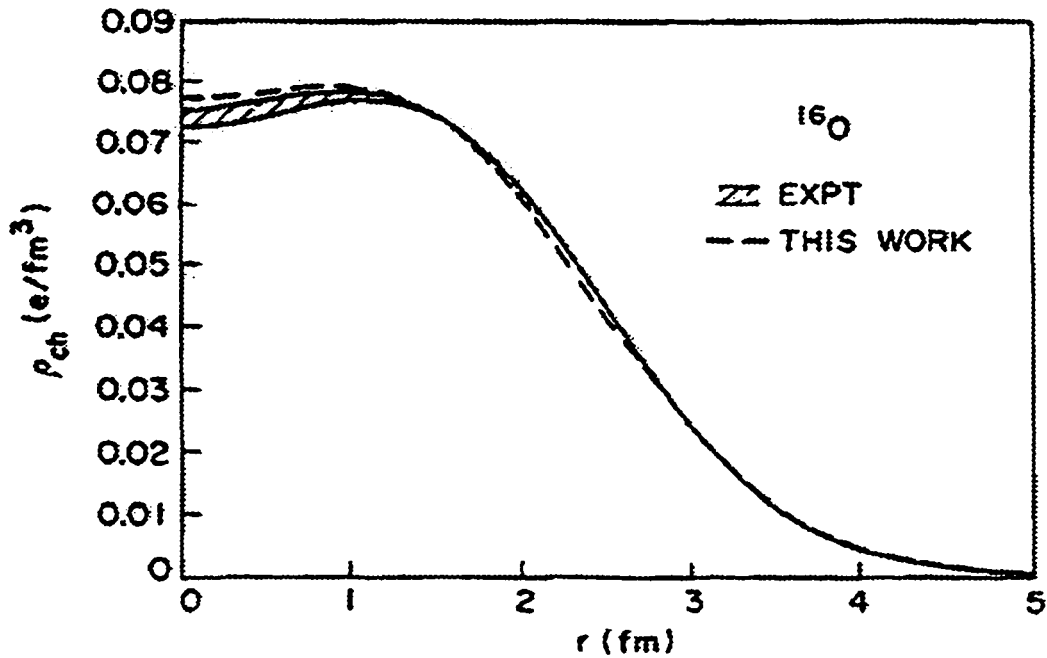
Figure 1.1: Charge density for the ^{16}O nucleus calculated in the relativistic Hartree analysis of finite nuclei in the QHD I model. The experimental results are explained very well. From Ref. [32].

Within this theory one can, for example, reproduce closely charge density

7

curves for closed-shell nuclei [32, 33], or account reasonably well for nuclear shell-model single-nucleon spectra (relativistic Hartree theory for finite nuclei) [32]. The quality of these results can be illustrated by Figure 1.1 - for the charge density of ^{16}O, and Figure 1.2 - for the ^{208}Pb nucleus occupied single-particle levels, correspondingly. One can also make a good prediction for the excitation spectrum of the closed shell nuclei (RPA and relativistic RPA calculations) [34].

It is equally important to include π-mesons in the model, which are responsible for the longest range effects in the problem, because only then can one incorporate chiral symmetry. To that end, the celebrated σ-model formalism is used to describe the $\pi - \sigma$ sector of the theory. This model has the following attractive features. First, it satisfies gauge and chiral symmetries. Second, it adequately describes a large number of meson processes. Third, it can be easily extended to incorporate the ω-meson exchange in a gauge and chirally invariant fashion [2]. And finally, it allows either a linear (Gell-Mann - Levy [35]) or a chirally transformed, non-linear (Weinberg [36]), realization. The σ-model lagrangian contains strong nonlinear couplings involving σ and π fields. If the chiral scalar field is identified with the low-mass scalar field of $m_s = 550$MeV required in the one-boson-exchange model of the phenomenological N-N potential [27], these terms would destroy the successful QHD I description of nuclear matter and finite nuclei. On the other hand, one can set the mass of the chiral scalar field very large ($m_s^2 \to \infty$) [36], while preserving chiral symmetry of the model. Then this scalar field decouples from the problem, and the QHD I picture remains valid. The low-mass scalar meson of QHD I is then produced as a broad dynamic resonance in the two pion exchange [37]. Alternatively, the low-mass scalar field required for modeling of the N-N potential can be introduced simply as an effective chiral scalar field in the non-linear realization of the σ-model. This procedure will be discussed in greater detail later.

Along with ensuring chiral symmetry of the theory, one automatically builds in

8
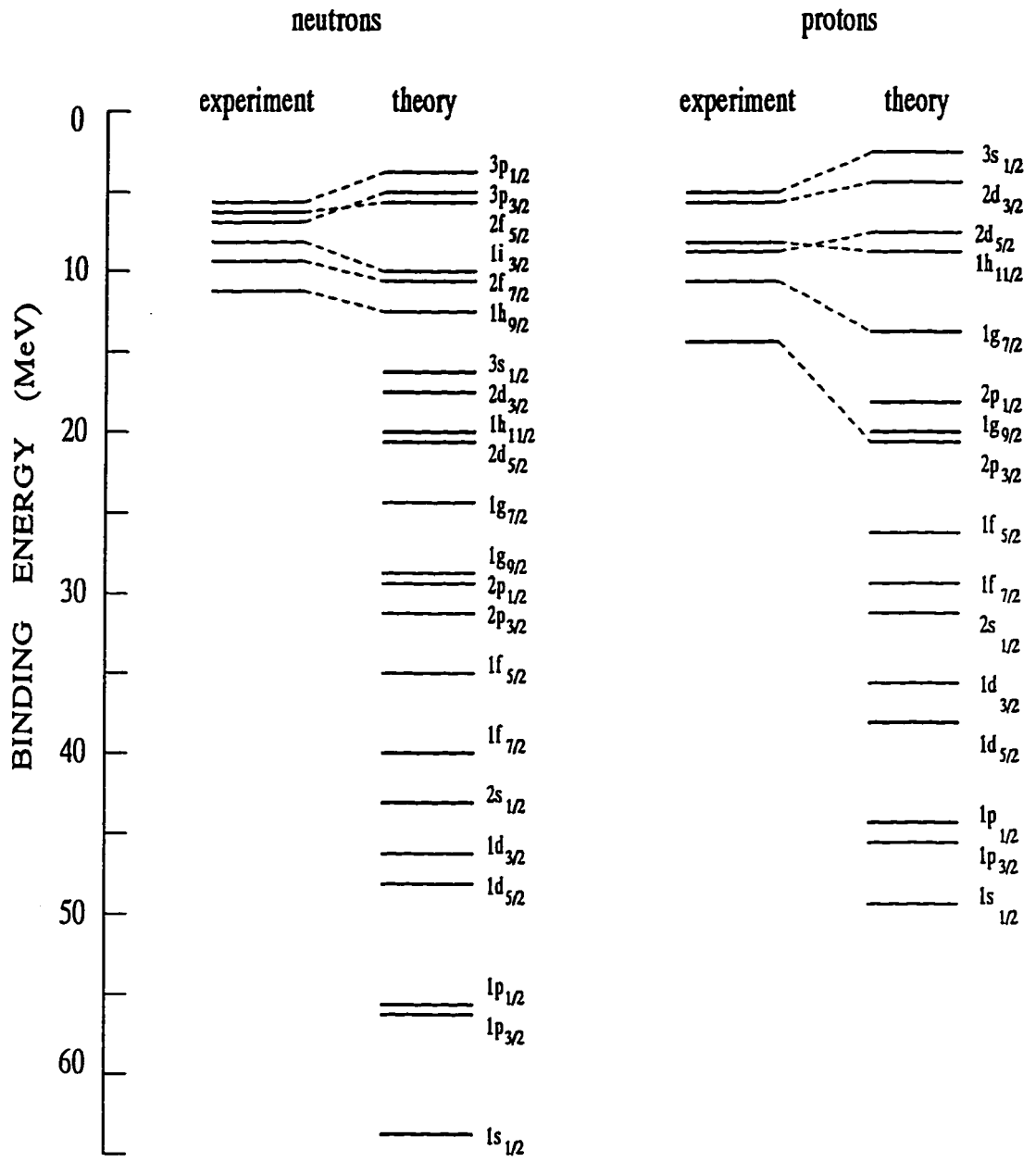
Figure 1.2: Predicted spectrum for occupied single-particle levels in ^{208}Pb. From Ref. [32].

9

a correct description of the pion physics - the longest range effect in the AXC problem. In the non-linear realization of the model, the part of the considered lagrangian that is responsible for the long-range physics coincides with the effective low-energy lagrangian of Weinberg [30]. Hence the present model can be viewed as an attempt to build a bridge between the traditional phenomenological approach and the χPT treatment of the AXC problem.

The vector, isovector ρ-meson and nucleon excitations are also known to play an important role in the short range nuclear dynamics [27]. These degrees of freedom have yet to be included in the present model. Other approaches exist, which take them into account [4,31,38]. In this work a consistent field-theoretical model is built, describing only the most distinct features of the nuclear dynamics.

The resulting chirally symmetric lagrangian model incorporating π, σ and ω mesons, will be referred to as the $\sigma - \omega$ model. Two realizations of the $\sigma - \omega$ model are studied: the linear realization with a non-derivative $\pi-$nucleon coupling, and a chirally transformed, or non-linear, realization, where the $\pi-$nucleon coupling contains a derivative, and all cancellations encountered in the pion$-$nucleon scattering are moved from the amplitude to the lagrangian itself. The reasons for investigating both models will be discussed below.

In the present work, AXC have been calculated in both realizations of the $\sigma - \omega$ model. It has been explicitly demonstrated that the way one splits relativistic many-body effects into AXC contributions, and one-body relativistic corrections to the traditional nuclear axial current, is model dependent. In particular, in the linear realization of the $\sigma - \omega$ model, satisfaction of PCAC to order O(1/M) in inverse nucleon mass requires consideration of the two-body AXC. These currents have been explicitly calculated and shown to restore the correct PCAC relation. In the non-linear realization of the $\sigma - \omega$ model, PCAC is satisfied for the one-body current identically without introduction of any two-body currents. Indeed, it has been shown

10

that there are no AXC of order $O(1/M)$ in this realization. However, to satisfy PCAC for the axial current interaction with a single nucleon to order $O(1/M^2)$ one now has to include a new one-body relativistic correction of order $O(1/M)$ into consideration.

The following general strategy is applied to the analysis of both the linear and non-linear realizations of the $\sigma - \omega$ model. A lagrangian model for the π and σ fields is first formulated, and the corresponding Noether's axial current is identified. The vector ω-meson is incorporated through the same "minimal substitution" procedure in both realizations of the σ-model in a chirally invariant fashion. The scheme for identification of the corresponding AXC consists of the three major steps:

1) The first step involves the analysis of the interaction of the axial current with a single nucleon (see Figure 1.3). It is well known [2] that from general symmetry considerations the axial current matrix element can be written in the form
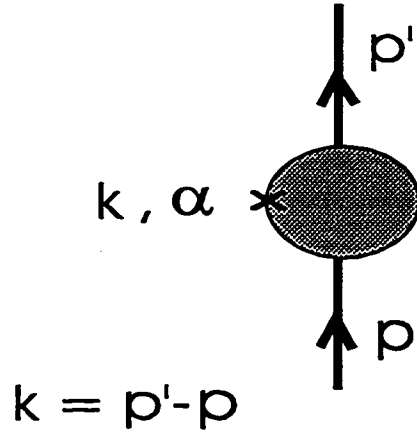
Figure 1.3: Full amplitude for the axial current — one nucleon interaction.

$$\langle p' \mid J_{5\mu}^{\pm}(0) \mid p \rangle = \frac{1}{\sqrt{2\epsilon_{p'} 2\epsilon_p}} \bar{u}(p') \left[F_A(k^2) \gamma_5 \gamma_\mu + F_P(k^2) \gamma_5 k_\mu \right] \tau_\pm u(p)$$

$$(1.1)$$

11

where F_A and F_P are the axial-vector and induced pseudoscalar form factors respectively, which must be determined from experiment, $k = p' - p$ is the four-momentum transferred to the nucleon, and α designates the isospin component of the coupled axial current. The matrices $\tau_\pm$ are defined in terms of hermitian isospin matrices as $\tau_\pm = \frac{1}{2}(\tau_1 \pm \tau_2)$. The factor $F_A(0) \equiv F_A = -1.23$ has been determined accurately from the nuclear beta-decay rates compared with the muon decay rate[1]. In these processes the exchanged momentum is so small that the second term in the current matrix element (1.1), which involves F_P, can be safely neglected. To derive the value of F_P, additional assumptions are usually made.

First, it is assumed that π-exchange dominates the interaction of the axial current with the nucleon in low-energy processes. This assumption works well because pions are so light that in the low-energy regime the pion propagator entering the interaction amplitude is not too far from its pole. It allows relating the pseudoscalar form factor F_P to the pion decay constant $F_\pi \simeq 0.92 m_\pi$ [2]:

$$F_P = \frac{\sqrt{2} g \, F_\pi}{k^2 - m_\pi^2} \tag{1.2}$$

where g is the π–nucleon coupling constant and m_π is the pion mass. The π-pole dominance is a major feature of low-energy nuclear processes in general. It is going to be one of the key elements of the model developed here.

Second, use is made of one consequence of the basic chiral symmetry of the underlying QCD, which is most important for consideration of the axial current: the partially conserved axial current (PCAC) hypothesis. For on-mass-shell particles it can be expressed in the form

$$\langle \partial^\mu J_{5\,\mu}^\pm \rangle = O(m_\pi) \tag{1.3}$$

Preservation of PCAC for the single-nucleon current is known to provide connection

---

[1]This result includes the Cabibo angle factor $\cos \theta_c = 0.97$.

12

of F_A to F_π in the Goldberger-Treiman relation:

$$-2M\,F_A = \sqrt{2}g\,F_\pi \qquad (1.4)$$

This formula produces the following relation between the axial and pseudoscalar form factors:

$$F_P = \frac{2M\,F_A}{k^2 - m_\pi^2} \qquad (1.5)$$

Analysis of the lowest order diagrams for the axial current interaction with a single nucleon in the $\sigma - \omega$ model (see Figure 1.4) allows one to derive a formula for the one-body axial current. The amplitude considered here represents also a building block entering the amplitudes for more complicated processes that involve a larger number of initial and final particles. PCAC must be satisfied in each order in the interaction constant for an on-mass-shell nucleon (for *any* nucleon in the non-linear $\sigma - \omega$-model) because partial chiral symmetry is one of the underlying symmetries of the full theory. As was mentioned before, the single-nucleon $-$ axial-current vertex is renormalized in the full theory by F_A. When going from the tree approximation to the full theory here, the correct π-pole structure is kept, as is required in the low-energy effective theory of strong interactions [29]. Then to preserve PCAC for the full amplitude, the $\pi -$ axial-current vertex has to be renormalized by F_A as well.

The one-body axial current is identified from the interaction amplitude according to the formula

$$\mathcal{J}_\mu^{(\pm)}(1) \simeq -\frac{1}{2M}\,iM_\mu^{(\pm)}(1) \qquad (1.6)$$

The invariant amplitude M_{fi} is defined below in Equations (1.9) and (1.10) through the scattering matrix S_{fi}.

To obtain the traditional single-nucleon axial current, a non-relativistic reduction of the axial current is performed, keeping only the lowest-order terms in inverse

13
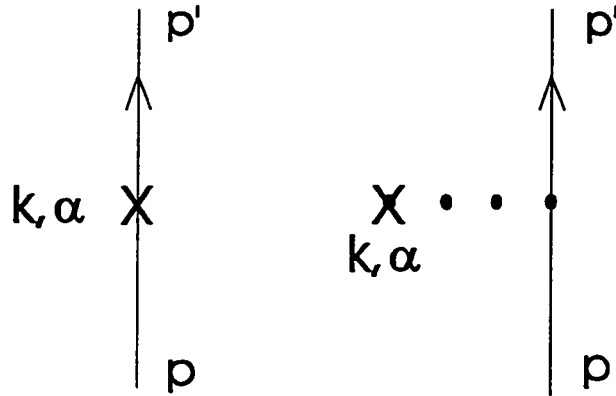
Figure 1.4: Lowest-order amplitude for the axial-current — one-nucleon interaction.

nucleon mass. Then, the one-body axial current operator in coordinate space is determined. This step involves switching to operator language that allows one to deal subsequently with the full many-body nuclear problem. It is assumed here that the many-body problem can be treated by considering one single-pair interaction at a time. One also implicitly assumes that an extension of results derived for the on-mass-shell particles, away from the mass shell, does not introduce significant error. It is then checked whether the one-body axial current satisfies PCAC in a nucleus to order $O(1/M)$ as an operator equation by itself, or if the PCAC enforcement requires consideration of axial two-body currents:

$$i\left[H_{nucl}, \rho_5(1)\right] + \nabla \cdot \mathbf{J}_5(1) \stackrel{?}{=} O(m_\pi) \tag{1.7}$$

Here H_{nucl} is the nuclear hamiltonian calculated in the same $\sigma - \omega$ lagrangian model. Different conclusions concerning the necessity of the two-body axial currents are drawn in the two different realizations of the $\sigma - \omega$ model.

2) The second step involves the analysis of pion production by the axial current on a nucleon (see Figure 1.5). First, the correct set of the lowest order $(O(g))$ diagrams for the amplitude is identified, insisting that this amplitude for the on-mass-shell

14
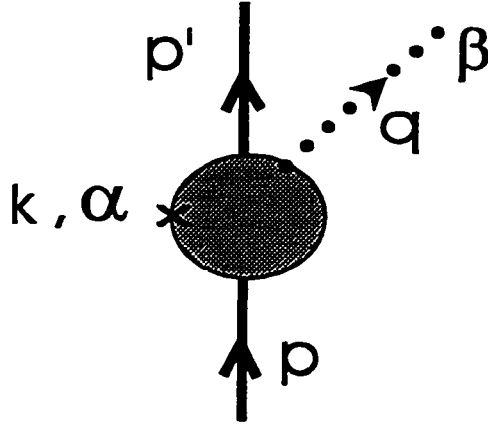
Figure 1.5: Full amplitude for pion production by the axial current on a single nucleon.

pion and nucleon should satisfy PCAC. This tree-level π-production amplitude will enter as a block into some diagrams for the coupling of the axial current to the two-nucleon system. Going to the full theory, the correct pion-pole structure is preserved again, while forcing the full amplitude to satisfy PCAC. This requires now *all* axial current vertices of the theory to be renormalized by the same F_A. Consideration of π-production provides also an additional test of the correctness of the formula obtained, since the low-energy limit of the amplitude can be checked against existing results. In both realization of the $\sigma - \omega$ model, the threshold amplitude for soft-pion production by the axial current satisfies the same low-energy theorem (see Chapter 2):

$$T_\mu^{\alpha\beta} \simeq \frac{1}{2M} M_\mu^{\alpha\beta} \simeq iF_A \frac{g}{M} \epsilon_{\alpha\beta\gamma} \frac{\tau^\gamma}{2} \delta_{\mu 0} \tag{1.8}$$

The formula obtained in the present work differs from the customary one, derived with the help of current algebra techniques, by an extra factor of $F_A{}^2$ (see Chapter 2). The difference originates from the way one takes into account the multi-pion processes, which are of higher order in the χPT small parameters, in the effective low-energy theory. In the current algebra approach, the commutator is calculated for the lowest tree-order currents [39]. In the present treatment the correct pion-pole structure and

15

PCAC for the full amplitude are preserved at each step of the calculation, i.e. the correct Goldberger-Treiman relation of Equation (1.4) is used. This forces one to renormalize each axial current vertex by F_A, thus introducing a factor F_A^2 to the formulae for the π-production amplitude, as well as to the result for the AXC (see step 3).

The scattering amplitude T_{fi} in the previous formula is defined in terms of the scattering matrix S_{fi} by

$$S_{fi} \equiv \delta_{fi} + i(2\pi)^4 \delta^{(4)}(P_f - P_i) \, T_{fi} \tag{1.9}$$

where P_f and P_i are the sums of all final and initial momenta, correspondingly. The invariant scattering amplitude M_{fi} is defined, in turn, by

$$T_{fi} \equiv \frac{M_{fi}}{(2\epsilon_1 \ldots 2\epsilon'_1 \ldots)^{1/2}} \tag{1.10}$$

where ϵ_i and ϵ'_i denote energies of each intitial and final particle participating in the process.

3) The final, third step involves consideration of the coupling of the axial current to the two-nucleon system (see Figure 1.6). Again, PCAC is used to determine the correct set of diagrams for the interaction amplitude to the lowest order in the interaction constant. Keeping only antinucleonic parts of the fermion propagators in the amplitude, the two-body axial meson exchange currents are identified according to the formula

$$\mathcal{J}_\mu^{(\pm)}(2) \simeq -\frac{1}{(2M)^2} \, iM_\mu^{(\pm)}(2) \tag{1.11}$$

Then one carries out the non-relativistic reduction of the current to the lowest order in $1/M$ to obtain the correction to the axial nuclear current in a customary form. Transition to the full theory is performed now by simple multiplication of all axial current vertices by F_A. This procedure ensures that the π-pole dominance and

16

PCAC are preserved in the full theory. The AXC obtained are compared with results of other work. The correction terms calculated are then incorporated in a unified analysis of some semileptonic electroweak processes for a few selected nuclei.
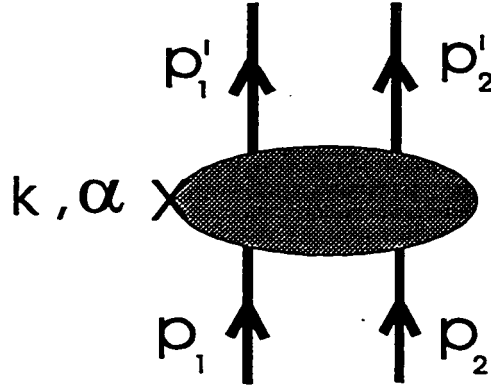
Figure 1.6: Full amplitude for the axial current − two-nucleons interaction.

Now, specific results obtained in the present work can be briefly discussed. The analysis is started by considering the linear realization of the $\sigma - \omega$ model, which serves mainly a pedagogical purpose, demonstrating the necessity and actual presence of AXC of order $O(1/M)$ in the present model. The corrections to the one-body axial current obtained in the non-linear realization are used in the analysis of actual semileptonic weak processes.

In the linear realization of the $\sigma - \omega$ model one obtains the familiar one-body axial current in coordinate space [2]. One piece of this current does not commute with the nuclear hamiltonian to order $O(1/M)$, thus not satisfying PCAC to this order:

$$\rho_5^{(\pm)}(\mathbf{x}) = F_A \sum_{j=1}^{A} \tau_{\pm}(j) \ \vec{\sigma}(j) \cdot \left[\frac{\hat{\mathbf{p}}(j)}{M}, \delta^3(\mathbf{x} - \mathbf{x}_j) \right]_{sym} \tag{1.12}$$

It is most easy to see in the momentum space representation of the current that a

17

combination of all other terms satisfies PCAC through order $O(1/M)$. No specific form for a wave function is involved in this proof, thus the corresponding operators in coordinate space satisfy PCAC as well. The commutator of $\hat{\rho}_5^{(\pm)}(x)$ with the nuclear hamiltonian does not vanish because of the derivative term in the axial charge operator, which fails to commute with nuclear potentials arising from the inclusion of mesons in the hamiltonian. The presence of the isoscalar (due to σ-exchange and, after including ω meson, due to ω-exchange) potentials, which are of order $O(1)$ in inverse nucleon mass, breaks PCAC for the one-body axial current to order $O(1/M)$:

$$\left[\hat{H}_{nucl}, \hat{\rho}_5^{(\pm)}\right] \simeq \left[V_\sigma + V_\omega, \, \hat{\rho}_5^{(\pm)}\right] = O(\frac{1}{M}) \neq O(m_\pi{}^2) + O(\frac{1}{M^2}) \qquad (1.13)$$

Partially conserved chiral symmetry is the most important symmetry which any low-energy effective hadronic theory should satisfy. It must hold in the present many-body problem. To preserve PCAC of the theory, consideration of corresponding two-body spatial axial currents of order $O(1/M)$ is necessary in the linear realization of the $\sigma - \omega$ model.

Meson exchange currents of order $O(1/M)$ are explicitly calculated in this work for the linear realization of the σ-model, and it is shown that the single-nucleon axial current indeed satisfies PCAC to order $O(1/M)$ as an operator equation in coordinate space upon inclusion of these AXC in the problem. This is consistent with the observation of [9] that the one-pion exchange effects will not describe the space components of the axial current.

At the same time, the well-known formula for the meson-exchange axial charge operator of order $O(1/M^2)$ due to the π-exchange [9,17] is reproduced up to the factor F_A^2 discussed above in step 2, inherited from the π-production amplitude:

$$\begin{aligned}
A_0^\alpha(2)(x_1, x_2, k) \simeq & -F_A \frac{g^2}{4\pi} \left(\frac{m_\pi}{2M}\right)^2 \left[\tau(1) \times \tau(2)\right]^\alpha \\
& \times \left(1 + \frac{1}{x_\pi}\right) \frac{e^{-x_\pi}}{x_\pi} \left[e^{i\mathbf{k} \cdot \mathbf{x}_1} \vec{\sigma}(2) \cdot \hat{\mathbf{r}} + e^{i\mathbf{k} \cdot \mathbf{x}_2} \vec{\sigma}(1) \cdot \hat{\mathbf{r}}\right] \qquad (1.14)
\end{aligned}$$

18

where

$$x_\pi \equiv m_\pi |\mathbf{r}|, \quad \mathbf{r} \equiv \mathbf{x_1} - \mathbf{x_2}$$

An extra factor of $F_A^2 \simeq 1.5$ present in the formulae of this work, enhances the AXC contributions by about fifty percent. This enhancement has the order of magnitude to which the presence of the AXC has been tested in nuclei [40].

The non-linear realization of the $\sigma - \omega$ model is much better suited for the description of low-energy nuclear physics because here the soft-pion limit is *built into the model explicitly*, and no cancellations of large quantities occur in the amplitudes. Now the amplitude for the axial-current — single-nucleon interaction explicitly satisfies PCAC because of a projection operator that can be pulled in front of the matrix element:

$$iM_\mu^\alpha(1) = \frac{\tau^\alpha}{2} \underbrace{\left(g_{\mu\nu} - \frac{k_\mu k_\nu}{k^2 - m_\pi^2} \right)}_{\text{projector}} \bar{u}(p_1')\gamma_5\gamma^\nu u(p_1) \qquad (1.15)$$

The PCAC equation for the single-nucleon axial current is satisfied to order $O(1/M)$ *identically* without requiring introduction of any two-body axial currents. Indeed, explicit calculation shows that there are now no AXC of order $O(1/M)$ in this model. However, the very same PCAC argument requires now consideration of a new relativistic correction to a single-nucleon axial current of order $O(1/M)$:

$$\delta A^{(\pm)}(1) \simeq - F_A \tau_\pm \frac{\mathbf{k}}{\mathbf{k}^2 + m_\pi^2} k_0 \frac{\vec{\sigma} \cdot \mathbf{P}}{2M} \qquad (1.16)$$

where $\mathbf{P} \equiv \mathbf{p} + \mathbf{p'}$ and m_π is the pion mass. The corresponding operator in coordinate space will be discussed in detail in Chapter 4. Since PCAC is taken to be one of the cornerstones of the effective theory, one has to include systematically the effects of this correction in the calculation of all weak processes.

In addition, the same formula (1.14) for the axial exchange charge of order $O(1/M^2)$ due to the π-exchange is obtained in this realization of the $\sigma - \omega$ model.

19

These are the two corrections to the traditional nuclear one-body axial current that are included in the analysis of weak processes in the present work.

When calculating the weak interaction operators matrix elements, one has to use some specific wave functions for the nuclear states involved. The lack of reliable nuclear wave functions is the second major source of uncertainty in the analysis of nuclear weak processes. It is the key element of the present strategy, to treat the nuclear wave function part of all the electroweak nuclear matrix elements consistently. In order to eliminate the nuclear wave function uncertainties from the problem, the unified analysis of electroweak nuclear processes is performed in this work within the shell-model framework. The nuclear wave function is parameterized in terms of the shell-model single-particle levels, and corresponding parameters are determined from available electromagnetic data[2]. Following the results of Donnelly and Walecka [41], use is made here of the low-q^2 experimental data to determine the single-body densities for the nucleus under consideration, which is parameterized in terms of the shell-model single-nucleon state contributions:

$$\langle \Psi_f \mid \hat{T}_{JM_J,TM_T}(q) \mid \Psi_i \rangle = \sum_{\alpha,\beta} \langle \alpha \mid T_{JM_J,TM_T}(q) \mid \beta \rangle \, \psi_{\alpha\beta}^{fi} \qquad (1.17)$$

with numerical coefficients

$$\psi_{\alpha\beta}^{fi} \equiv \langle \Psi_f \mid c_\alpha^+ c_\beta \mid \Psi_i \rangle \qquad (1.18)$$

The electromagnetic current is assumed here to be a one-body operator[3].

A simple harmonic oscillator basis is used for the single-nucleon orbits in this work. First, some reasonable truncation of the number of shells important for the considered processes is performed. Then the corresponding coefficients ψ^{fi}, as well

---

[2]Electromagnetic exchange currents have been calculated in this approach by Dubach, Koch and Donnelly in [6].

[3]The two-body currents introduce only small corrections in the low-q^2 regime, which is important for weak processes considered.

20

as the oscillator parameter of the radial eigenfunctions, are calculated in the "model independent way" by fitting available low-q^2 electromagnetic experimental results. Those coefficients are used to compute the weak rates under consideration.

The present procedure eliminates to a large extent nuclear structure uncertainties from the analysis of weak rates and cross sections. Thus one no longer needs to use phenomenological N-N potentials for calculation of a nuclear wave function. Here, instead of these phenomenological potentials, the $\sigma - \omega$ model containing a set of meson fields that reproduces qualitatively the most important features of the N-N potential, and, in the MFT framework, adequately describes many nuclear spectra, is used.

As applications, corrections to the one-body axial currents obtained in this work, have been included in the analysis of the three charge-changing semileptonic weak process:

1) β^--decay: $A(N, Z) \to A^*(N - 1, Z + 1) + e^- + \bar{\nu}_e$

2) μ^--capture: $\mu^- + A(N - 1, Z + 1) \to A^*(N, Z) + \nu_\mu$

3) antineutrino scattering: $\bar{\nu}_l + A^*(N - 1, Z + 1) \to A(N, Z) + l^+$

for two light nuclear systems. These systems are the ^{3}H$-^3$He isospin doublet, and the ^{6}He$-^6$Li neighboring nuclei. The objective here is to see how large the contributions to the specified semileptonic weak processes from the corrections (1.14) and (1.16) are, compared to the traditional one-body axial currents.

Corrections to the one-body *vector* part of the weak currents can be obtained from the electromagnetic exchange currents through the isospin rotation. They will not be included in the present analysis[4]. The prime goal of the present treatment is

---

[4]The processes considered in this work: muon capture, nuclear beta decay and charge-changing neutrino scattering - are predominantly Gamow-Teller transitions for the nuclear systems considered. Selection rules determine that contributions from the vector part of the weak current are suppressed in these processes by extra powers of the ratio of the transferred momentum to nucleon mass.

21

to estimate effects of the corrections to the "canonical" axial one-body currents [2].

22

Ground state $(J^\pi T) = (\frac{1}{2}^+\frac{1}{2})$ isodoublet of the A=3 system

$$\rule{4cm}{0.1cm} \qquad \rule{4cm}{0.1cm} \qquad \frac{1}{2}^+\frac{1}{2}$$

$${}^3_1\text{H} \qquad\qquad {}^3_2\text{He}$$
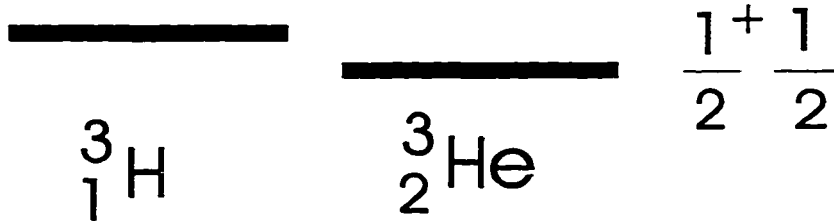
Figure 1.7: The ^{3}H $-{}^3$He isodoublet ground states.

The ^{3}H$-{}^3$He system depicted in Figure 1.7 consists of the most simple nuclei featuring the weak processes of interest here. Very accurate calculations of the wave functions for these three-body nuclear systems from first principles exist [42]. However, the objective of the present analysis is to estimate the scale of the effects due to the calculated corrections. For this purpose it is sufficient to implement the most straightforward description of the involved wave functions in terms of the single-particle shell-model states. As a model for the ground states of the isodoublet, the $(1s_{\frac{1}{2}})^{-1}$ hole state in the filled $(1s_{\frac{1}{2}})$ shell is used. The only parameter of the model, $b_{osc} = 1.59$ fm, is determined by fitting the elastic electromagnetic form factors in the low transferred momentum region [41]. Figure 1.8 shows that the simple model adopted for the description of the ground states, models well the electromagnetic form factors in the low-q^2 region, which is of prime interest for the treatment of the weak processes considered here. The data for the form factors has been taken from [43-45]. Results for the semileptonic weak rates for the ^{3}H $\leftrightarrow{}^3$He transitions

23

with the corrections to the one-body axial current included, are compared to the previous calculations with no exchange currents or relativistic corrections present [41].

Within the assumed model for the isodoublet ground state there is *no contribution to any of the weak processes considered from the one-body relativistic correction* to the axial current. This happens because only the reduced matrix elements of operators between the $1s$-states are required in the calculation. The only non-zero multipoles of the relativistic correction are expressed through the Ω_{1M_1} operator defined in [46], but

$$\langle 1s \parallel \Omega'_1 \parallel 1s \rangle = 0 \qquad (1.19)$$

For calculating effects of the AXC on this system, one can consider the ground state of the isodoublet as a $(1s_{\frac{1}{2}})^3$ state. Then the two-body AXC contribution to the weak ground state processes with this isodoublet can be analyzed with the help of the fractional parentage coefficients reduction of the three-body matrix element to the combination of the two-body matrix elements [47,48] (see Appendix C for details). Within the present model of the AXC, only $\rho_5^a(2)$ - pseudoscalar, isovector - operator has to be considered to order $O(1/M^2)$. Only Coulomb multipoles of this operator are non-zero. Due to the angular momentum selection rules, the two-body matrix elements vanish for $J > 1$. The $\hat{M}_0^5$ operator is prohibited by parity conservation arguments. Thus there are only two terms left, with the $\hat{M}_{11}^5(2)$ operator in them. However, these matrix elements cancel each other for the AXC operator considered. Thus the three-body matrix elements of the AXC vanish to order $O(1/M^2)$. *There are no effects of the AXC on the processes involving transitions between the ground states in the ^3H–^3He isodoublet in this model whatsoever.*

These results justify the close agreement of the previous one-body calculations [7,41,49] with experimental results, at least as far as the dominant axial vector current

24
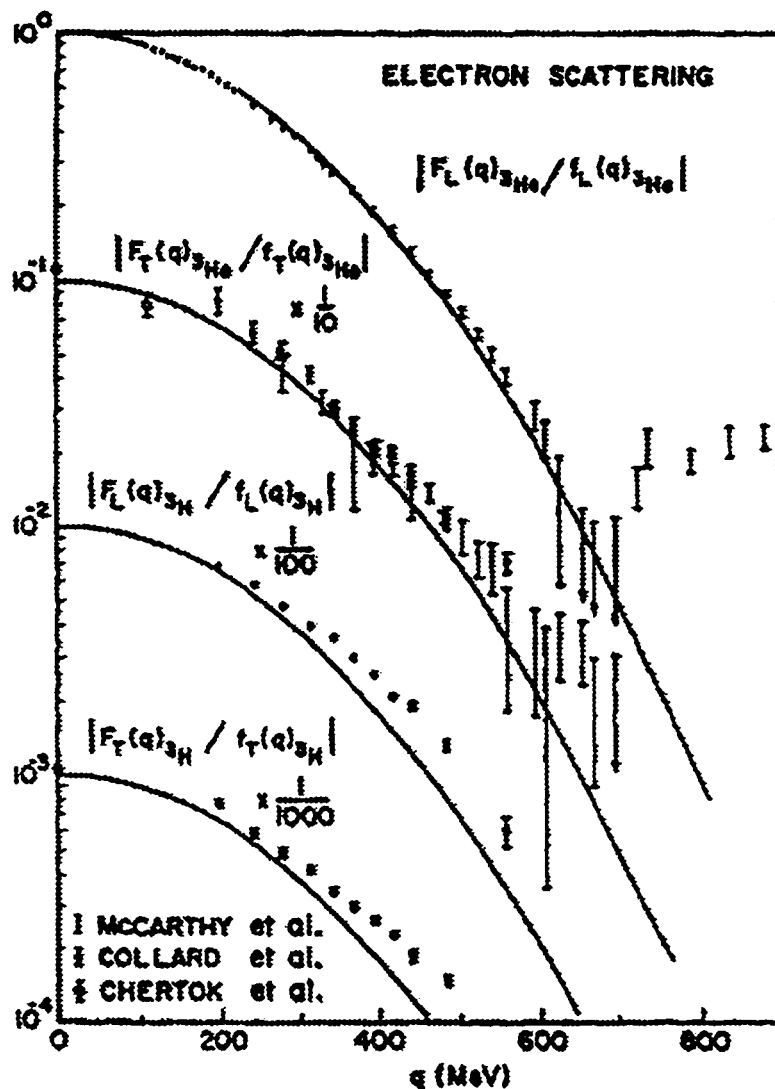
Figure 1.8: Elastic electron scattering form factors for the A=3 system: $b_{osc} = 1.59\,\mathrm{fm}$ is obtained. From Ref. [41].

25

contributions are concerned (see Table 1.1). $\bar{\omega}_\mu$ designates the muon capture rate, statisticaly averaged over different hyperfine states of the muonic atom.

	exper.	1-body theory	+relativ. correction	+ pion X current
β^--decay: $\omega_\beta(10^{-9}\mathrm{sec}^{-1})$	1.79 ± 0.007^5	1.84	1.84	1.84
μ^--capture: $\bar{\omega}_\mu$ (sec^{-1})	1505 ± 46^6	1534	1534	1534

Table 1.1: ^{3}H$-^3$He weak transition rates.

26

$(1^+0) \leftrightarrow (0^+1)$ transitions in A=6 system

3.562 MeV
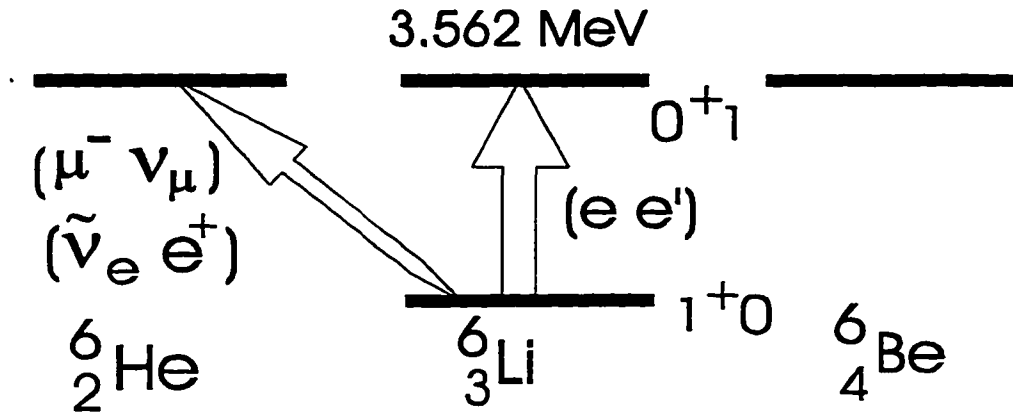
Figure 1.9: The ^{6}He $-^6$Li nuclei lowest energy levels.

The second system investigated here consists of the A=6 neighboring nuclei (see Figure 1.9): the ^{6}He$\leftrightarrow$ ^{6}Li transitions are considered. The following three facts make this system interesting for the present analysis:

1) These are non-trivial nuclei. It would be a daunting task to calculate the required wave functions from first principles.

2) There are high precision electromagnetic data available for these nuclei.

3) This is the simplest system where one can now expect to see some nontrivial effects of the derived corrections to the one-body axial currents.

The following model for the A=6 nucleus is assumed here: an *inert* core (closed $1s$-shell) + two valence nucleons producing the wave function of the form:

$$|1^+0\rangle = A|(1p_{\frac{3}{2}})^2 1^+0\rangle + B|(1p_{\frac{3}{2}} 1p_{\frac{1}{2}})1^+0\rangle + C|(1p_{\frac{1}{2}})^2 1^+0\rangle$$

$$|0^+1\rangle = D|(1p_{\frac{3}{2}})^2 0^+1\rangle + E|(1p_{\frac{1}{2}})^2 0^+1\rangle \tag{1.20}$$

Again the simple harmonic oscillator basis is used for parameterizing the nuclear

27
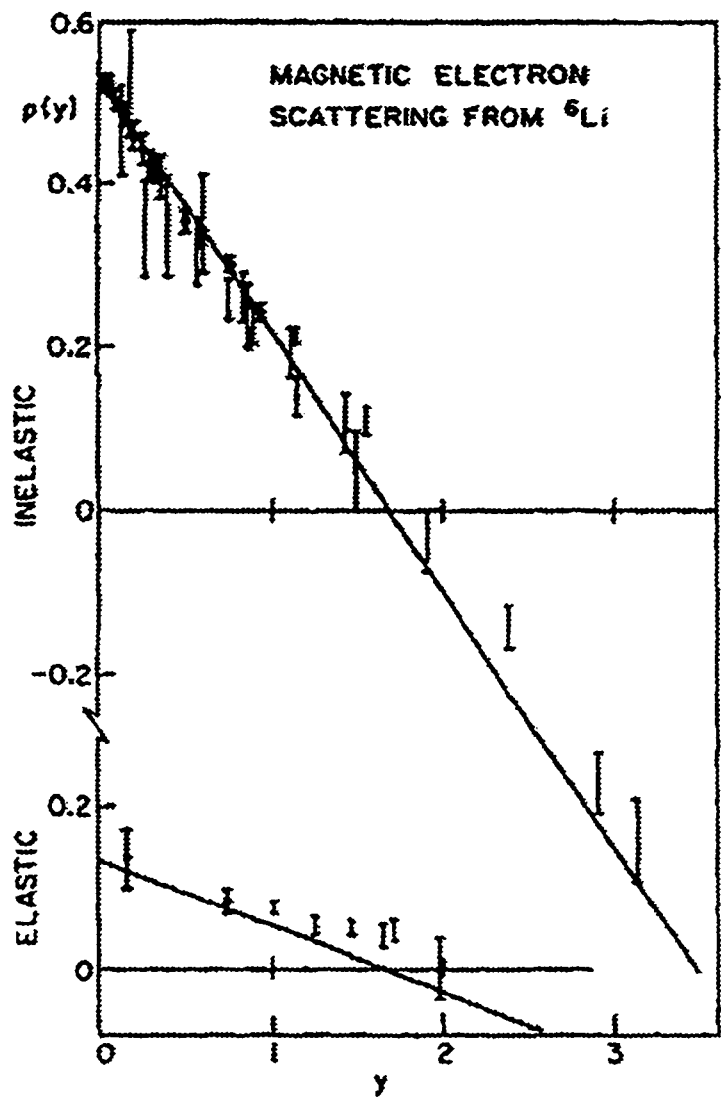
Figure 1.10: Elastic electron scattering form factors for ^{6}Li. From Ref. [41].

28

wave function. This model works well for description of electromagnetic processes with the system. Parameters of the model are determined through simultaneously fitting the magnetic dipole and electric quadrupole moments of the ^{6}Li ground state, as well as the elastic and inelastic magnetic form factors, calculated in terms of the model wave function of (1.20). For instance, the elastic magnetic form factor is

$$\frac{\langle 1^+ 0 \| \hat{T}_{1,0}^{mag} \| 1^+ 0 \rangle}{\sqrt{3}(i|q|/m)e^{-y}f_{sn}f_{cm}} \equiv p(y) = \alpha_e + \beta_e y \qquad (1.21)$$

where $y \equiv (| q | b_{osc}/2)^2$ and α_e, β_e are certain constants. The result for the inelastic form factor differs from (1.21) only by different values of the constants involved (see Figure 1.10). The best set of the simultaneous values of the parameters is given in Table 1.2 [52]:

A	B	C	D	E	b_{osc}(fm)
0.810	-0.581	0.084	0.80	0.60	2.03
±0.001	±0.001	±0.002	±0.03	±0.04	±0.02

Table 1.2: Parameters of the wave function.

These parameters are used in the corresponding nuclear wave functions to calculate the weak current matrix elements for the A=6 system. Details of these calculations are presented in Chapter 5.

For the consideration of the two-body operators, the proper description of the wave function at small interparticle separations becomes an important issue. To estimate effects of the incorrect behavior of the simple harmonic oscillator basis wave functions at short distances, a phenomenological correlation function $g(r)$ has been introduced in the calculation, following Dubach [6], in the following way:

$$R_{N_A'L_A'}(r) R_{N_A L_A}(r) \rightarrow g(r) R_{N_A'L_A'}(r) R_{N_A L_A}(r) \qquad (1.22)$$

29

Only the s-state relative wave functions must be modified by this correlation function. The function $g(r)$ was chosen to have the form:

$$g(r) = C(N_A) \left[1 - \exp(-\frac{r^2}{d^2}) \right] \qquad (1.23)$$

where $d = 0.84\,\mathrm{fm}$ has been determined from a fit to the nuclear matter properties [6], and the $C(N_A)$ coefficient is introduced to preserve the normalization of the s-state wave function. This *ad hoc* correlation function forces the wave functions to vanish at short distances, mocking up the presence of the repulsive core. Calculations of the weak rates have been performed with and without this correlation function to see how significant is the error made when using the simple harmonic oscillator wave functions for the single-nucleon states.

The semileptonic weak rates in Table 1.3 have been calculated for the $(0^+1) \leftrightarrow (1^+0)$ transitions in ^{6}He$-^6$Li system, upon performing the numerical evaluation of the weak current multipole matrix elements with the wave function coefficients and the correlation function obtained above.

	exper.	1-body theory	+relativ. correction	+ pion X current	with corr. function	Total	Diff (%)
β^--decay:							
ω_β (sec^{-1})	0.864^7 ± 0.003	0.876	0.872	0.869	0.869	0.865	-1.3
μ^--capture:							
$\bar{\omega}_\mu$(sec^{-1})[8]	1600^{+330}_{-130}	1381	1381	1386	1385	1385	0.2
$\omega_\mu^{F=1/2}$(sec^{-1})		3843	3843	3865	3860	3860	0.4
$\omega_\mu^{F=3/2}$(sec^{-1})		150.2	150.2	137.1	140.3	140.3	-6.6

Table 1.3: Weak rates for the $(0^+1) \leftrightarrow (1^+0)$ transitions in the ^{6}He$-^6$Li system.

Here the F superscript, a quantum number of the $\mathbf{F} = \mathbf{J} + \mathbf{S}$ operator, distinguishes the μ-capture processes occuring from different hyperfine states of the muonic

atom. The $\bar{\omega}_\mu$ corresponds to the statistically averaged μ-capture rate.

Effects of the calculated corrections in the weak processes are seen to be small. In the first column of the table available experimental results are provided. The second column shows the traditional results of the weak rates calculations, where only the single-nucleon axial currents have been included [41,49,52]. The third and fourth columns of the table display the separate influences on the weak rates of the relativistic correction (1.16) and pion exchange charge (1.14), correspondingly. The fifth column shows the latter result with a correlation function included in the analysis. The next column shows the cumulative rates with both considered corrections included, while the last column expresses the effect due to both calculated corrections combined, in the percent fraction of the one-body result. The largest effect due to the corrections is predicted for the muon-capture rate from the hyperfine $F = 3/2$ state (-6.6%). The total effect for the beta-decay rate is small, but it is interesting that the one-body relativistic correction obtained in this work, produces here an effect of about the same size with the one from the pion axial exchange charge. Consideration of the phenomenological correlation function corrects the result for the axial exchange charge contribution by at most 20%, as was expected. In general, *the smallness of the calculated effects serve as a justification of the success of the previous analysis of weak processes in terms of the one-body currents* [41,49,52].

One arrives at the same conclusion upon consideration of the results for the charge-changing antineutrino cross section in the process

$$\bar{\nu}_e + {}^6\mathrm{Li} \rightarrow {}^6\mathrm{He(g.s.)} + e^+$$
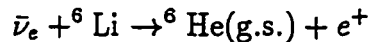
A prediction for the differential scattering cross section with the obtained corrections to the one-body effects included in the analysis, is shown in Figure 1.11. This result does not differ noticeably, up to high transferred momentum, from the curve obtained in the one-body analysis, again justifying the applicability of the previous one-body

31

analysis.

The second part of this dissertation is devoted to investigation of electroweak processes involving (0^+0) excitations in nuclei. It is based on the corresponding work presented in [55]. This work is discussed in detail in Part II. A short summary of the results obtained in this work is presented in the next paragraph.

Within the Standard Model, strong isospin invariance and the nuclear domain of u, d quarks and their antiquarks, the formula for the parity violating asymmetry in electron scattering is derived, and the neutrino scattering cross section is directly related to the electron scattering cross section, for inelastic $(0^+0)_{gnd} \rightarrow (0^+0)^*$ nuclear transitions (assuming pure quantum numbers for both states). With the inclusion of strange quarks, the asymmetry measures a new nuclear matrix element of the strangeness current, if the inelastic charge form factor for that transition is large enough for performing the experiment. The ground and first excited states of ^{4}He have $(J^\pi = 0^+, T = 0)$; thus the analysis is applicable to future CEBAF experiments on parity violation, as well as possible neutrino scattering experiments on this nucleus. Existing low momentum transfer q^2 data on the inelastic charge form factor for the $(0^+0)_{gnd} \rightarrow (0^+0)^*$ transition in ^{4}He (which show it growing relative to the elastic one) are fit within simple nuclear models, and predictions are made for higher q^2. A more quantitative analysis for ^{4}He is significantly complicated by the fact that the considered excited state lies just above the break-up threshold. It is desirable to first have an experimental measurement of this form factor to higher q^2, using the predicted magnitude as a guide.

32

$\overline{\nu}_e + {}^6Li \rightarrow {}^6He + e^+$ scattering cross section
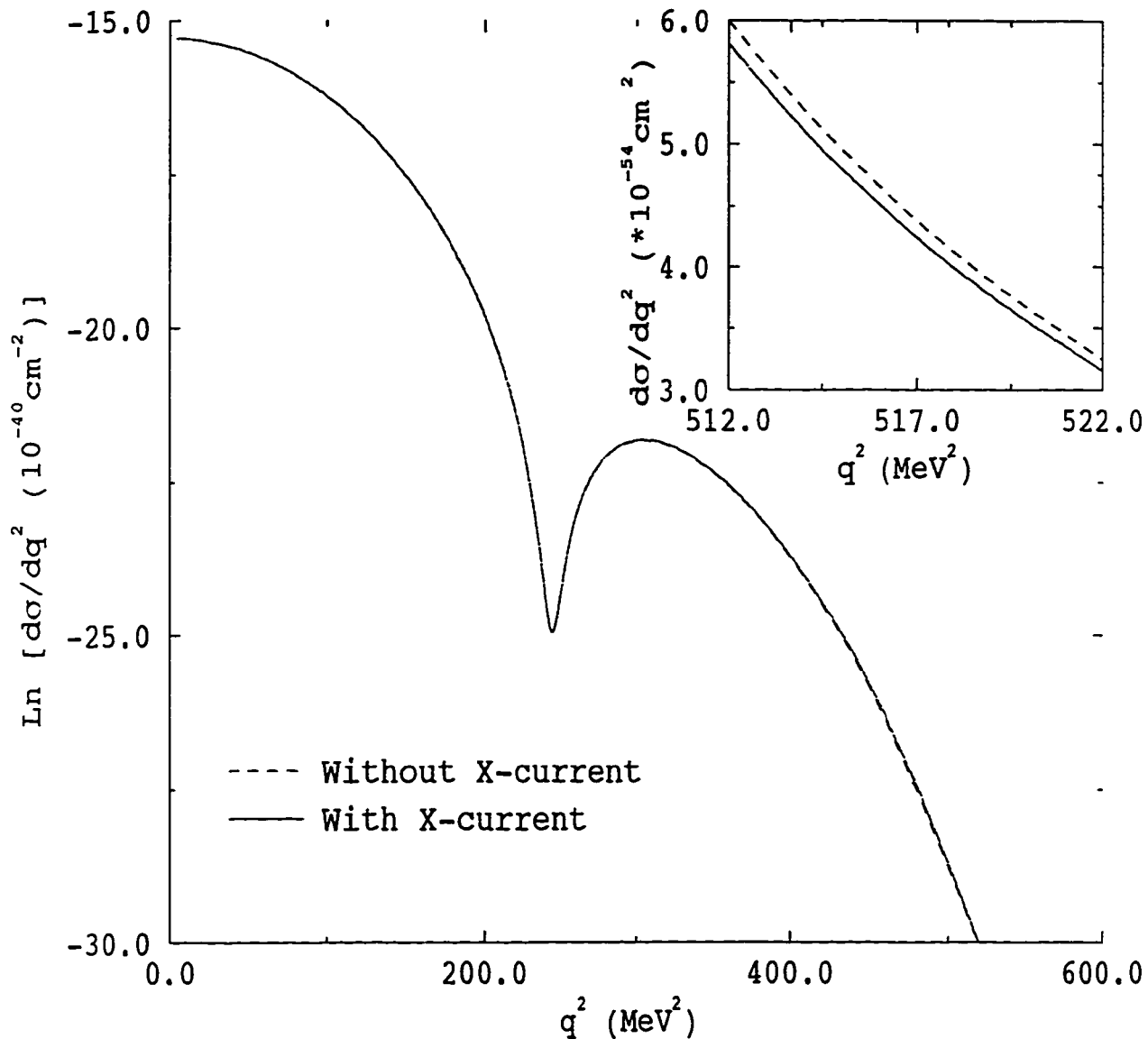
Figure 1.11: Charge-changing antineutrino scattering cross section on ${}^6Li$. The linear-scale insertion in the upper right corner of the graph represents the blown-up figure of the same results at some large q^2 where effects of exchange currents are expected to be more pronounced.

33

Part I

A consistent hadronic model of weak meson exchange currents in nuclei

34

Chapter 2

Linear realization of the $\sigma - \omega$ model

As was outlined in the introduction, the objective of this work is to build a consistent $\sigma - \omega$ model involving three mesons: π, σ and ω, that would describe most of conventional nuclear physics results while preserving the basic symmetries of the underlying QCD, and then to calculate AXC in the framework of this model. One can start the analysis by considering the "linear realization" of the σ-model with π and σ fields entering in the combination $\sigma - i\vec{\tau} \cdot \vec{\pi}\gamma_5$ (with no other mesons included at first). There are some known drawbacks to this model: it does not incorporate explicitly the correct soft-pion limit of the theory because of the non-derivative character of the $\pi - N$ coupling used. In addition, fine cancellations of large quantities in the amplitudes are required for reproduction of the experimental results. The non-linear realization of the $\sigma - \omega$ model, which is free of these problems, is a natural framework for the analysis of the present problem. It will be utilized in the next chapter for calculating corrections to the traditional one-body axial currents, which are used later in the actual analysis of weak rates. Nevertheless, the linear realization of the model allows

35

one to obtain an additional insight into the MEC problem and to set certain checks on the intermediate results, which will be helpful for analysis of the non-linear model. Here Noether's axial current of the theory can be identified easily for future use in the non-linear model, and the low-energy theorem for pion production by the axial current on a nucleon derived. Still more important, the need for the AXC of order O(1/M) for the satisfaction of PCAC as an operator equation, and the actual presence of these AXC in the linear model are demonstrated. In the linear realization of the σ-model the π-N coupling has a pseudoscalar character, and the nucleon mass M appears in the investigated lagrangian as a result of spontaneous chiral symmetry breaking, in the form of a vacuum expectation value of the scalar field.

The model is developed starting with the following chirally symmetric lagrangian [2]

$$
\mathcal{L}_\sigma = \bar{\psi}\left[i\not{\partial} + g(\sigma - i\gamma_5\vec{\tau}\cdot\vec{\pi})\right]\psi + \frac{1}{2}(\partial_\mu\sigma\,\partial^\mu\sigma + \partial_\mu\vec{\pi}\cdot\partial^\mu\vec{\pi}) - V(\vec{\pi}^2 + \sigma^2)
$$

where $\quad V(\vec{\pi}^2 + \sigma^2) = \dfrac{\lambda}{4}\left[(\sigma^2 + \vec{\pi}^2) - v^2\right]^2$ (2.1)

where g is the π-N interaction constant, while $\lambda > 0$, and $v > 0$ are some arbitrary parameters. The symmetry is realized in the Goldstone mode: the ground state is not symmetric under the chiral transformation. Addition to the potential of a small chiral-symmetry breaking term

$$
\delta V_{\text{csb}} \equiv \frac{M}{g}\,m_\pi^2\,\sigma
$$ (2.2)

singles out the correct vacuum state, bringing the theory in line with the observation that the vacuum must have a definite parity. The coefficient on the right hand side of equation (2.2) has been included in anticipation of the identification of the nucleon mass M in the world with the spontaneously broken chiral symmetry. When one redefines the scalar field to describe excitations of a new scalar field ϕ built over the

36

proper ground state

$$\sigma = -\frac{M}{g} + \phi \tag{2.3}$$

one obtains the following σ-model lagrangian density for the linear representation of the model:

$$\mathcal{L} = \bar{\psi}\left[i\partial\!\!\!/ - M + g(\phi - i\gamma_5\vec{\tau}\cdot\vec{\pi})\right]\psi + \frac{1}{2}(\partial_\mu\phi\,\partial^\mu\phi - m_s^2\phi^2) + \frac{1}{2}(\partial_\mu\vec{\pi}\cdot\partial^\mu\vec{\pi} - m_\pi^2\vec{\pi}^2)$$

$$+\frac{g}{2M}(m_s^2 - m_\pi^2)\,\phi\,(\phi^2 + \vec{\pi}^2) - \frac{g^2}{8M^2}(m_s^2 - m_\pi^2)\,(\phi^2 + \vec{\pi}^2)^2 \tag{2.4}$$

In this lagrangian the constants λ and v have been reabsorbed into the mass parameters of the fields m_s and m_π.

One can identify $m_\pi = 139\,\text{MeV}$ as the mass of the pion, the particle playing the most important role in low-energy strong interaction physics. Correct identification of the mass of the scalar field m_s is known to be more problematic. It might be tempting to put this mass equal to the mass (about 550 MeV) of a scalar field required in the phenomenological N-N potential. However, this is not consistent with the traditional nuclear physics results obtained in the QHD I model of Walecka [32]. The strong non-linear coupling terms in the last line of the lagrangian (2.4) would then destroy successful nuclear physics applications calculated in the MFT limit of QHD I. To reconcile results obtained in the two models, one has to take the σ-model scalar field mass to be very large. As discussed in the next Chapter, such an isoscalar field then decouples from the problem, and results of QHD I get rescued. The low-mass scalar field of QHD I (entering also the phenomenological N-N potential) is then produced dynamically as a (broad) resonance in the isoscalar channel of the two-pion exchange [37]. It is not clear, however, how to include such a dynamic σ-field in the analysis of the AXC problem. A better phenomenological way of including an additional low-mass scalar field in the model as a chiral singlet can be achieved in the non-linear realization of the $\sigma - \omega$ model discussed in the next chapter.

37

$$N \quad \phi \qquad N \quad q, \alpha \qquad \phi \qquad \pi \quad q_1, \alpha$$

$$\pi \qquad \qquad \pi \quad q_2, \beta$$

$$i g \qquad\qquad g \gamma_5 \tau^\alpha \qquad\qquad i \frac{g}{M}(m_s^2 - m_\pi^2)\, \delta_{\alpha\beta}$$
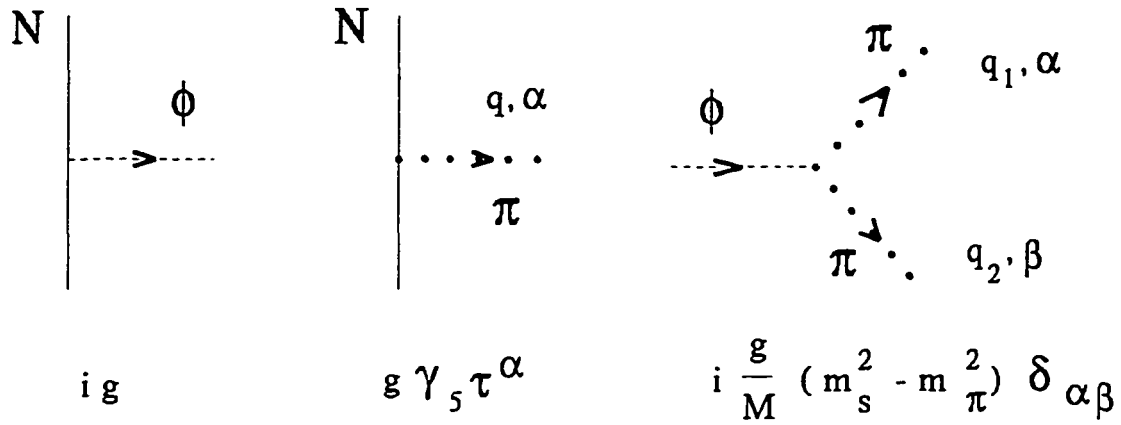
Figure 2.1: Strong interaction vertices relevant for the present calculation in the linear realization of the $\sigma - \omega$ model.

The limit of a very large mass scalar field of the σ-model will be considered in most of the present work. Nevertheless, one can imagine for a moment considering the σ-model with a low-mass scalar field as a purely phenomenological model of the AXC, with no recourse to any other nuclear physics results. To take this possibility into acount, one can treat m_s as an arbitrary mass parameter for a while, taking the required large-scalar-mass limit only at the final stage of the calculations.

The strong interaction vertices relevant for the future calculation of AXC are depicted in Figure 2.1. As is well known [2], Noether's theorem allows writing down the axial current corresponding to the lagrangian (2.4):

$$A^{\alpha\mu} = \bar{\psi}\gamma_5\gamma^\mu \frac{\tau^\alpha}{2}\psi - \pi^\alpha\partial^\mu\phi + \phi\partial^\mu\pi^\alpha - \frac{M}{g}\partial^\mu\pi^\alpha \tag{2.5}$$

This current satisfies the PCAC theorem

$$\partial_\lambda A^\lambda = \frac{M}{g} m_\pi^2 \, \vec{\pi} \tag{2.6}$$

The axial current vertices are shown in Figure 2.2. Now both, strong interaction and axial-current, sets of vertices of the theory have been identified in terms of

38

$$\gamma_5 \gamma_\mu \frac{\tau^\alpha}{2} \qquad\qquad i\,2\,(q_\mu - r_\mu)\,\delta_{\alpha\beta} \qquad\qquad -i\frac{M}{g}\,q_\mu$$
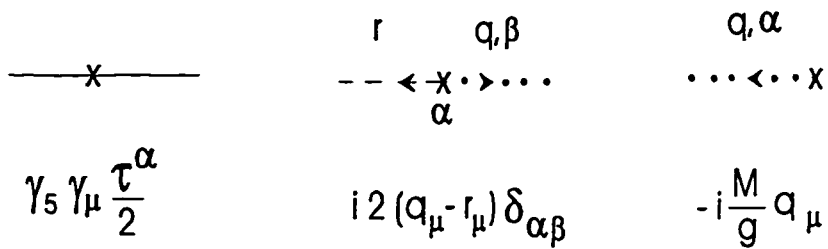
Figure 2.2: Axial current vertices in the linear realization of the $\sigma - \omega$ model.

just three parameters: the pion—nucleon interaction constant g, the pion mass m_π and the scalar field mass m_s. Note that the ω-meson can also be easily incorporated in the present model in a chirally-invariant fashion by introducing a chiral-singlet Lorentz-vector field V_μ, changing the partial derivative in the first term in the lagrangian (2.4) to

$$\not{\mathcal{D}} = \not{\partial} - ig_v\,\gamma^\mu V_\mu \qquad\qquad (2.7)$$

and adding kinetic and mass terms for the ω-field to the lagrangian:

$$i\,g_v\gamma_\mu$$
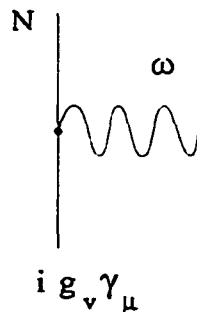
Figure 2.3: Nucleon — vector-meson vertex in the linear $\sigma - \omega$ model.

39

$$-\frac{1}{4}F_{\mu\nu}F^{\mu\nu} + \frac{1}{2}m_v^2 V_\mu V^\mu \tag{2.8}$$

Here g_v is the ω-meson$-$N coupling constant, and $F^{\mu\nu} \equiv \partial^\mu V^\nu - \partial^\nu V^\mu$. In QHD I the vector meson parameters are taken to be

$$\frac{g_v^2}{4\pi} \simeq 10.8 \quad \text{and} \quad m_v = 782\text{MeV}$$

An additional Feynman vertex due to the included ω-meson, of interest in the problem investigated, is shown in Figure 2.3. It should be noted that the presence of this additional field in the lagrangian does not change the form of Noether's axial current. In the present treatment, the first non-trivial contribution of the ω-meson will be to the axial current interaction with the two-nucleon system. The resulting model is referred to as the *linear representation of the $\sigma - \omega$ model.*

Following the general analysis framework, first some familiar results are reproduced, corrections to which will be derived later. The lowest order $(O(g^0))$ amplitude for the interaction of the axial current with a single nucleon can be read off Figure 1.4 and is given by the expression:

$$iM^{\alpha\mu}(1) = \frac{\tau^\alpha}{2}\, \bar{u}(p')\gamma_5 \left(\gamma^\mu + 2M\frac{k^\mu}{k^2 - m_\pi^2}\right) u(p) \tag{2.9}$$

where k^μ is the four-momentum transferred to the nucleon. This amplitude satisfies PCAC for an on-mass-shell nucleon. Note that use of Dirac equation for an on-mass-shell nucleon is explicitly involved in deriving the PCAC result here. Thus PCAC will *not* be satisfied as an operator equation for the corresponding one-body current operator alone in coordinate space.

As was outlined in the introduction, when making transition to the full many-body nuclear problem, one assumes the π-pole dominance and satisfaction of the correct Goldberger-Treiman relation (1.4) for the on-mass-shell nucleon. Then the $\pi-$ axial-current vertex should be renormalized by the same F_A as the nucleon$-$axial-current vertex. The one-body axial current in momentum space is identified then at

40

low energies from the interaction amplitude $iM^{\alpha\mu}(1)$ in accordance with the formula (1.6).

When one considers the non-relativistic limit of the amplitude, assuming all momenta in the problem to be small compared to the nucleon mass M, the familiar one-body axial current [2] is obtained in momentum space:

$$J_5^{(\pm)0}(1) = F_A \, \tau_\pm \left[\frac{\vec{\sigma} \cdot \mathbf{P}}{2M} + \frac{k_0}{k^2 - m_\pi^2} \, \vec{\sigma} \cdot \mathbf{k} \right]$$

$$\vec{J}_5^{(\pm)}(1) = F_A \, \tau_\pm \left[\vec{\sigma} + \frac{\mathbf{k}}{k^2 - m_\pi^2} \, \vec{\sigma} \cdot \mathbf{k} \right] \tag{2.10}$$

where $\mathbf{P} = \mathbf{p} + \mathbf{p}'$ and $\mathbf{k}$ is the momentum transferred to the *nucleon* (see Figure 1.4).

For the currents (2.10) one obtains, of course, the well-known coordinate space axial current operators [2], corrections to which will be calculated in this work. These coordinate space current operators are provided below for ease of future reference:

$$\hat{J}_5^{(\pm)0}(\mathbf{x}) = \hat{\rho}_5^{(\pm)}(\mathbf{x}) + \hat{\rho}_{ps}^{(\pm)}(\mathbf{x}) \tag{2.11}$$

$$\hat{\mathbf{J}}_5^{(\pm)}(\mathbf{x}) = \hat{\mathbf{A}}^{(\pm)}(\mathbf{x}) + \nabla \hat{\phi}_{ps}^{(\pm)}(\mathbf{x}) \tag{2.12}$$

where

$$\hat{\rho}_5^{(\pm)}(\mathbf{x}) = F_A \sum_{j=1}^{A} \tau_\pm(j) \; \vec{\sigma}(j) \cdot \left[\frac{\hat{\mathbf{p}}(j)}{M}, \; \delta^3(\mathbf{x} - \mathbf{x}_j) \right]_{sym} \tag{2.13}$$

$$\hat{\mathbf{A}}^{(\pm)}(\mathbf{x}) = F_A \sum_{j=1}^{A} \tau_\pm(j) \; \vec{\sigma}(j) \, \delta^3(\mathbf{x} - \mathbf{x}_j) \tag{2.14}$$

$$\hat{\phi}_{ps}^{(\pm)}(\mathbf{x}) = -\frac{1}{k^2 - m_\pi^2} \, \nabla \cdot \hat{\mathbf{A}}^{(\pm)}(\mathbf{x}) \tag{2.15}$$

$$\hat{\rho}_{ps}^{(\pm)}(\mathbf{x}) = \frac{1}{i} \left[\hat{H}_{nucl} \, , \, \hat{\phi}_{ps}^{(\pm)}(\mathbf{x}) \right] \tag{2.16}$$

with $\hat{H}_{nucl}$ standing for the full nonrelativistic nuclear hamiltonian calculated in the framework of the same hadronic $\sigma - \omega$ model developed here.

41

It is easy to see in the momentum space representation of the current that a combination of all the terms in (2.11) except the first one satisfies PCAC through order $O(1/M)^1$. Thus one needs only to check whether $\hat{\rho}_5^{(\pm)}(x)$ satisfies PCAC to the same order in M. In fact, its commutator with the nuclear hamiltonian does not vanish because of a derivative term in the axial charge operator, which does not commute with potentials arising due to exchange of various mesons. The presence of the isoscalar potentials (due to σ-exchange and, after including ω-meson, due to ω-exchange), which are of order $O(1)$ in inverse nucleon mass, breaks PCAC for the one-body axial current to order $O(1/M)$:

$$\left[\hat{H}_{nucl}, \hat{\rho}_5^{(\pm)}\right] \simeq \left[V_\sigma + V_\omega, \hat{\rho}_5^{(\pm)}\right] = O(\frac{1}{M}) \neq O(m_\pi^2) + O(\frac{1}{M^2}) \qquad (2.17)$$

However, partially conserved chiral symmetry is the most important symmetry to be satisfied by any low-energy effective hadronic theory [29]. It must hold in the present many-body problem. Hence, consideration of corresponding two-body axial currents of order $O(1/M)$, required to preserve PCAC in the theory, is necessary in the present model. These axial MEC are indeed present in the linear realization of the $\sigma - \omega$ model. They will be calculated explicitly below and shown to rescue the PCAC relation in coordinate space (see Appendix A). Two-body exchange axial current operators, which must represent the most significant correction to the one-body operators, will be the focus of the present work. Three-body effects are omited, following the standard nuclear physics arguments that they are negligible [5].

Next, one has to write down the amplitude for π-production by the axial current on a nucleon to the lowest order in the interaction constant ($O(g)$). The relevant

---

[1] It is sufficient here to consider the momentum space relation because one does not need to use any specific form for the wave function to obtain this result.

π^β k, α

q

π^β q   k, α

π^β q   k, α
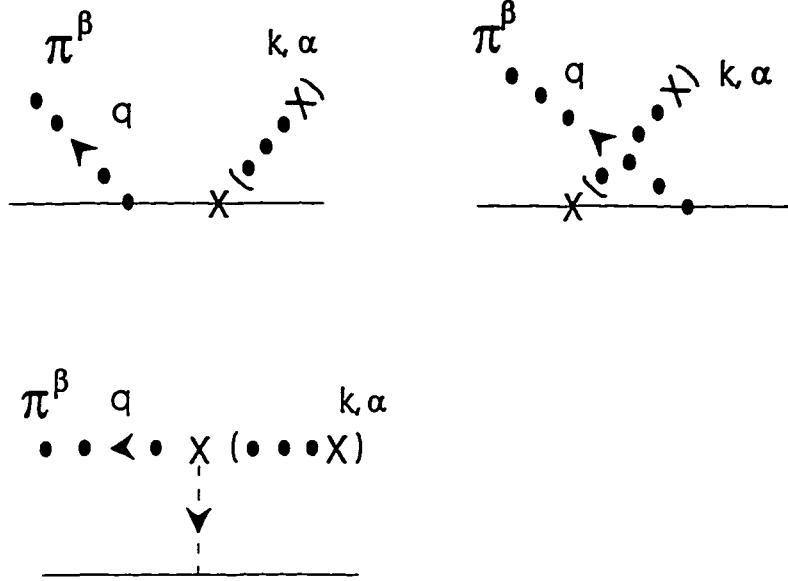
Figure 2.4: Lowest order amplitude for pion production by the axial current on a single nucleon in the linear realization of the $\sigma - \omega$ model.

diagrams are shown in Figure 2.4. They correspond to the amplitude:

$$
\begin{aligned}
iM_\mu^{\alpha\beta}(\pi) \;=\; & ig\,\bar{u}(p_1')\Bigg[\; \frac{\tau^\beta\tau^\alpha}{2}\,\frac{-1}{(\not{p}_1'+\not{q})+M}\left(\gamma_\mu + 2M\frac{k_\mu}{k^2 - m_\pi^2}\right) \\
& +\; \frac{\tau^\alpha\tau^\beta}{2}\left(-\gamma_\mu + 2M\frac{k_\mu}{k^2 - m_\pi^2}\right)\frac{-1}{(\not{p}_1-\not{q})+M} \\
& +\; \frac{\delta^{\beta\alpha}}{(l^2 - m_s^2)}\left(-2q_\mu + k_\mu - (m_s^2 - m_\pi^2)\frac{k_\mu}{k^2 - m_\pi^2}\right)\Bigg]u(p_1) \quad (2.18)
\end{aligned}
$$

Again, the π-production amplitude satisfies PCAC for the on-mass-shell pion and nucleon. This fact adds to the confidence that all the diagrams contributing to the considered order in the interaction constant has been included in the analysis. Consideration of PCAC for the amplitude in the full many-body problem, while preserving π-pole dominance and the Goldberger-Treiman relation, forces one now to renormalize *all* axial current vertices by the same F_A. For soft-pion production at the

43

threshold one obtains the following result:

$$T_\mu^{\alpha\beta} \simeq \frac{1}{2M} M_\mu^{\alpha\beta} \simeq iF_A \frac{g}{M} \epsilon_{\alpha\beta\gamma} \frac{\tau^\gamma}{2} \delta_{\mu 0} \tag{2.19}$$

where $g \equiv g_\pi$ is the pion-nucleon interaction constant. Definitions of various amplitudes in terms of scattering S-matrix have been provided in Equations (1.9) and (1.10).

Comparing this formula with the result of Kubodera, Delorme and Rho [9]

$$T_\mu^{\alpha\beta} = -i\frac{\sqrt{2}}{F_\pi} \epsilon_{\alpha\beta\gamma} \frac{\tau^\gamma}{2} \delta_{\mu 0} \tag{2.20}$$

$$= i\frac{1}{F_A} \frac{g}{M} \epsilon_{\alpha\beta\gamma} \frac{\tau^\gamma}{2} \delta_{\mu 0} \tag{2.21}$$

obtained using the current algebra approach, one can see that the two results coincide except for an extra F_A^2 factor in the amplitude derived in the present work. This discrepancy originates from the different techniques used for calculating the result.[2] The fact that the correct form of the Goldberger-Treiman relation, with F_A present in it, has been used throughout the present calculation, leads one to believe that an extra F_A^2 factor should be actually present in the expression for the π-production amplitude. This extra factor will be inherited as well in the formulae for the AXC derived below. The numerical difference between the two results is about 50% - the order of magnitude to which corrections due to the presence of the AXC effects have been tested in nuclei so far.

Next, the analysis of the interaction of the axial current with the two-nucleon system is performed. All corresponding diagrams of the lowest order in the interaction constants ($O(g^2)$ and $O(g_v^2)$) are shown in Figures 2.5 and 2.6. Amplitudes corresponding to both figures satisfy PCAC, as they should. At the same time, one notes that separate nonzero contributions coming from the first line (involving the

---

[2]The difference lies in the method of calculation of the corrections of higher order in m_π/M and Q/M, which will not be discussed here.

44
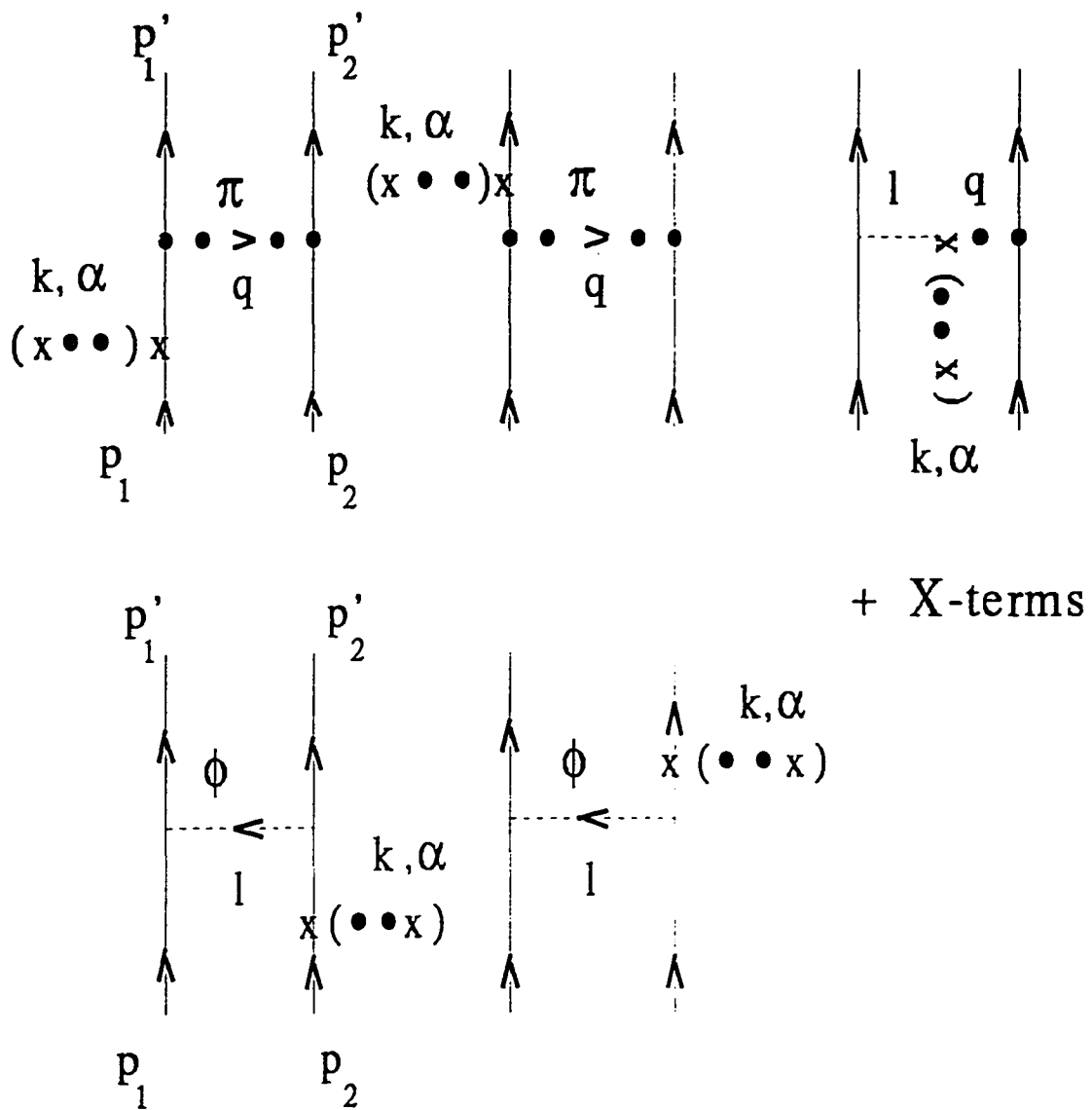
Figure 2.5: Lowest order amplitude for the axial current interaction with the two-nucleon system in the linear realization of the σ-model.

45

pion production amplitude) and the second line of Figure 2.5 have to cancel each other to arrive at the PCAC result. It again shows that the pion and scalar meson contributions have to be carefully balanced in the linear σ-model calculations. They are separated in the non-linear realization of the model discussed in the next Chapter. When identifying AXC from the considered interaction amplitude according to the
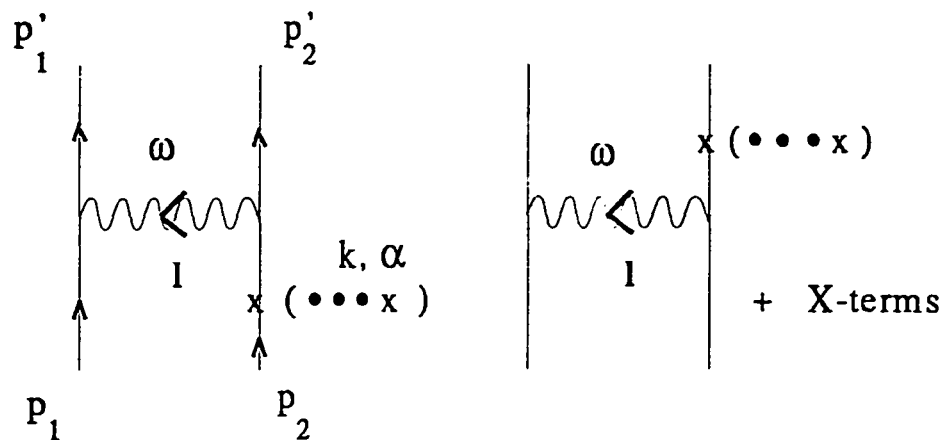
Figure 2.6: Additional lowest order diagrams for the axial current interaction with the two-nucleon system in the $\sigma - \omega$ model.

formula (1.11), one has to keep only antinucleonic parts of the nucleon propagators in the amplitude to avoid double counting of terms [6].

One remembers that PCAC for the single-nucleon axial current requires the presence of two-body currents in the model. Actual calculation of the interaction amplitudes of Figures 2.5 and 2.6 in the linear $\sigma - \omega$ model, followed by the axial current identification and non-relativistic reduction, shows that *there are indeed space*

46

components of axial meson exchange currents of order O(1/M) present in this model:

$$\mathbf{A}^{(\pm)}(\pi + \sigma) \simeq \frac{g^2}{M} \tau_{\pm} \frac{1}{\mathbf{l}^2 + m_s^2} \left[\frac{\vec{\sigma}(1) \cdot \mathbf{q}}{\mathbf{q}^2 + m_\pi^2} \left(1 - \mathbf{q} - \mathbf{k} \frac{\mathbf{l}^2 + m_\pi^2}{\mathbf{k}^2 + m_\pi^2} \right) \right.$$
$$\left. + \frac{\mathbf{k}}{\mathbf{k}^2 + m_\pi^2} \vec{\sigma}(1) \cdot \mathbf{q} \right] + X - \text{terms} \quad (2.22)$$

$$\mathbf{A}^{(\pm)}(\omega) \quad \simeq \quad \frac{g_v^2}{M} \tau_{\pm} \frac{\mathbf{k}}{\mathbf{k}^2 + m_\pi^2} \frac{\vec{\sigma}(2) \cdot \mathbf{l}}{\mathbf{l}^2 + m_v^2} \quad + \quad X - \text{terms} \quad (2.23)$$

where g_v and m_v are the $\omega{-}N$ interaction constant and ω-meson mass, correspondingly. The X-terms designate contributions from the set of diagrams with the two nucleons interchanged.

It is shown in Appendix A that the presence of these two spatial AXC makes the respective operator PCAC equation in coordinate space satisfied through order O(1/M), when proper potentials arising from the σ- and ω-meson exchange are included in the analysis.

Corrections to the axial-charge operator are not required for satisfying the PCAC equation. Nevertheless, they can be explicitly calculated in the present model. The first non-vanishing term in the axial-charge operator is the pion contribution of order O(1/M²) identified from the same set of the lowest-energy diagrams in Figure 2.5:

$$A_0^\alpha(\mathbf{k}, \mathbf{q}) \simeq -\left(\frac{g}{2M} \right)^2 [\tau(1) \times \tau(2)]^\alpha \frac{\vec{\sigma}(2) \cdot \mathbf{q}}{\mathbf{q}^2 + m_\pi^2} + X - \text{term} \quad (2.24)$$

This is a familiar result [9, 17]. The formula from previous work is reproduced again up to a factor of $F_A{}^2(0)$ inherited directly from the π-production amplitude.

There are also terms of order O(1/M²) in the axial charge due to the exchange of isoscalar (Lorentz scalar and vector) mesons. However, in view of the same interaction range arguments that led to the pion-pole dominance hypothesis, these contributions are expected to be much smaller than the main π-exchange charge correction (2.24).

47

Now one can return to the question of reconciling the $\sigma - \omega$ model with the MFT results of QHD I and take m_s to be very large. Successful applications of QHD I are then rescued. The result for the axial current π-production on a nucleon still holds in this limit. The σ-meson potential and $A^{(\pm)}(\pi + \sigma)$ of equation (2.22) vanish. However, the second piece $A^{(\pm)}(\omega)$ (2.23) of the AXC of order $O(1/M)$ due to the ω-meson exchange *is still present*, and PCAC is satisfied with the isoscalar potential and AXC coming from the ω-meson exchange only.

It is useful to summarize the advantages and disadvantages of using the linear realization of the $\sigma - \omega$ model to describe AXC in nuclei. It is very important that this model preserves PCAC. This helps one to determine the correct set of diagrams for each of the processes considered and, when the π-pole dominance requirement and correct Goldberger-Treiman relation are incorporated in the model, to perform the renormalization of all axial current vertices in the full theory unequivocally. This renormalization of the axial-current vertices of the theory introduces an extra factor F_A^2 into the results for π-production and AXC. The linear realization of the model allowed derivation of the low-energy result (2.19) for the π-production amplitude, as well as calculation of the spatial AXC (2.22) and (2.23) of order $O(1/M)$ due to the isoscalar mesons exchange, and the axial exchange charge correction (3.19) due to pion exchange.

Among disadvantages of the present realization of the model is the fact that to ensure chiral invariance of the theory, sensitive cancellations of large quantities have to occur in the amplitudes (for example, contributions of the sets of diagrams in the first and second rows in Figure 2.5 have to cancel each other's non-zero contributions to arrive at the PCAC result). Also the soft-pion limit is not built into the theory because of the non-derivative character of the $\pi-$ N coupling in this model. These were the major considerations that brought to existance the non-linear realization of the σ-model [36]. One additional problem that is encountered when building a

48

consistent model for calculating AXC starting from the σ-model, is how to include the phenomenological low-mass scalar field in the model. There seems to be no easy way to perform this in the linear realization of the $\sigma - \omega$ model. The low-mass scalar field can be obtained here only as a dynamic resonance in the two-pion exchange, whose contribution to the two-body axial currents is not simple to calculate. All these difficulties motivate one to perform the transition to the non-linear realization of the model and to compare the results obtained in the two approaches.

Chapter 3

Non-linear realization of the $\sigma - \omega$ model

Acceptance of the non-linear realization of the $\sigma - \omega$ model to be the framework for calculating AXC solves all the difficulties listed in the end of the previous chapter. This is a natural approach to the present problem. In addition, corrections to the "customary" (2.10) single-body axial nuclear current, obtained in the non-linear model, are simpler than those calculated within the linear model. In the present work these corrections are included in the analysis of some semileptonic weak transitions in a few selected nuclei. The ω-meson is introduced in the lagrangians of both realizations of the $\sigma - \omega$ model through the same procedure, so one can forget about this meson for a moment, returning to calculating its contributions later when discussing axial exchange currents in the non-linear model[1].

The non-linear (Weinberg) realization of the σ-model can be obtained in either one of two independent ways. In the first derivation scheme, one assumes the point

---

[1] The ω-meson does not interact with the axial current or pions directly. Hence it makes no contribution to the axial-current — one-nucleon interaction or pion production by the axial current on a nucleon to the lowest order in the interaction constant.

50

of view that chiral symmetry is not realized in a customary way which would provide linear relations between various fields and their commutators with the symmetry generators. Instead, chiral symmetry here implies relations between processes involving different number of pions [31]. In this approach one makes no recourse to the linear realization of the σ-model, deriving the transformation laws for various fields from the consideration of the $SU(2)_L \times SU(2)_R$ symmetry group algebra. The corresponding lagrangian of the model is then built out of the chiral-invariant combinations of fields and their derivatives.

In the second derivation scheme [36], one obtains the non-linear realization of the σ-model upon carrying out a chiral rotation of the field variables in the linear realization lagrangian (2.4) and the axial current operator (2.5). Utilization of the chirally transformed fields as independent particle variables ensures that the lagrangian for the new fields does not entail sensitive cancellations in the amplitudes as before. The intrinsic connection between the two realizations of the σ-model becomes very lucid in this way of derivation. All that is done here is the redefinition of fields and consideration of the same problem in terms of the new degrees of freedom. The two models are equivalent in the chiral limit $m_\pi^2 \to 0$. The consequences of this redefinition are, however, dramatic.

In the present work the second method of obtaining the non-linear σ-model lagrangian is utilized. One rewrites the meson − nucleon interaction term, introducing a position-dependent chiral rotation angle $\vec{\Omega} = \vec{\Omega}(x)$ [2] through

$$M - g\phi + ig\gamma_5 \vec{\tau} \cdot \vec{\pi} \equiv \sqrt{(M - g\phi)^2 + g^2 \vec{\pi}^2} \; e^{\frac{i}{2}\vec{\Omega} \cdot \vec{\tau} \gamma_5} \tag{3.1}$$

The quantity under the square root is chirally invariant because it is equivalent to an explicitly chiral-invariant combination $g^2 (\sigma^2 + m_\pi^2)$ (see equation (2.3) for the definition of the ϕ-field). Next, one defines a new baryon field N to be

$$N \equiv e^{\frac{i}{2}\vec{\Omega} \cdot \vec{\tau} \gamma_5} \psi \tag{3.2}$$

51

so that

$$\bar{\psi}\left[M - g\phi + ig\gamma_5\vec{\tau}\cdot\vec{\pi}\right]\psi = \sqrt{\left(M - g\phi\right)^2 + g^2\vec{\pi}^2}\,\bar{N}N \qquad (3.3)$$

Thus, the π-N pseudoscalar interaction diasappears from the lagrangian. The left hand side of the previous equation is invariant under the chiral rotation and the square root is also invariant in the chiral limit. Thus the combination $\bar{N}N$ also satisfies partial chiral invariance. This fact will be used later when introducing a phenomenological low-mass scalar field in the model as a chiral singlet.

One more new field can be defined

$$\vec{\xi} \equiv \frac{1}{(M - g\phi) + \sqrt{(M - g\phi)^2 + g^2\vec{\pi}^2}}\,g\vec{\pi} \qquad (3.4)$$

and new pion π' and scalar ϕ' fields introduced as

$$\sqrt{(M - g\phi)^2 + g^2\vec{\pi}^2} \equiv M - g\phi'$$

$$\vec{\xi} \equiv \frac{g}{2M}\vec{\pi}' \qquad (3.5)$$

Upon performing the transformation to the newly defined fields, the lagrangian (2.4) takes the form [2]

$$\mathcal{L} = \bar{N}\left\{i\gamma^\lambda\partial_\lambda - M + g\phi' + \frac{1}{1 + \xi^2}\left[\gamma^\lambda\gamma_5\,\vec{\tau}\cdot\partial_\lambda\vec{\xi} - \gamma^\lambda\,\vec{\tau}\cdot(\vec{\xi}\times\partial_\lambda\vec{\xi})\right]\right\}N$$

$$+ \frac{1}{2}\mathcal{R}\left[\mathcal{R}\,\partial^\lambda\vec{\pi}'\cdot\partial_\lambda\vec{\pi}' - m_\pi^2\vec{\pi}^2\right] + \frac{1}{2}\left[\partial^\lambda\phi'\partial_\lambda\phi' - m_s^2\phi'^2\right] + (m_s^2 - m_\pi^2)\left[F\phi'^3 - \frac{1}{2}F^2\phi'^4\right]$$

where

$$\mathcal{R} = \frac{1 - 2F\phi'}{1 + \xi^2}\,, \quad F \equiv \frac{f}{m_\pi} \equiv \frac{g}{2M} \quad \text{and} \quad \vec{\xi} \equiv F\vec{\pi}' \qquad (3.6)$$

The new fields in the lagrangian represent: N - nucleons, $\vec{\pi}$ - pions, and ϕ' - scalar mesons with the same masses as in the linear realization of the σ-model. This particle content of the theory can be identified upon setting the coupling constant $F = 0$. All

52

pion couplings now have at least one derivative of the π field, so the soft-pion limit is built into the model explicitly.

One can define yet another generalized scalar field χ with an equation

$$m_s \phi' \equiv \chi \tag{3.7}$$

The above σ-model lagrangian is chirally invariant (when $m_\pi = 0$) for *any* value of m_s. It is possible to take the formal limit $m_s \to \infty$. Then

$$
\begin{aligned}
\mathcal{L}(N, \pi', \chi) &= \bar{N}\left\{ i\gamma^\lambda \partial_\lambda - M + \frac{1}{1+\xi^2}\left[\gamma^\lambda \gamma_5 \, \vec{\tau} \cdot \partial_\lambda \vec{\xi} - \gamma^\lambda \, \vec{\tau} \cdot (\vec{\xi} \times \partial_\lambda \vec{\xi}) \right] \right\} N \\
&\quad + \frac{1}{2}\mathcal{R}\left[\mathcal{R} \, \partial^\lambda \vec{\pi}' \cdot \partial_\lambda \vec{\pi}' \right] - \frac{1}{2}\chi^2
\end{aligned}
$$

where

$$\mathcal{R} = \frac{1}{1+\xi^2} \tag{3.8}$$

The scalar field χ decouples from the problem. There are no strong non-linear coupling terms involving the scalar field left in the model. This way the σ-model development can be reconciled with the results obtained in the QHD I model.

Nevertheless, again in this work the $\sigma - \omega$ model will be developed keeping m_s a general parameter. The limit $m_s \to \infty$ is postponed until later in the calculation, prior to obtaining the final results. Some of the intermediate results derived this way will be used later for analyzing contribution of the phenomenological low-mass scalar field to the axial exchange currents.

To the first order in the interaction constant ($O(g)$ or $O(F)$) one then arrives at the following interaction lagrangian:

$$
\begin{aligned}
\mathcal{L}_{\text{int}} &= g\phi' \bar{N} N + \bar{N}\gamma^\lambda \gamma_5 \, \vec{\tau} \cdot \partial_\lambda \vec{\xi} N - \bar{N}\gamma^\lambda \, \vec{\tau} \cdot (\vec{\xi} \times \partial_\lambda \vec{\xi}) N \\
&\quad - 2F \phi' \left(\partial^\lambda \vec{\pi}' \cdot \partial_\lambda \vec{\pi}' - \frac{1}{2} m_\pi^2 \vec{\pi}^2 \right) + (m_s^2 - m_\pi^2) F \phi'^3
\end{aligned} \tag{3.9}
$$

53

$$i\,g$$

$$-F\,\slashed{q}\,\gamma_5\tau^\alpha$$

$$F^2(\slashed{q}+\slashed{k})\,\varepsilon_{\alpha\beta\gamma}\tau^\gamma$$

$$i\,4F\left(q_1\cdot q_2+\frac{m_\pi}{2}\right)\delta_{\alpha\beta}$$

$$i\,6(m_s^2-m_\pi^2)\,F$$
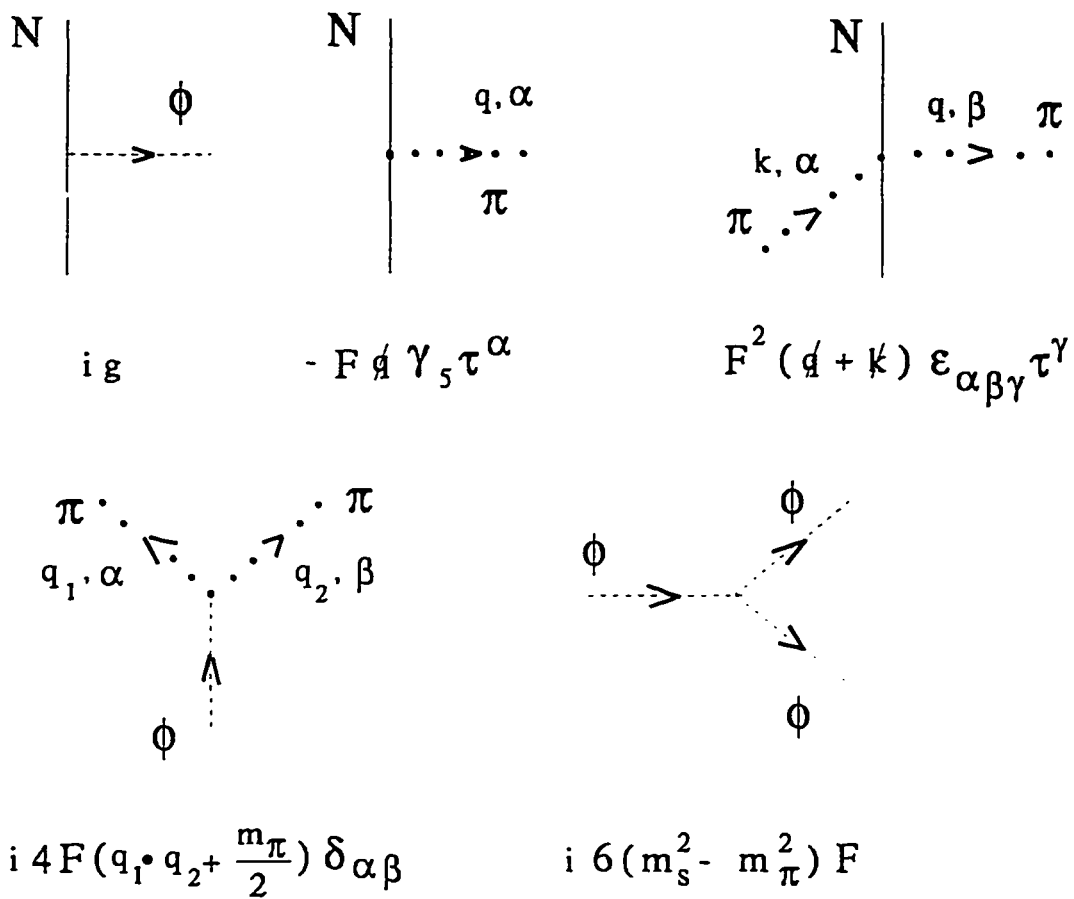
Figure 3.1: Strong interaction vertices for the non-linear realization of the $\sigma-\omega$ model.

All the corresponding strong interaction vertices are depicted in Figure 3.1. One can transform also the axial Noether's current to the new fields, obtaining to the lowest order in the interaction constant

$$A_\mu^\alpha \simeq \bar{N}\gamma_5\gamma_\mu\frac{\tau^\alpha}{2}N - F\epsilon_{\alpha\beta\gamma}\,\bar{N}\gamma_\mu\pi'^\beta\tau^\gamma N + 2\phi'\,\partial_\mu\pi'^\alpha - \frac{1}{2F}\,\partial_\mu\pi'^\alpha + O(F)$$

$$(3.10)$$

The second term, which is of order O(F), has been included in the current because the tree-diagrams for the processes considered here, which contain this term, involve one less π—N vertex of order O(F). The axial current vertices are shown in Figure 3.2. Summarizing, after the chiral transformation of the lagrangian one has a different set of effective degrees of freedom, all the vertices have changed, and hence, there is a new set of diagrams for each process considered.
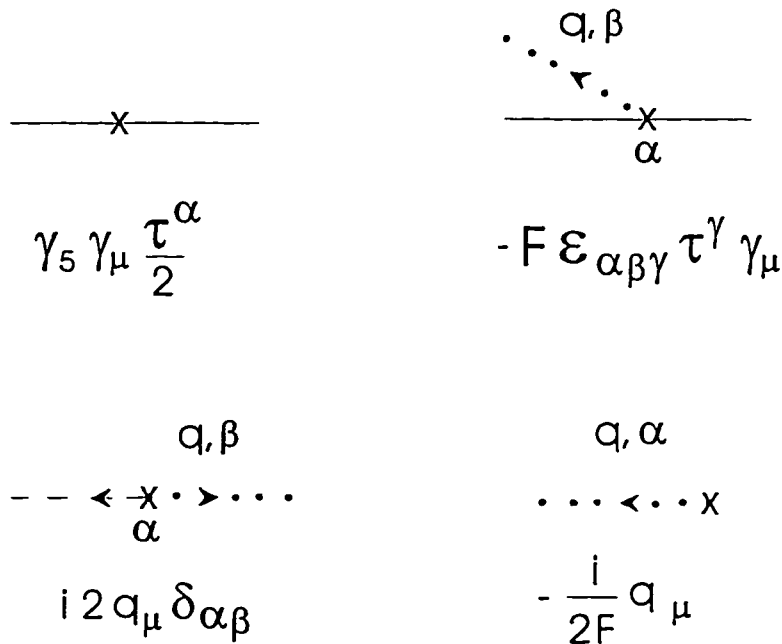
Figure 3.2: Lowest order axial-current vertices in the non-linear realization of the $\sigma - \omega$ model.

Following the general analysis scheme outlined in the introduction, one first considers the axial current interaction with a single nucleon. The tree-level diagrams (which are of order $O(g)$ in the interaction constant) have the same appearance as in the linear realization of the σ-model (see Figure 1.4). However, since the vertices of the theory have changed, the interaction amplitude assumes a different form:

$$iM_\mu^\alpha(1) = \bar{u}(p_1') \left[\gamma_5 \gamma_\mu \frac{\tau^\alpha}{2} + F \not{k} \gamma_5 \tau^\alpha \frac{1}{k^2 - m_\pi^2} \frac{1}{2F} k_\mu \right] u(p_1) \tag{3.11}$$

It is easy to see that, just as in the linear realization, PCAC is satisfied again for the on-mass-shell nucleon. However, in the present case one does not have to use the Dirac equation for demonstrating PCAC, so the symmetry is satisfied for the off-mass-shell nucleon as well. This fact can be illustrated by pulling out of the Dirac spinors in the nuclear matrix element an operator, which becomes a projection operator in the chiral limit $m_\pi^2 \to 0$

$$iM_\mu^\alpha(1) = \frac{\tau^\alpha}{2} \underbrace{\left(g_{\mu\nu} - \frac{k_\mu k_\nu}{k^2 - m_\pi^2} \right)}_{\text{projector}} \bar{u}(p_1')\gamma_5\gamma^\nu u(p_1) \tag{3.12}$$

The bracketed operator projects out a four-vector that is orthogonal to k_μ in the chiral limit, thus ensuring that the interaction amplitude satisfies PCAC *identically* in this realization of the model. Hence the corresponding one-body axial current, identified from this amplitude according to (1.6),

$$A_\mu^\alpha(1) = -\frac{1}{2M} F_A \frac{\tau^\alpha}{2} \left(g_{\mu\nu} - \frac{k_\mu k_\nu}{k^2 - m_\pi^2} \right) \bar{u}(p_2) \gamma_5\gamma^\nu u(p_1) \tag{3.13}$$

satisfies PCAC identically by itself in momentum space. The result for the pion — axial-current vertex renormalization by F_A in the full theory is obtained here exactly as in the linear model before.

When performing the non-relativistic reduction of this axial current, PCAC should be satisfied in each order in $1/M$, and, due to the presence of the projection

56

operator in the current, all the relevant terms should come from the one-body axial current alone. For the axial current interaction with a free nucleon the transferred energy k_0 is of order $O(1/M)$. It proves useful to consider the non-relativistic one-body current with the next-to-leading order relativistic correction included

$$J_5^{(\pm)0}(1) \;=\; F_A \, \tau_\pm \left[\overbrace{\frac{\vec{\sigma} \cdot \mathbf{P}}{2M}}^{1} + \overbrace{\frac{k_0}{k^2 - m_\pi^2} \vec{\sigma} \cdot \mathbf{k}}^{2} - \overbrace{\frac{k_0^2}{k^2 - m_\pi^2} \frac{\vec{\sigma} \cdot \mathbf{P}}{2M}}^{5} \right] \qquad (3.14)$$

$$\vec{J}_5^{(\pm)}(1) \;=\; F_A \, \tau_\pm \left[\underbrace{\vec{\sigma}}_{3} + \underbrace{\frac{\mathbf{k}}{k^2 - m_\pi^2} \vec{\sigma} \cdot \mathbf{k}}_{4} - \underbrace{\frac{\mathbf{k}}{k^2 - m_\pi^2} k_0 \frac{\vec{\sigma} \cdot \mathbf{P}}{2M}}_{6} \right] \qquad (3.15)$$

where $\mathbf{P} = \mathbf{p} + \mathbf{p}'$. The terms 1 through 4 comprise the familiar non-relativistic nuclear one-body axial current [2]. As is well known, the combination of terms 2, 3 and 4 satisfies PCAC to order $O(1/M)$. One can see that if the customary first term is included in the analysis, its contribution to the PCAC equation is of order $O(1/M^2)$. Then to facilitate PCAC satisfaction to this order, one additional relativistic correction term (term 6) must also be considered:

$$\sim k_0 \frac{\vec{\sigma} \cdot \mathbf{P}}{2M} + \frac{\mathbf{k}^2}{k^2 - m_\pi^2} k_0 \frac{\vec{\sigma} \cdot \mathbf{P}}{2M} \simeq \left(1 - \frac{\mathbf{k}^2}{k^2 + m_\pi^2} \right) k_0 \frac{\vec{\sigma} \cdot \mathbf{P}}{2M}$$

$$= \frac{m_\pi^2}{k^2 + m_\pi^2} k_0 \frac{\vec{\sigma} \cdot \mathbf{P}}{2M} = O(m_\pi^2) \qquad (3.16)$$

The contribution of term 5 to the PCAC equation is suppressed by two extra powers of $1/M$. This term is not needed to satisfy PCAC to the considered order in $1/M$ and, thus, can be safely neglected.

Let us discuss in more detail the transition to the analysis of the axial current operators in the full many-body nuclear problem. Transformation from the momentum space result for a free nucleon to the axial current operators in coordinate space involves one subtle point. These operators are going to be used in the analysis of weak processes with nuclei, rather than with free nucleons only. Some quantities in the momentum space current are small for on-mass-shell nucleons but, in principle,

can introduce a significant contribution when nuclear matrix elements of the current operators are considered. For instance, k_0 is of order $O(1/M)$ for a free nucleon, but it might not be small in some nuclear processes. Since the treatment here started with the consideration of the axial-current — free-nucleon interaction amplitude in momentum space, one has the freedom to include these terms in the current operator in coordinate space, or to leave them out. In the present work it is chosen to consider such terms only when their presence facilitates satisfaction of PCAC to considered order in $O(1/M)$. Then, following the reasoning of the previous paragraph, one is forced to include in the analysis a new leading relativistic correction to the customary axial nuclear currents from (2.10), which helps preserving PCAC to order $O(1/M^2)$ [2]

$$\delta A^{(\pm)}(1) \simeq - F_A \, \tau_\pm \, \frac{\mathbf{k}}{k^2 - m_\pi^2} \, k_0 \, \frac{\vec{\sigma} \cdot \mathbf{P}}{2M} \qquad (3.17)$$

The corresponding operator in coordinate space will be included in the analysis of weak processes with nuclei. It should be noted, however, that effects of this correction are small because $k_0/2M$ is generally small in the weak processes. The procedure for calculating effects of the relativistic correction will be presented in the next chapter.

Since PCAC holds now for *any* particular wave function chosen to calculate the matrix element, it will also hold for the one-body axial current derived in this model *as an operator equation* in coordinate space. Thus, *no two-body currents are required by PCAC to be present in this model.*

Indeed, through a direct reduction of the interaction amplitude of the axial current with the two-nucleon system performed below, *it has been shown explicitly that there are in fact no axial MEC of order O(1/M) present in the non-linear model.* This result demonstrates the model-dependent character of the way one splits the whole many-body problem corrections to the one-body analysis into the one-body relativistic corrections to the customary current and MEC effects. One would like to find a model where the semileptonic weak interactions have the simplest description.

58

As the preceding analysis demonstrates, corrections to the one-body axial current become simple when considering the non-linear realization of the $\sigma - \omega$ model.

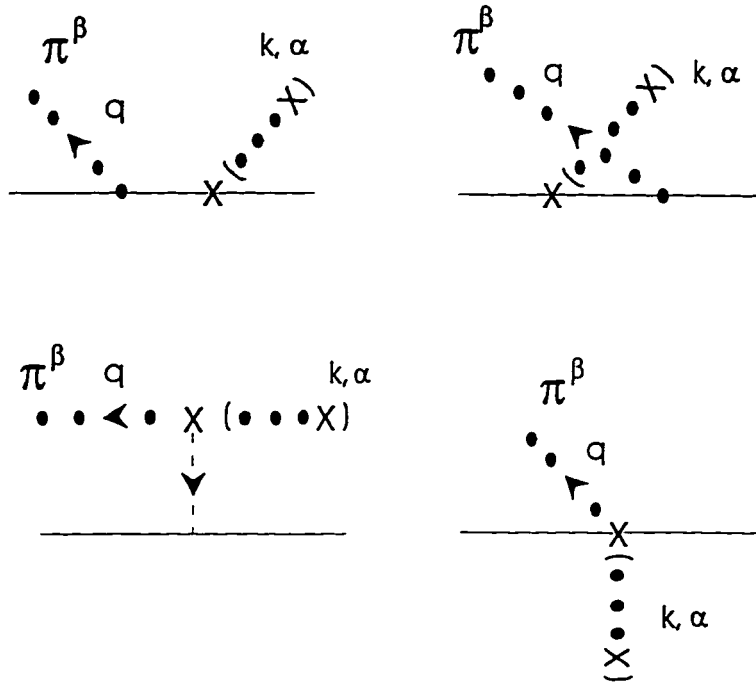Figure 3.3: Lowest order amplitude for pion production by the axial current on a single nucleon in the non-linear realization of the $\sigma - \omega$ model.

As a second step of the investigation. one considers the axial current π-production on a nucleon. A set of diagrams contributing to this process at the tree level (to first order in the interaction constant) is presented in Figure 3.3. The corre-

sponding amplitude has the following form

$$
\begin{aligned}
iM_\mu^{\beta\alpha}(\pi) &= -iF\,\bar{u}(p')\left\{ \slashed{q}\gamma_5 \frac{1}{(\slashed{p}_1+\slashed{q})-M}\gamma_5\left(\gamma_\mu-\slashed{k}\frac{k_\mu}{k^2-m_\pi^2}\right)\frac{\tau^\alpha\tau^\beta}{2}\right. \\
&+ \left(\gamma_\mu-\slashed{k}\frac{k_\mu}{k^2-m_\pi^2}\right)\gamma_5\frac{1}{(\slashed{p}_1-\slashed{q})-M}\gamma_5\,\slashed{q}\frac{\tau^\beta\tau^\alpha}{2} \\
&+ \delta^{\beta\alpha}\frac{2M}{(k-q)^2-m_s^2}\left[2q_\mu+2(-k\cdot q+\frac{m_\pi^2}{2})\frac{k^\mu}{k^2-m_\pi^2}\right] \\
&+ \left. i\epsilon_{\alpha\beta\gamma}\frac{\tau^\gamma}{2}\left[(\slashed{q}+\slashed{k})\frac{k^\mu}{k^2-m_\pi^2}-2\gamma_\mu\right]\right\}u(p)
\end{aligned}
\tag{3.18}
$$

This amplitude satisfies PCAC for the on-mass-shell particles, as should be the case. It also reproduces the same low-energy result (2.19) for soft-pion ($m_\pi^2 = 0$) production by the axial current at the threshold as has been obtained in the linear realization of the σ-model. These two facts provide confidence that all the relevant diagrams have been included into the analysis. The argument for renormalization of all the axial current vertices by F_A follows here exactly the linear $\sigma - \omega$ model reasoning.

The final step of the general analysis scheme is to consider the interaction of the axial current with the two-nucleon system. All the tree-level diagrams of the non-linear σ-model, contributing to this process to the first nonvanishing order in the interaction constant ($O(g^2)$), are shown in Figure 3.4.

It is interesting to observe that the sets of diagrams in the first and the second rows of Figure 3.4 now satisfy PCAC *separately*, each by itself. Graphs including pion-production and those coming from the scalar meson exchange do not have to be considered together any more. This will allow introducing the low-mass scalar field in the analysis, whose contribution to the AXC calculation diagrams looks exactly the same as the set of digrams in the second line of Figure 3.4.

Now one recalls that in order not to destroy successful mean field theory results of QHD I by the large cubic and quartic terms in the lagrangian, one has to consider the limit of a very large scalar meson mass ($m_s^2 \rightarrow \infty$). In this limit the three diagrams
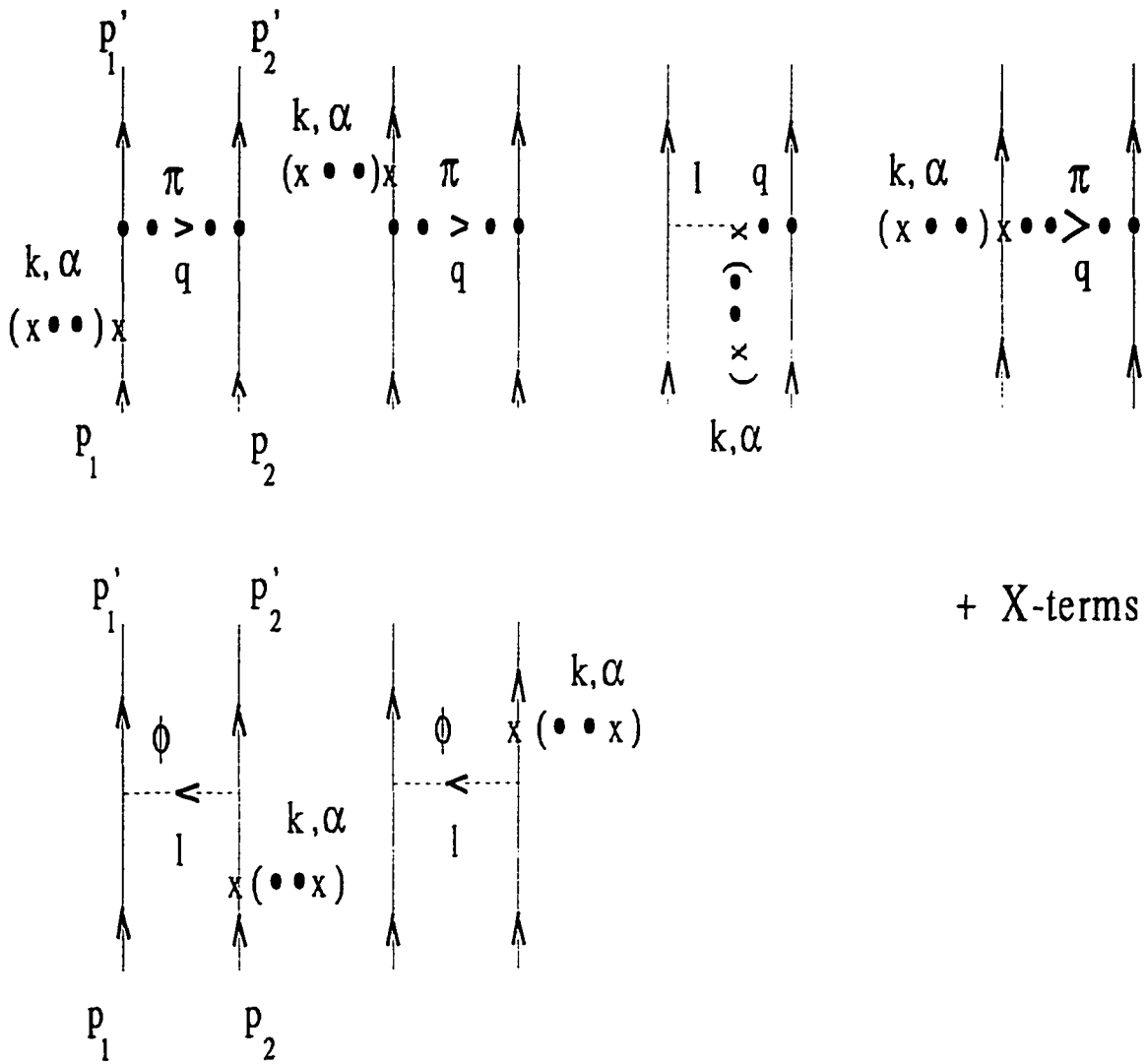
60

Figure 3.4: Lowest order amplitude for the axial current interaction with the two-nucleon system in the non-linear realization of the σ-model.

61

of Figure 3.4 that include the scalar meson propagator disappear, simplifying the analysis. Performing $1/M$ power counting, one shows that the contribution of the last diagram in the first line is larger by an order of M^2 than the contribution from the first two diagrams. One can note that this term also satisfies PCAC separately, as it should. This last diagram provides the leading pion exchange axial charge term of order $O(1/M^2)$, which has exactly the same form as the one in equation (2.24) in the linear realization of the $\sigma - \omega$ model. The corresponding charge operator in coordinate space is

$$
\begin{aligned}
A_0^\alpha(2)(x_1, x_2, k) \simeq & -F_A \frac{g^2}{4\pi} \left(\frac{m_\pi}{2M}\right)^2 [\tau(1) \times \tau(2)]^\alpha \\
& \times \left(1 + \frac{1}{x_\pi}\right) \frac{e^{-x_\pi}}{x_\pi} \left[e^{ik \cdot x_1} \vec{\sigma}(2) \cdot \hat{r} + e^{ik \cdot x_2} \vec{\sigma}(1) \cdot \hat{r} \right] \quad (3.19)
\end{aligned}
$$

where

$$
x_\pi \equiv m_\pi |r|, \quad r \equiv x_1 - x_2
$$

This is a familiar result [9,17] again up to the same factor of $F_A{}^2(0)$. This charge operator is the second correction to the one-body current anlysis of the relativistic many-body problem of semileptonic weak processes with nuclei that is considered in this work. The contribution of the investigated terms to the spatial components of AXC is of order $O(1/M^3)$ and thus can be neglected.

The ω-meson is included in the present analysis exactly as this has been done in the linear realization of the $\sigma - \omega$ model. The chiral rotation performed does not influence the ω-field, thus the $\omega-N$ vertex is exactly the same as before. A set of diagrams for calculating the ω-exchange axial current also looks the same (see Figure 2.6).

And at last an additional phenomenological low-mass scalar field σ' can be introduced in the present model as a chiral singlet. Since the $\bar{N}N$ combination is chirally symmetric, the scalar-meson—nucleon interaction term of the form $g_\sigma \sigma' \bar{N} N$

is also chirally invariant. Such an interaction does not upset the QHD I calculations, so one can assign the new scalar field the mass $m_\sigma = 550$ MeV and the interaction constant $g_\sigma^2/4\pi \simeq 7.3$ required in QHD I or in the phenomenological N-N potential. The same set of diagrams in the second line of Figure 3.4, with the new mass and interaction constant, represents the interaction amplitude of the axial current with the two-nucleon system.

Nucleon mass power counting arguments for the diagrams involving the ω and low-mass σ meson exchange, show that their contributions to the spatial part of AXC start only with the terms of order $O(1/M^3)$. *Thus no AXC of order O(1/M) are present in the non-linear realization of the $\sigma - \omega$ model in accord with the conclusion that no axial two-body currents of that order are required by PCAC to be present in the model (unlike the results obtained in the linear realization of the model).* There are yet corrections from the exchange of these mesons in the axial exchange charge of order $O(1/M^2)$. They have an isospin structure different from that of the pion-exchange correction. For example, the σ-field axial exchange charge has the form

$$A_0^{(\pm)}(\sigma') = \frac{g_\sigma^2}{2M^2} \frac{\vec{\sigma}(2) \cdot \mathbf{P}_2}{\mathbf{l}^2 + m_\sigma^2} \tau_\pm(2) + X - \text{terms} \tag{3.20}$$

where $\mathbf{P}_2 \equiv \mathbf{p}'_2 - \mathbf{p}_2$. However, these contributions will not be considered in the present analysis. They are argued to be negligible in the processes considered due to a very short range of such heavier meson exchanges, comparing to the pion exchange[2].

In summary, two leading corrections to the traditional axial current have been calculated in this Chapter in the non-linear realization of the $\sigma - \omega$ model: the spatial one-body relativistic correction (3.17) and the two-body axial exchange charge (3.19). Only these two corrections will be included in the following chapters in the analysis of few semileptonic weak processes with some selected nuclei.

---

[2]This is the same argument that lead to the pion-pole dominance hypothesis. These contributions are predicted though to play an important role in some processes in heavy nuclei [16,56].

63

Chapter 4

Matrix elements

The general expressions for observed experimental quantities for the processes of interest here - the muon-capture and beta-decay rates, and the charge-changing antineutrino scattering cross section - involving transitions between discrete nuclear states, have been derived in [7] in terms of the matrix elements of the various multipoles of the weak currents. The relevant formulae are provided in Appendix B. The only assumptions made in the derivation of these results are that there exists a local weak current density operator $\hat{\mathcal{J}}_\mu(x)$ for the target, that this current is localized in space, and that initial and final target states have definite angular momentum and parity quantum numbers J^π. Target recoil effects are taken into account in these formulae only through the kinematic factors.

To introduce the two corrections (the one-body relativistic correction to the traditional axial current, and the two-body axial exchange charge due to π-exchange), obtained in the previous chapter, in this general analysis of the weak nuclear semileptonic processes, one has to take the isospin structure of the considered operators into account correctly, and also to project out the multipoles of the calculated additional

operator terms

$$\hat{M}^5_{JM}(k) \equiv \int d\mathbf{x}\, j_J(kx) Y_{JM}(\Omega_x) \hat{\rho}_5(\mathbf{x})$$

$$\hat{L}^5_{JM}(k) \equiv \frac{i}{k} \int d\mathbf{x}\, \{\nabla \left[j_J(kx) Y_{JM}(\Omega_x) \right]\} \cdot \hat{J}_5(\mathbf{x})$$

$$\hat{T}^{mag5}_{JM}(k) \equiv \int d\mathbf{x}\, \left[j_J(kx)\, \mathcal{Y}^M_{JJ_1}(\Omega_x) \right] \cdot \hat{J}_5(\mathbf{x})$$

$$\hat{T}^{el5}_{JM}(k) \equiv \frac{1}{k} \int d\mathbf{x}\, \left\{ \nabla \times \left[j_J(kx)\, \mathcal{Y}^M_{JJ_1}(\Omega_x) \right] \right\} \cdot \hat{J}_5(\mathbf{x}) \tag{4.1}$$

First, one can carry out the calculation of the contributions due to the relativistic correction. This calculation is simple because the considered correction is a one-body operator, and also its isospin structure is identical to that of the traditional one-body axial current. The multipole projections of the one-body relativistic correction to the axial current can be identified by splitting the new contribution to the interaction hamiltonian matrix element into leptonic and nucleonic parts somewhat differently than is done usually. Consider the weak interaction hamiltonian matrix element

$$\langle f \| \hat{H}_W \| i \rangle = -\frac{G}{\sqrt{2}} l^\mu \int d\mathbf{x}\, e^{-i\mathbf{k}\cdot\mathbf{x}} \langle f \| \hat{J}_\mu(\mathbf{x}) \| i \rangle$$

$$= -\frac{G}{\sqrt{2}} [\mathbf{l} \cdot \mathbf{J}_{fi}(\mathbf{k}) - l_0 \, J_{0\,fi}(\mathbf{k})] \tag{4.2}$$

and assume the calculated relativistic correction 3.17 to be the only current contributing to this expression:

$$\delta \langle f \| \hat{H}_W \| i \rangle = -\frac{G}{\sqrt{2}} \left[\frac{k_0}{k^2 - m_\pi^2} \mathbf{l} \right] \cdot \left[-F_A \, \tau_\pm \, \mathbf{k}\, \frac{\vec{\sigma} \cdot \mathbf{P}}{2M} \right] \equiv \mathbf{l}' \cdot \delta \mathbf{J}_5^{(\pm)}(\mathbf{k}) \tag{4.3}$$

The new lepton term $\mathbf{l}'$ is different from the usual one $\mathbf{l}$ by an extra scalar factor

$$\frac{k_0}{k^2 - m_\pi^2}$$

65

This factor will not influence the calculation of the lepton traces, but rather will be passed directly to the final results. Now the $\delta \hat{\mathbf{J}}_5^{(\pm)}(\mathbf{x})$ operator in coordinate space is easily identified to be

$$\delta \hat{\mathbf{J}}_5^{(\pm)}(\mathbf{x}) = i \, \nabla \hat{\rho}_5^{(\pm)}(\mathbf{x}) \tag{4.4}$$

where $\hat{\rho}_5^{(\pm)}(\mathbf{x})$ is the familiar one-body axial charge operator (2.13). Upon separating isospin dependence and projecting multipoles of this extra axial vector current, for the multipole operators one obtains:

$$\delta \hat{T}_{JM}^{\text{mag}\, 5\,(1)}(\kappa) = \delta \hat{T}_{JM}^{\text{el}\, 5\,(1)}(\kappa) = \delta \hat{M}_{JM}^{5\,(1)}(\kappa) = 0 \tag{4.5}$$

$$-i \, \delta \hat{L}_{JM}^{5\,(1)}(\kappa \mathbf{x}) = F_A^{(1)} \frac{\kappa^2}{M} \, \Omega_J^{\prime M}(\kappa \mathbf{x}) \tag{4.6}$$

where $\kappa = |\mathbf{k}|$ is the absolute value of the momentum transferred to the nucleus, and $\Omega_J^{\prime M}(\kappa \mathbf{x})$ is an operator defined in [46]

$$\Omega_J^{\prime M}(\kappa \mathbf{x}) = M_J^{M_J}(\kappa \mathbf{x})\vec{\sigma} \cdot \frac{1}{q} \nabla + \frac{1}{2q}[\nabla \, M_J^{M_J}(\kappa \mathbf{x})] \cdot \vec{\sigma}$$

$$M_J^{M_J}(\kappa \mathbf{x}) = j_J(\kappa \mathbf{x}) \, Y_J^{M_J}(\Omega_x)$$

Matrix elements of this operator in the simple harmonic oscillator basis have been tabulated in [46].

Thus, only the longitudinal multipoles of the relativistic correction are non-zero, and the whole contribution of this term to the weak axial current interactions can be calculated by performing the substitution

$$\hat{L}_{JM}^5(\kappa) \to \hat{L}_{JM}^5(\kappa) + \frac{k_0}{k^2 - m_\pi^2} \, \delta \hat{L}_{JM}^5(\kappa) \tag{4.7}$$

in all formulae for weak rates and cross sections. This trick simplifies significantly calculation of the effects due to the relativistic correction.

Next one needs to perform multipole decomposition of the two-body pion-exchange current, as well as decomposition of the corresponding matrix elements in

66

terms of invariant quantities. This calculation is rather straightforward but very tedious.

It is not difficult to write down the general matrix element reduction formula for the two-body operator obtained:

$$\langle J_f; T_f\, M_{T_f} \parallel \hat{T}_{J,1}^{M_T}(2) \parallel J_i; T_i\, M_{T_i} \rangle \;=$$

$$(-1)^{T_f - M_{T_f}} \begin{pmatrix} T_f & T & T_i \\ -M_{T_f} & M_T & M_{T_i} \end{pmatrix} \underbrace{\langle T_f \parallel [\tau(1) \times \tau(2)] \parallel T_i \rangle}_{\text{isospin}} \underbrace{\langle J_f \parallel \hat{T}_J(2) \parallel J_i \rangle}_{\text{space-spin}} \quad (4.8)$$

For calculating discrete nuclear state wave functions, their parameterization in terms of the combinations of the shell model single-particle states is used here. The coefficients of this decomposition are determined by fitting available moderate-q^2 electromagnetic experimental data. In this analysis the electromagnetic two-body currents (whose magnitude is smaller by an extra factor of q/M) have been neglected.

A simple harmonic oscillator basis is used in this work for the nuclear wave function parameterization. It is known that this basis allows one to account well for the low-transferred-momentum electromagnetic properties of nuclei while utilizing in the model just a few lowest single-particle states, to easily include kinematical corrections due to the center-of-mass motion, and to perform simply the eigenstates transition from the individual particle coordinates to the relative and center-of-mass coordinates (making use of Moshinski brackets [57]) defined by

$$\mathbf{R} \;=\; \frac{1}{2}(\mathbf{x}_1 + \mathbf{x}_2)$$

$$\mathbf{r} \;=\; \mathbf{x}_1 - \mathbf{x}_2 \qquad\qquad (4.9)$$

The above mentioned coordinate substitution is important because the two-body AXC operators have been calculated in terms of the relative and center-of-mass coordinates, and, in order to calculate their matrix elements, one needs to have nuclear wave functions expressed correspondingly in these coordinates.

67

Coulomb multipoles are the only terms appearing in this calculation, since the current has only the axial charge component to order $O(1/M^2)$. Following [6], one can calculate the two-body nuclear matrix elements of the relevant two-body axial charge. In order to project multipoles, it is useful to first calculate matrix elements of the *two-body axial charge* operator between the two-body nuclear states.

The isospin part of the matrix elements can be separated and calculated trivially. The two-body axial exchange charge is an isovector. The isospin operator involved can be expressed through irreducible tensor operators:

$$[\tau(1) \times \tau(2)]^\pm = -i\sqrt{2}\,[\tau(1) \odot \tau(2)]_{1\,\pm 1} \tag{4.10}$$

Then the reduced isospin matrix element is

$$\left\langle \left(\frac{1}{2}\right)^2 ; T_f \|[\tau(1) \times \tau(2)]_1\| \left(\frac{1}{2}\right)^2 ; T_i \right\rangle = -i6\sqrt{6}[T_i][T_f] \left\{ \begin{array}{ccc} \frac{1}{2} & \frac{1}{2} & 1 \\ \frac{1}{2} & \frac{1}{2} & 1 \\ T_f & T_i & 1 \end{array} \right\} \equiv \zeta(T_i, T_f) \tag{4.11}$$

These results are obtained using the eigenstate phase conventions and general formulae from the book by Edmonds [58].

The two-body operators calculated in the previous chapters were all expressed there in terms of relative and center-of-mass coordinates of the two nucleons. The nuclear states are considered to be built from the shell-model single-nucleon states in the j-j coupling scheme, obtained in the center-of-well coordinate system. To calculate the space-spin parts of the axial-charge matrix elements, one has to transform to the L-S coupling scheme and then use Moshinski transformation brakets [57] to arrive at eigenfunctions in the relative and center-of-mass coordinate system.

Now one can decompose everything in terms of irreducible tensor operators and combine various terms to express the matrix element (which must be invariant under rotations) through possible invariant constructions. This procedure is similar

68

to one used by Dubach [6] for the decomposition of the electromagnetic MEC matrix elements. To ensure consistency of the present approach with previous work, Dubach's result for the electromagnetic case has been reproduced. After that a new result, allowing one to calculate exchange axial charge matrix elements in a j-j coupling two-particle states basis, has been obtained. Upon performing a rather lengthy but straightforward calculation involving a number of angular momentum recouplings, one arrives at the following formula:

$$\frac{1}{\sqrt{4\pi}}\langle(j_1'j_2')J_f\|A_0^\alpha(x_1,x_2,k)\|(j_1j_2))J_i\rangle =$$

$$\sqrt{6}\sum_{\substack{LS,L'S'\\\{A\}\{B\}}}\sum_{\substack{\mathcal{L}\mathcal{L}'\,l\,l_R\\J\,M_J}} i^{l+l_R}\,\mathcal{A}\,\mathcal{A}'\,X(N_A'\,L_A',\,N_B'\,L_B';\,l\,l_R)\,X(N_A\,L_A,\,N_B\,L_B;\,l\,l_R)$$

$$\times\,[j_1]\,[j_2]\,[L]^2\,[S]^2\,[j_1']\,[j_2']\,[L']^2\,[S']^2\,[J_i]\,[J_f]\,[J]^2\,[\mathcal{L}]^2\,[\mathcal{L}']^2\,[l]^2\,[l_R]^2\,[L_A]\,[L_B]\,[L_A']\,[L_B']$$

$$\times(-1)^{S-\mathcal{L}'-M_J+L_A+L_B}
\begin{Bmatrix} l_1' & l_2' & L' \\ \tfrac{1}{2} & \tfrac{1}{2} & S' \\ j_1' & j_2' & J_f \end{Bmatrix}
\begin{Bmatrix} l_1 & l_2 & L \\ \tfrac{1}{2} & \tfrac{1}{2} & S \\ j_1 & j_2 & J_i \end{Bmatrix}
\begin{Bmatrix} L' & L & \mathcal{L} \\ S' & S & 1 \\ J_f & J_i & J \end{Bmatrix}
\begin{Bmatrix} L_A' & L_A & \mathcal{L} \\ L_B' & L_B & l_R \\ L' & L & \mathcal{L}' \end{Bmatrix}$$

$$\times\begin{Bmatrix} \tfrac{1}{2} & S' & \tfrac{1}{2} \\ S & \tfrac{1}{2} & 1 \end{Bmatrix}
\begin{Bmatrix} \mathcal{L}' & 1 & J \\ l\,l_R & \mathcal{L} \end{Bmatrix}
\begin{pmatrix} l & 1 & \mathcal{L} \\ 0 & 0 & 0 \end{pmatrix}
\begin{pmatrix} l & l_R & J \\ 0 & 0 & 0 \end{pmatrix}
\begin{pmatrix} L_A' & \mathcal{L} & L_A \\ 0 & 0 & 0 \end{pmatrix}
\begin{pmatrix} L_B' & l_R & L_B \\ 0 & 0 & 0 \end{pmatrix}$$

$$\times(1+(-1)^{l+S'-S})\,I_R(l_R,B,B')\,I_r(l,A,A')\,Y_{J,-M_J}(\Omega_k) \tag{4.12}$$

where the summation over $\{A\}$ implies summation over all the quantum numbers

69

$N_A, L_A; N'_A, L'_A$. The factor

$$(1 + (-1)^{l+S'-S})$$

arises from combining the two terms contributing to the axial charge operator expression; $\mathcal{A}$'s are the symmetry factors required for incorporating proper antisymmetry and normalization of the initial and final nuclear states

$$A = \begin{cases} 1 & \text{if } j_1 = j_2 \\ \frac{1}{\sqrt{2}}(1 - (-1)^{L_i+S_i+T_i}) & \text{if } j_1 \neq j_2 \end{cases} \tag{4.13}$$

The shorthand notation $[j] = \sqrt{2j+1}$ is utilized. The $X(N_A L_A, N_B L_B; l\, l_R)$ factors are Moshinski brakets [57], which allow transformation of the eigenfunctions from the center-of-well coordinates to the relative and center-of-mass coordinates. The radial integrals are defined as

$$I_R(l_R, B, B') = \int R^2 dR\, j_{l_R}(kR)\, \mathcal{R}_{N_B L_B}(R)\, \mathcal{R}_{N_{B'} L_{B'}}(R) \tag{4.14}$$

$$I_r(l, A, A') = \alpha' \int r^2 dr\, f(r) j_l(\frac{kr}{2})\, \mathcal{R}_{N_A L_A}(r)\, \mathcal{R}_{N_{A'} L_{A'}}(r) \tag{4.15}$$

where

$$\begin{aligned} \alpha' &= -F_A \frac{g^2}{4\pi}\left(\frac{m_\pi}{2M}\right)^2 \\ f(r) &= \left(1 + \frac{1}{x_\pi}\right)\frac{e^{-x_\pi}}{x_\pi} \\ x_\pi &= m_\pi r \end{aligned} \tag{4.16}$$

The radial oscillator wave functions $\mathcal{R}(x)$ entering the integrals are the radial oscillator eigenfunctions normalized by

$$\int r^2 dr\, |\mathcal{R}_{N_A L_A}(r)|^2 = 1$$

These functions are calculated with the following oscillator parameters: $b_R = \sqrt{\frac{1}{2}}b_{osc}$ - for the integral over the center-of-mass coordinate, $b_r = \sqrt{2}b_{osc}$ - for the integral

over the relative coordinate. The integral over the the center-of-mass coordinate can be done in terms of the confluent hypergeometric function [7], while the integral over the relative coordinate will be done numerically.

One may now observe that the axial charge matrix element is expressed in the form

$$\frac{1}{\sqrt{4\pi}} \langle (j_1' j_2') J_f \| A_0^\alpha(\mathbf{x}_1, \mathbf{x}_2, \mathbf{k}) \| (j_1 j_2) J_i \rangle = \sum_{J'M_j'} C_{fi}(k, J', M_j') \, Y_{J',-M_j'}(\Omega_k)$$

(4.17)

On the other hand, consider the irreducible tensor operator decomposition of the axial charge operator:

$$\hat{A}_0^\alpha(\mathbf{k}) \equiv \int d\mathbf{x} \, e^{-i\mathbf{k}\cdot\mathbf{x}} \hat{A}_0^\alpha(\mathbf{x})$$

$$= 4\pi \sum_{JM} (-i)^J Y_{JM}^*(\Omega_k) \int d\mathbf{x} \, j_J(kx) \, Y_{JM}(\Omega_x) \, \hat{A}_0^\alpha(\mathbf{x})$$

(4.18)

Hence the Coulomb multipole operator can be rewritten as

$$M_{JM}^5(k) = \frac{i^J}{4\pi} \int d\Omega_k \, Y_{JM}(\Omega_k) \, \hat{A}_0^\alpha(\mathbf{k})$$

(4.19)

Substituting the result (4.17) for the axial charge matrix element and utilising the relation

$$Y_{J',-M_j'}(\Omega_k) = (-1)^{M_j'} Y_{J',M_j'}^*(\Omega_k)$$

one obtains

$$\langle f \| M_{JM}^5(k) \| i \rangle = \frac{i^J}{4\pi} \sum_{J'M_j'} C_{fi}(k, J', M_j') \, (-1)^{M_j'} \int d\Omega_k \, Y_{J,M_J}(\Omega_k) \, Y_{J',M_j'}^*(\Omega_k)$$

(4.20)

Making use of the orthonormality of the spherical harmonics, one arrives at the following formula for the reduced matrix elements of the Coulomb multipoles:

$$\langle f \| M_{JM}^5(k) \| i \rangle = \frac{(-1)^M i^J}{4\pi} C_{fi}(k, J, M)$$

(4.21)

71

Reduction of the many-body nuclear matrix elements to the one- and two-body matrix elements can be performed by making use of the fractional parentage coefficients technique developed in [47]. In the present work simple models for the light nuclei under consideration are used for calibration of the effects of the calculated corrections to the axial current. In most cases it will be possible to model the nuclear states as having only one or two nucleons present (or absent). The application of the fractional parentage coefficients formalism will be actually required only once (in the first case).

Chapter 5

Numerical Results

The obtained corrections to the one-body axial current operator have complex isospin and space-spin structure. To get a feeling for the size of these corrections, one needs to estimate the magnitude of effects of the calculated corrections on the weak nuclear processes in the some real nuclei. As applications, the corrections to the one-body axial current obtained in this work have been included in the analysis of the three semileptonic weak process:

1) β^--decay: $A(N, Z) \to A^*(N - 1, Z + 1) + e^- + \bar{\nu}_e$

2) μ^--capture: $\mu^- + A(N - 1, Z + 1) \to A^*(N, Z) + \nu_\mu$

3) antineutrino scattering: $\bar{\nu}_l + A^*(N - 1, Z + 1) \to A(N, Z) + l^+$

for two light nuclear systems. These systems are the ^{3}H$-^3$He isospin doublet, and the ^{6}He$-^6$Li neighboring nuclei. The objective here is to estimate the size of the extra contributions from the corrections to the traditional one-body axial currents, written out in equations (1.14) and (1.16), to the specified nuclear processes. One recalls that the weak current consists of the vector and axial-vector parts. Corrections to the one-body vector part of the weak currents can be obtained from the analysis of the electromagnetic exchange currents by performing the isospin rotation. They will

73

not be included in the present treatment[1]. The prime goal of the present treatment is to estimate effects of the axial-vector corrections to the "canonical" axial one-body currents [2]. To achieve this goal, the results for weak rates and cross sections obtained in the one-body approach [7] have been rederived here, and then the contributions from the two calculated corrections (3.17) and (3.19) to the traditional one-body axial current have been included.

When calculating the weak interaction operator matrix elements, one has to calculate specific wave functions for the nuclear states involved. It is the second key element of the present strategy to treat the nuclear wave function part of all the electroweak nuclear matrix elements consistently. To eliminate the nuclear wave function uncertainties from the problem, the unified analysis of electroweak nuclear processes is performed in this work within the shell-model framework. The nuclear wave function is parameterized in terms of the shell-model single-particle levels, and corresponding parameters are determined from fitting electromagnetic data[2]. Following the results of Donnelly and Walecka [41], use is made here of these data to determine single-body densities for the nucleus under consideration, parameterized in terms of the shell-model single-nucleon state contributions[3]:

$$\langle \Psi_f \mid \hat{T}_{JM_J,TM_T}(q) \mid \Psi_i \rangle = \sum_{\alpha,\beta} \langle \alpha \mid T_{JM_J,TM_T}(q) \mid \beta \rangle \, \psi_{\alpha\beta}^{fi} \tag{5.1}$$

with numerical coefficients

$$\psi_{\alpha\beta}^{fi} \equiv \langle \Psi_f \mid c_\alpha^+ c_\beta \mid \Psi_i \rangle \tag{5.2}$$

---

[1]The processes considered in this work: muon capture, nuclear beta decay and charge-changing neutrino scattering - are predominantly Gamow-Teller transitions for the nuclear systems considered. Selection rules determine that contributions from the vector part of the weak current are suppressed in these processes by extra powers of the ratio of the transferred momentum to the nucleon mass.

[2]Electromagnetic exchange currents have been calculated in this approach in [6].

[3]Electromagnetic meson exchange currents are not included in the present analysis. Their introduction would produce a small correction to the obtained results, while significantly complicating the calculations involved.

74

A simple harmonic oscillator basis, with an oscillator parameter determined by fitting the low transferred momentum $(e\,e')$ scattering data, is used for the single-nucleon orbits in this work. First, some reasonable truncation of the number of shells important for the considered processes is performed. Then the corresponding coefficients ψ^{fi} are calculated in the "model independent way" by fitting available experimental electromagnetic results. The low-q^2 properties of the two nuclear systems considered can be fit very well by expressing them in terms of a few shell-model states. The low-q^2 region is important also for majority of considered weak processes. Thus in the present work the *nuclear wave function* for the simple systems considered can be determined purely from the electromagnetic data. One does not need to use any specific N-N potential as must be done in, for example, TDA or RPA calculations. The obtained densities are used to compute weak rates. The present procedure eliminates most of the usual nuclear structure uncertainties, arising from calculating the nuclear wave function in some specific model, from the analysis of weak rates and cross sections.

5.1 Ground state $(J^\pi\, T) = (\frac{1}{2}^+\frac{1}{2})$ isodoublet of the A=3 system

The $^3\text{H}-^3\text{He}$ system depicted in Figure 5.1 consists of the most simple nuclei featuring the weak processes of interest here. Very accurate calculations of the wave function for these three-body nuclear systems from first principles exist [42]. However, the objective of the present analysis is to estimate the scale of the effects due to the calculated corrections. For this purpose it is sufficient to implement the most straightforward description of the wave functions involved, in terms of the single-particle shell-model states. This approach simplifies calculations considerably. As a
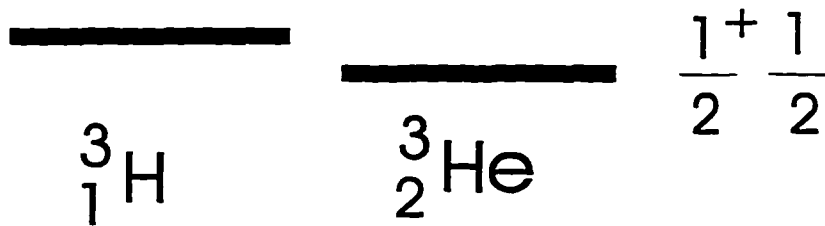
75

$$\frac{1}{2}^+ \frac{1}{2}$$

$${}^{3}_{1}H \qquad {}^{3}_{2}He$$

Figure 5.1: The ^{3}H $-{}^{3}$He isodoublet ground states.

model for the ground states of the isodoublet, the three nucleons in the $(1s_{\frac{1}{2}})$ shell picture is used. When calculating contribution of the one-body operator, it can be also viewed even simpler as a $(1s_{\frac{1}{2}})^{-1}$ hole state in the filled $(1s_{\frac{1}{2}})$ shell. Isospin is considered to be a good symmetry for description of the ground states of the investigated nuclei. The only parameter of the model, $b_{osc} = 1.59$ fm, is determined by fitting the elastic electromagnetic form factors in the low-transferred-momentum region [41]. Figure 1.8 shows that the simple model adopted for the description of the ground states of the isodoublet, models well the elastic electromagnetic form factors of the two A=3 nuclei in the low-q^2 region, which is of prime interest for the treatment of the weak processes considered here. Results for the semileptonic weak rates for the ^{3}H $\leftrightarrow {}^{3}$He transitions with the corrections to the one-body axial current included, are compared in Table 5.1 with experimental results and the previous calculations in the one-body approach, where no exchange currents or relativistic corrections were present [41].

Transverse multipoles have been shown in the previous chapter to have no contribution from the obtained corrections to the one-body axial current. Only Coulomb and longitudinal multipoles of these corrections are non-zero. Selection rules originating from the symmetries of the considered system reduce the number of multipole

76

terms which are able to contribute to just a few. Angular momentum selection rules determine that only $J = 0, 1$ multipoles can contribute to the transitions between the $J = \frac{1}{2}$ states. Parity conservation arguments eliminate M_0^5 and L_0^5 - half of the multipole terms remaining. Thus only the L_1^5 multipole due to the relativistic one-body correction to the axial current and M_1^5 - due to axial exchange charge could have non-zero matrix elements in the transitions under consideration.

Within the assumed model for the isodoublet ground state there is *no contribution to any of the weak processes considered from the one-body relativistic correction to the axial current*. This happens because the reduced matrix elements of operators between the 1s-states only are required in the calculation:

$$\langle \frac{1}{2}^+ ; \frac{1}{2}, \pm\frac{1}{2} \| \hat{T}_J^\pm \| \frac{1}{2}^+ ; \frac{1}{2}, \mp\frac{1}{2} \rangle = \mp (-1)^J \sum_{ab} \langle a\|T_J\|b\rangle = \mp (-1)^J \langle 1s\|T_J\|1s\rangle \quad (5.3)$$

The only non-zero multipole of the relativistic correction L_1^5 is expressed through the Ω_{1M_1} operator defined in [46], but

$$\langle 1s \| \Omega_1' \| 1s \rangle = 0 \tag{5.4}$$

For calculating effects of the AXC on this system, one can consider the ground state of the isodoublet as a $(1s_{\frac{1}{2}})^3$ state. Then the two-body AXC contribution to the weak ground state processes with this isodoublet can be analyzed with the help of the fractional parentage coefficients reduction of the three-body matrix element to the combination of the two-body matrix elements [47,48] (see Appendix C for details).

$$\langle \left(\frac{1}{2}\right)^3 ; \frac{1}{2}^+ \frac{1}{2} :: \hat{M}_{11}^5(2) :: \left(\frac{1}{2}\right)^3 ; \frac{1}{2}^+ \frac{1}{2} \rangle =$$

$$- 2 \left[\left(\frac{1}{2}\right)^3 \left(\frac{1}{2}^+ \frac{1}{2}\right) \left\{ \Big|\frac{1}{2} \left(\frac{1}{2}\right)^2 (01) \right] \left[\left(\frac{1}{2}\right)^3 \left(\frac{1}{2}^+ \frac{1}{2}\right) \left\{ \Big|\frac{1}{2} \left(\frac{1}{2}\right)^2 (10) \right]$$

$$\times \left\{ \langle \left(\frac{1}{2}\right)^2 ; 01 :: \hat{M}_{11}^5(2) :: \left(\frac{1}{2}\right)^2 ; 10 \rangle + \langle \left(\frac{1}{2}\right)^2 ; 10 :: \hat{M}_{11}^5(2) :: \left(\frac{1}{2}\right)^2 ; 01 \rangle \right\} \quad (5.5)$$

77

The objects of the form $[j^3 \, (J^\pi T)\{|j\,j^2 \, (J_{11}T_{11})]$ are *coefficients of fractional parentage* defined in [47]. Here these coefficients determine contributions of various possible two+one particle states to the resulting totally antisymmetric three-particle state $(J^\pi T)$.

To simplify the analysis of the contribution of the M_1^5 multipole due to axial exchange charge operator, one additional symmetry of the considered system can be utilized. Hermiticity of the charge and current operators and time reversal symmetry considerations combined, produce a general formula (obtained in [46]) for the *one-body* operator matrix elements

$$\langle J_f T_f \mathbin{\vdots\vdots} \hat{T}_{JT}(\kappa) \mathbin{\vdots\vdots} J_i T_i \rangle = (-1)^{J+\eta+J_f-J_i+T_f-T_i} \langle J_i T_i \mathbin{\vdots\vdots} \hat{T}_{JT}(\kappa) \mathbin{\vdots\vdots} J_f T_f \rangle$$

(5.6)

where

$$\eta \equiv \begin{cases} 1 - \text{for current} \\ 0 - \text{for charge} \end{cases} \text{multipoles}$$

(5.7)

If a similar relation were true for *two-body* operators between the two-body states, it would simplify the analysis drastically.

There are two places where the one-body character of the operators involved had been used in the derivation of this formula. The first of them is the following relation for the isospin part of the current operator:

$$\hat{J}^\dagger_{T,M_T} = (-1)^{M_T} \hat{J}_{T,-M_T}$$

(5.8)

which is true because of the simple isospin dependence of a one-body current operator. It is interesting to see whether a similar relation would hold for the two-body charge operator (3.19) obtained. Recalling the isospin structure of this operator, one can

78

write for an isovector spherical component

$$\left(\, [\tau(1) \times \tau(2)]^\alpha \, \right)^\dagger = \left(-i\sqrt{2} \sum_{m_1 m_2} \tau(1)_{m_1} \tau(2)_{m_2} \, \langle 1m_1; 1m_2 | 1\alpha \rangle \, \right)^\dagger$$

$$= i\sqrt{2} \sum_{m_1 m_2} (-1)^{m_1 + m_2} \, \tau(1)_{-m_1} \tau(2)_{-m_2} \, \langle 1m_1; 1m_2 | 1\alpha \rangle \quad (5.9)$$

Now symmetry relations of the vector coupling coefficients from Edmonds [58] are used

$$m_1 + m_2 = \alpha \quad (5.10)$$

$$\langle j_1 m_1; j_2 m_2 | j_3 \alpha \rangle = (-1)^{j_1 + j_2 - j_3} \, \langle j_1, -m_1; j_2, -m_2 | j_3, -\alpha \rangle \quad (5.11)$$

Then one obtains a relation

$$\left(\, [\tau(1) \times \tau(2)]^\alpha \, \right)^\dagger = (-1)^\alpha \, [\tau(1) \times \tau(2)]^{-\alpha} \quad (5.12)$$

which has exactly the same form as (5.8).

The second potential difference is in the transformation of the two-body states under time reversal. Recalling the transformation law of a single-body state

$$\hat{T} \, |JM_J; \, TM_T\rangle = (-1)^{J + M_J} |J, -M_J; \, TM_T\rangle \quad (5.13)$$

where $\hat{T}$ is a time reversal operator, and constructing the proper two-body states by angular momentum coupling

$$|J_i M_{J_i}\rangle \sum_{M_J M_J'} \langle JM_J, J'M_J' | J_i M_{J_i}\rangle \, |JM_J\rangle \, |J'M_J'\rangle \quad (5.14)$$

one can obtain the transformation law of the two-body state.

$$\hat{T} \, |J_i M_{J_i}\rangle = (-1)^{J + J'} \sum_{M_J M_J'} (-1)^{M_J + M_J'} \langle JM_J, J'M_J' | J_i M_{J_i}\rangle \, |J, -M_J\rangle \, |J', -M_J'\rangle$$

$$= (-1)^{J + J'} (-1)^{M_{J_i}} \sum_{M_J M_J'} \langle J, -M_J, J', -M_J' | J_i M_{J_i}\rangle \, |JM_J\rangle \, |J'M_J'\rangle \quad (5.15)$$

79

Using again a vector coupling formula (5.10) from Edmonds [58], one arrives at

$$\hat{T} \, |J_i M_{J_i}\rangle = (-1)^{J_i + M_{J_i}} |J', -M'_J\rangle \tag{5.16}$$

This is again exactly the same relation as the one for the single-nucleon state. Thus the general formula (5.6) is still valid and can be used for the analysis of the matrix element of interest here (where $J_f = J_i$ and $T_f = T_i$). Application of this formula to equation (5.5) results in exact cancellation of the two matrix elements of the M_1^5 multipole.[4] Thus *there are no effects of the AXCs on the processes involving transitions between the ground states of the ^3H–^3He isodoublet in this model.*

These results serve to justify the close agreement of the weak rates calculated within the one-body approach, with experimental results, at least as far as the dominant axial vector current contributions are concerned (see Table 5.1).

	exper.	1-body theory	+relativ. correction	+ pion X current
β^--decay:				
$\omega_\beta(10^{-9}\text{sec}^{-1})$	1.79 ± 0.007^5	1.84	1.84	1.84
μ^--capture:				
$\bar{\omega}_\mu$ (sec^{-1})	1505 ± 46^6	1534	1534	1534

Table 5.1: ^{3}H–^{3}He weak transition rates.

5.2 $(1^+0)\leftrightarrow(0^+1)$ transitions in the A=6 system

The second system investigated in the present work consists of two A=6 neighboring nuclei (shown in Figure 5.2): the ^{6}He$\leftrightarrow$ ^{6}Li transitions are considered. Three

---

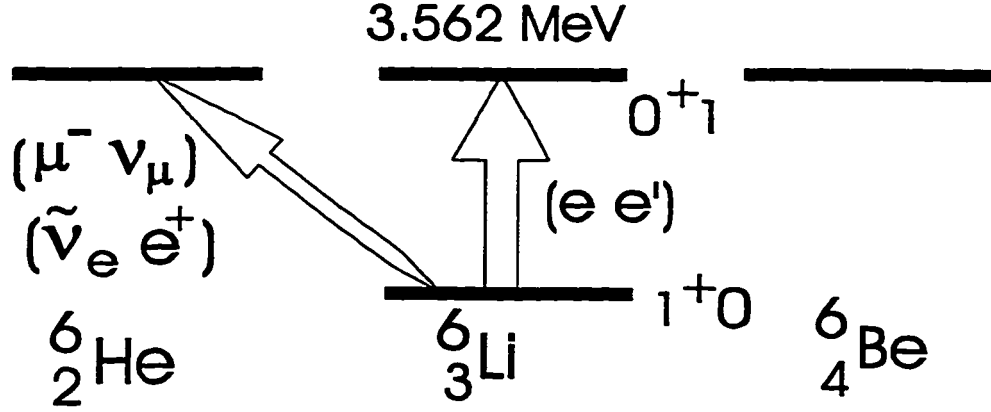[4]This cancellation was first obtained by explicit calculation of the two-body matrix elements involved.

Figure 5.2: The ^{6}He $-^6$Li nuclei lowest energy levels.

facts make this system interesting for the present analysis:

1) These are non-trivial nuclei. It would be a daunting task to calculate the required wave functions from the first principles.

2) There are high precision electromagnetic data available for these nuclei.

3) This is the simplest system where one can now expect to see some nontrivial effects of the calculated corrections to the one-body axial currents.

The following model for the ^{6}Li nucleus is assumed here (after [52]): an *inert* core (closed 1s-shell) + two valence nucleons producing the following general wave function for the ground or first excited states, correspondingly:

$$|1^+0\rangle = A|(1p_{\frac{3}{2}})^2 1^+0\rangle + B|(1p_{\frac{3}{2}} 1p_{\frac{1}{2}})1^+0\rangle + C|(1p_{\frac{1}{2}})^2 1^+0\rangle$$

$$|0^+1\rangle = D|(1p_{\frac{3}{2}})^2 0^+1\rangle + E|(1p_{\frac{1}{2}})^2 0^+1\rangle \qquad (5.17)$$

Again the simple harmonic oscillator basis is used for parameterizing the nuclear wave function. This model works well for a description of electromagnetic processes with the system. Parameters of the model are determined through simultaneous fitting the magnetic dipole and electric quadrupole moments of the ^{6}Li ground state, as well as the elastic and inelastic magnetic form factors, calculated in terms of the model

81

wave function of (5.17). For instance, the elastic magnetic form factor is

$$\frac{\langle 1^+ 0 \parallel \hat{T}_{1,0}^{mag} \parallel 1^+ 0 \rangle}{\sqrt{3}(i\,|q|/m)e^{-y}f_{sn}f_{cm}} \equiv p(y) = \alpha_e + \beta_e y \qquad (5.18)$$

where $y \equiv (|q|\,b_{osc}/2)^2$ and α_e, β_e are certain constants. The result for the inelastic form factor differs from (5.18) only by diferent values of the constants involved (see Figure 1.10). The best set of the simultaneous values of parameters is given in Table 5.2 [52]:

A	B	C	D	E	b_{osc}(fm)
0.810	-0.581	0.084	0.80	0.60	2.03
±0.001	±0.001	±0.002	±0.03	±0.04	±0.02

Table 5.2: Parameters of the wave function.

For the considered transition the angular momentum selection rules determine that only the $J = 1$ multipoles can contribute. Thus to estimate effects of the calculated corrections to the axial current, one has to calculate the matrix elements of the L_1^5 operator due to the relativistic one-body correction, and the matrix elements of the M_1^5 operator projected from the axial exchange charge.

For the weak charge changing processes with the ^{6}He$-^6$Li system two combinations of the initial and final isospins of the system are possible: $(T_i = 0, T_f = 1)$ or $(T_i = 1, T_f = 0)$. In both these cases the isospin matrix element is easily calculated to be

$$\zeta = -2i\sqrt{3} \qquad (5.19)$$

In the adopted model nuclear wave functions are just linear superpositions of simple two-nucleon states. Thus the general formula (4.12) can be utilized to calcu-

82

late the required matrix elements of the two-body axial exchange charge operator. Numerical evaluation of the required spatial matrix elements has been performed.

For consideration of the two-body operators, proper description of the wave function at small interparticle separations becomes an important issue. To estimate effects of the incorrect behavior of the simple harmonic oscillator basis wave functions at short distances, a phenomenological correlation function $g(r)$ (as in [6]) has been introduced in the calculation in the following way:

$$R_{N'_A L'_A}(r)\, R_{N_A L_A}(r) \;\to\; g(r)\; R_{N'_A L'_A}(r)\, R_{N_A L_A}(r) \tag{5.20}$$

Only the s-state wave functions must be modified by this correlation function. The function is chosen to have the form:

$$g(r) = C(N_A) \left[1 - \exp(-\frac{r^2}{d^2}) \right] \tag{5.21}$$

where $d = 0.84\,\text{fm}$ has been determined from a fit to the nuclear matter properties, and the $C(N_A)$ coefficient is introduced to preserve the normalization of the s-state wave function. This *ad hoc* correlation function forces the wave functions to vanish at the short distances, mocking up the presence of the repulsive core. Calculations of the weak rates have been performed with and without this correlation function to see how significant is the error made when using the simple harmonic oscillator wave functions for the single-nucleon states.

The semileptonic weak rates in Table 1.3 have been calculated for the $(0^+1)\leftrightarrow(1^+0)$ transitions in ^{6}He$-^6$Li system, upon performing the numerical evaluation of the weak current multipole matrix elements with the wave function coefficients and the correlation function obtained above.

Here the F superscript, a quantum number of the $\mathbf{F} = \mathbf{J} + \mathbf{S}$ operator, distinguishes μ-capture processes from different hyperfine states. The $\bar{\omega}_\mu$ corresponds to the statistically averaged μ-capture rate.

83

	exper.	1-body theory	+relativ. correction	+ pion X current	with corr. function	Total	Diff (%)
β^--decay:							
ω_β (sec^{-1})	0.864^7 ± 0.003	0.876	0.872	0.869	0.869	0.865	-1.3
μ^--capture:							
$\bar{\omega}_\mu(\text{sec}^{-1})^8$	1600^{+330}_{-130}	1381	1381	1386	1385	1385	0.2
$\omega_\mu^{F=1/2}(\text{sec}^{-1})$		3843	3843	3865	3860	3860	0.4
$\omega_\mu^{F=3/2}(\text{sec}^{-1})$		150.2	150.2	137.1	140.3	140.3	-6.6

Table 5.3: Weak rates for the $(0^+1) \leftrightarrow (1^+0)$ transitions in the ^{6}He$-^6$Li system.

In the first column of the table available experimental results are provided. The second column shows the traditional results of the weak rates calculations, where only the single-nucleon axial currents have been included [41,49,52]. The third and fourth columns of the table display the separate influences on the weak rates of the relativistic correction and pion exchange charge, correspondingly. The fifth column shows the latter result with a correlation function (5.21) included into consideration. The next column shows the cumulative rates with both considered corrections included, while the last column expresses the effect due to the corrections in the percent fraction of the one-body result. The largest effect due to the corrections is predicted for the muon-capture rate from the hyperfine $F = 3/2$ state (-6.6%). The total effect of the corrections for the beta-decay rate is small, but it is interesting that the one-body relativistic correction obtained in this work, produces here an effect of about the same size with the one from the pion axial exchange charge. Consideration of the phenomenological correlation function corrects the result for the axial exchange charge contribution by at most 20%, as was expected. In general, *the smallness of the calculated effects serve as a justification of the previous successful analysis of weak processes in terms of the one-body currents* [41,49,52].

84

The same conclusion is made upon consideration of the results for the charge-changing antineutrino cross section in the process

$$\bar{\nu}_e + {}^6\text{Li} \rightarrow {}^6\text{He(g.s.)} + e^+$$
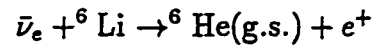
A prediction for the differential scattering cross section with the obtained corrections to the one-body effects included in the analysis, are shown in Figure 5.3. These results do not differ significantly, up to high transferred momentum, from the curve obtained in the one-body analysis, again justifying the legitimacy of the previous one-body analysis.
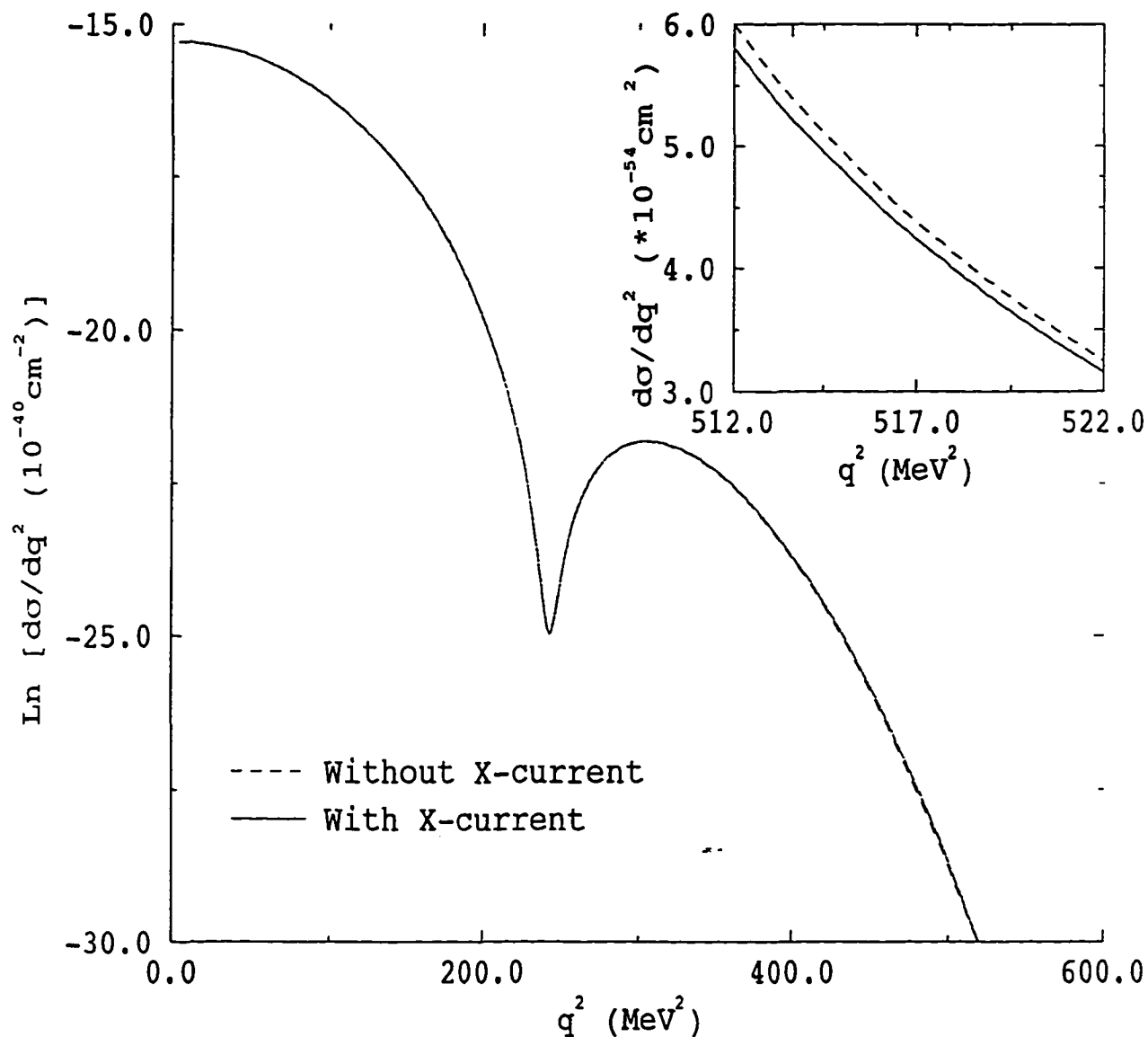
Figure 5.3: Charge-changing antineutrino scattering cross section on ^{6}Li. The linear-scale insertion in the upper right corner of the graph represents the blown-up figure of the same results at some large q^2 where effects of exchange currents are expected to be more pronounced.

86

Chapter 6

Conclusions to Part I

1. In the present work AXC up to order $O(1/M^2)$ are calculated consistently in the linear and non-linear realizations of the $\sigma - \omega$ model. The $\sigma - \omega$ model is a chirally symmetric lagrangian model containing π, σ and ω mesons, as well as nucleons, that provides systematic explanation of a vast number of nuclear physics results.

2. Splitting the corrections to the traditional one-body nonrelativistic approximation of the full many-body nuclear problem is explicitly shown to be a model-dependent procedure.

3. In the linear realization of the $\sigma - \omega$ model, AXC of order $O(1/M)$ due to the isoscalar, scalar and vector, meson exchange are shown to be required to satisfy PCAC. These AXC are calculated explicitly and shown to help in preserving PCAC in this model.

4. In both realizations, a familiar axial exchange charge operator of order $O(1/M^2)$ due to pion exchange is reproduced, differing from the result of other work by an extra factor of $F_A^2 \simeq 1.5$. This extra factor appears in the present approach because the correct Goldberger-Treiman relation and pion-pole dominance are preserved at each step of the calculation.

87

5. In the non-linear realization of the $\sigma - \omega$ model, a new leading one-body relativistic correction of order $O(1/M)$ to the one-body axial current, required for the PCAC satisfaction in momentum space to order $O(1/M^2)$, is derived.

6. The last two corrections to the traditional nuclear one-body axial current are included in the analysis of the weak charge-changing semileptonic processes in two selected light nuclear systems.

7. To determine the nuclear wave functions necessary for calculating matrix elements of the axial charge operators, a unified analysis of electroweak nuclear processes is performed in this work within the simple harmonic oscillator shell-model framework. The nuclear wave function is parameterized in terms of the shell-model single-particle levels, and the corresponding parameters are determined from the available electromagnetic data. This procedure eliminates most nuclear structure uncertainties from the analysis of weak rates and cross sections.

8. Effects of the calculated corrections on the weak cross sections and rates are shown to be very small (never exceeding a few percent). In general, *the smallness of the calculated effects serves as a justification for the success of the previous analysis of weak processes considered in terms of the one-body weak currents.*

9. There can be other nuclear systems where the calculated corrections would contribute significantly to some weak processes. It is important to find such nuclear systems and test carefully the obtained results. However, such a search appears to be a highly non-trivial endeavor due to the large number and complexity of matrix elements which have to be analyzed.

Part II

Electroweak processes involving (0^+0) excitations in nuclei

89

Chapter 7

Introduction to the problem

The simple ground state quantum numbers of $(0^+0)_{gnd}$ nuclei are known to allow relations connecting various elastic electroweak processes for the same nucleus. Some of these relations provide new unique tools to study nuclear and nucleon structure. For example, strange quark pairs $(s, \bar{s})$ appear to contribute significantly to the properties of the nucleon [59]. So far little is known about various strange quark matrix elements of the nucleon, and ways to obtain experimental information on these matrix elements are intensively discussed in the literature [60-64]. Parity violating (PV) elastic polarized electron scattering and elastic neutrino scattering experiments on light $(J^\pi = 0^+, T = 0)$ nuclei have been proposed as probes of the electric strange form factor of the nucleon [65]. As noted in [66], because of potential isospin mixing and decrease in the figure-of-merit, only ^{4}He and ^{12}C (and possibly ^{16}O) nuclei appear to be suitable targets for such experiments. Experiments aimed at determination of the ground state matrix element of the weak strange current from the PV asymmetry in elastic polarized electron scattering on ^{4}He are planned for CEBAF [67,68]. All of the discussed nuclei have low-lying $(0^+0)^*$ excited states. Analysis shows that one can obtain results similar to the elastic case when the same electroweak processes excite

90

a $(0^+0)_{gnd}$ nucleus to its $(0^+0)^*$ state. In the following discussion, inelastic processes will mean just such excitations. The present work has been motivated by the questions of what new issues of nuclear structure can be addressed, and whether any of the proposed measurements can be enhanced if, in addition to an elastic electroweak experiment, one measures excitation of a $(0^+0)^*$ state in the same nucleus.

Chapter 8 describes in detail general relations for the cross sections of inelastic electron and neutrino scattering. It is shown, for example, that within the *single nucleon picture* of the nucleus the inelastic and elastic PV asymmetries are identical. Measuring the PV asymmetry in the inelastic polarized electron scattering cross section could enable one to extract information about a new transition nuclear matrix element of the vector strange quark current in the nucleus under consideration. Knowledge of the inelastic charge form factor of the nucleus for the region of intermediate transfered momentum q^2 (here $q \equiv |\mathbf{q}|$ is the absolute value of the transferred three-momentum) will be necessary to design such experiments. The central goal of the present analysis is to urge experimental investigation of how well the inelastic $(0^+0)^*$ resonance in the electron scattering can be seen at intermediate q^2, and to provide some theoretical guidance for such experiments.

In Chapter 9 the existing low transfered momentum ($q^2 < 2.4$ fm^{-2}) data on the inelastic charge form factor of ^{4}He is explained, and its higher q^2 (up to 10 fm^{-2}) behavior is predicted with the help of three simple models used for the ^{4}He nucleus. While the $(0^+0)^*$ state is indeed the first excited state of ^{4}He, the situation here is complicated by the fact that this state lies just above the break-up threshold. Although the $(0^+0)^*$ states in ^{12}C and ^{16}O are distinct bound states, the ^{4}He nucleus is considered in this work because the PV electron scattering experiment *will* actually be done on this nucleus, and corresponding neutrino experiments are under consideration. The relatively crude estimates of the inelastic electron scattering form factor in the present work are aimed at the determination of the size of the form

91

factor prior to attempting to perform state-of-the-art calculations of the structure of the $(0^+0)^-$ excitation of the ^{4}He nucleus. Thus the questions of the break-up background, radiative corrections, parity and isospin mixing, and meson exchange currents (MEC) contributions are set aside in the present analysis. The form factor is shown to be large enough to be seen in future CEBAF experiments. CEBAF will have luminosity and resolution sufficient to measure the inelastic charge form factor and PV asymmetry in the inelastic polarized electron scattering on ^{4}He up to high momentum transfers q^2.

The inelastic transition is, however, estimated to play only a marginal role in PV experiments aimed at extracting information about the small strangeness current contribution because experiments of sufficient accuracy will be very difficult, and their interpretation complicated.

Chapter 8

General Electroweak Relations

The analysis is started by considering two inelastic electroweak processes caus-
ing a $(0^+0)_{gnd} \to (0^+0)^*$ transition of a target nucleus (assuming pure quantum
numbers for both states): polarized electron scattering and neutrino scattering. The
only assumptions made in the analysis are the validity of the Standard Model and
strong isospin symmetry. Spin and isospin selection rules then allow one to derive
simple relations between weak and electromagnetic inelastic processes with a nucleus
in the same way as for elastic processes. The fact that isospin T=0 for initial and final
states of the target implies that only the isoscalar part of the weak neutral current can
contribute to hadronic matrix elements. In the nuclear domain approximation, when
a nucleus is assumed to contain only u, d quarks and their antiquarks, this implies
that only the following term of the weak neutral current of quarks contributes [2]:

$$J_\mu^{(0)} \doteq -2 \sin^2 \Theta_w \, J_\mu^\gamma \tag{8.1}$$

Thus, in the nuclear domain, PV asymmetry in polarized electron scattering is inde-
pendent of the nuclear structure, and the neutrino scattering cross section is propor-
tional to the electron scattering cross section. Corresponding formulae are discussed
below.

93

In the real world, heavy quarks of other flavors will contribute to the isoscalar part of the weak current. These quarks can exist as virtual $q, \bar{q}$ pairs in a nucleus. Only the contribution of s, $\bar{s}$ quarks will be taken into account because quarks of other flavors are much heavier and their influence can be neglected. The additional isoscalar piece of the weak neutral current is then

$$\delta J_\mu^{(0)} = -\frac{1}{2} \bar{s} \gamma_\mu (1 - \gamma_5) s \tag{8.2}$$

The axial-vector part of this current cannot contribute to the processes considered here because initial and final states of the target have $J^\pi = 0^+$. Thus the vector part of the strange current can be studied by observing the contribution it makes to the processes discussed here.

Let us consider the PV part of the inelastic polarized electron scattering. The PV asymmetry A is defined in the usual way:

$$A \equiv \frac{d\sigma_\uparrow - d\sigma_\downarrow}{d\sigma_\uparrow + d\sigma_\downarrow} \tag{8.3}$$

Then the same way of reasoning that was used in the case of PV in the elastic scattering [2] generates the result (within the one-photon-exchange approximation)

$$A_{\text{inel}} = \left(\frac{Gq^2}{\sqrt{2}\pi\alpha} \right) \sin^2\Theta_{\text{w}} \, \xi \tag{8.4}$$

where ξ is defined by

$$\xi \equiv \left[1 - \frac{\delta F_{\text{inel}}^{(0)}(q^2)}{2 \, \sin^2\Theta_{\text{w}} \, F_{\text{inel}}^{\text{ch}}(q^2)} \right] \tag{8.5}$$

Precise definition of the form factors is given in the next chapter. Here Q designates the absolute value of the space-like four-vector of the transferred momentum squared: $Q^2 = -q_\mu q^\mu$.

The same formula without the ξ factor represents asymmetry in the nuclear domain. Deviation of A_{inel} from the simple nuclear domain result measures either

94

the strange quark contribution to the nuclear transition considered, or the degree of strong isospin symmetry breakdown. For light nuclei, isospin symmetry holds well [66] and the measured deviation would come from the strange quark effects. $\delta F_{\text{inel}}^{(0)}(q^2)$ measures directly a new nuclear matrix element of the vector strange current for all q^2 considered. To perform an informative PV electron scattering experiment, one would have to measure the inelastic charge form factor at least up to q^2 around which the figure-of-merit for the transition reaches its maximum (in reality - to still higher q^2, so that the elastic scattering radiation tail can be separated).

For neutrino-nucleus inelastic scattering the same argument as the one used for the elastic process generates the result

$$\left(\frac{d\sigma}{d\Omega d\epsilon_2}\right)_{\text{inel}}^{\nu\nu'} = \left(\frac{G q^2}{\sqrt{2}\pi\alpha}\right)^2 \sin^4\Theta_w \left(\frac{d\sigma}{d\Omega d\epsilon_2}\right)_{\text{inel}}^{ee'} \xi^2 \qquad (8.6)$$

where the factor ξ has been defined above in (8.5). Here one encounters the second power of the small quantity G on the right hand side, so the effect is very small. However, in principle, this relation can be used to make a model-independent prediction of the inelastic neutrino scattering cross section in the nuclear domain approximation[1] (the same formula with no ξ^2 factor). One can use the corresponding elastic relation to determine neutrino flux (which is the largest source of uncertainty in neutrino experiments [69, 70]), and thus to predict the counting rate for the inelastic case.

It is important to note that the above relations are true to all orders in QCD.

If one neglects meson exchange currents (MEC), the Coulomb multipole operator becomes a one-body operator. If one further assumes both ground and excited $(0^+0)^*$ states to consist of nucleons in s-states only, then the spin-orbit part of the Coulomb operator does not contribute to the inelastic form factor (spin-orbit corrections to A_{el} due to 15% D-state admixture in $(0^+0)_{\text{gnd}}$ have been estimated to be

---

[1]This excitation is, in principle, easier to detect than the elastic scattering. The excited state is unstable, and one would observe two new slow charged particles in the final state p+^{3}H (one of which, ^{3}H, experiences β-decay) rather than just recoiling neutral ^{4}He in the elastic case.

95

negligible [71]). Then the nuclear structure cancels from the ratio of the form factors, leaving only single nucleon form factors behind:

$$\left. \frac{\delta F_{\text{inel}}^{(0)}(q^2)}{F_{\text{inel}}^{\text{ch}}(q^2)} \right|_{S-\text{state}} \rightarrow \frac{G_E^{(s)}(q^2)}{G_E^{(T=0)}(q^2)} \tag{8.7}$$

Here G_E are Sachs electric form factors. In this limit, nuclear structure does not enter the results for the PV asymmetry, and for the same q^2

$$\frac{A_{\text{inel}}}{A_{\text{el}}} = 1 \tag{8.8}$$

Deviations of the magnitude of the ratio from unity could allow one to test (independently of the nucleon strangeness issue) the validity of the nuclear picture that neglects MEC. In this test one compares (for a pure excited state) two experimental quantities rather than an experiment to a (model-dependent) impulse approximation calculation as is usual. If one measures elastic and inelastic asymmetries in the same experiment, their ratio is independent of the polarization of the electron beam. Some of the helicity−beam-parameters correlations, which constitute the most important class of systematic errors in asymmetry measurements [72], will also be reduced in this ratio.

The foregoing analysis is valid for any light (0^+0) nucleus. In the rest of the present work, however, the ^{4}He nucleus will be considered, because it is a practically important example. Experiments to determine the ground-state nuclear matrix element of the strange current from the asymmetry in the elastic polarized electron scattering on that nucleus are planned for CEBAF [67, 68]. It could be possible to use the same equipment to measure the analogous inelastic process. The possibility of measuring inelastic neutrino scattering on ^{4}He is also discussed [73]. It should be noted that isospin symmetry holds well for the ^{4}He nucleus [66]. To be able to make real use of the relations of this chapter between elastic and inelastic processes, one should measure $F_{\text{inel}}^{\text{ch}}(q^2)$ for higher momentum transfers. To make an estimate of

96

where in q^2 the figure-of-merit for the PV asymmetry has a maximum, and whether it is reasonable to expect that the inelastic charge form factor is large enough at this q^2 to allow measuring the cross section, the existing low-q^2 data for ^{4}He is explained here within three simple models for the $(0^+0)^*$ state. The corresponding curves for the inelastic form factor are projected to higher q^2. Very few measurements of $F_{inel}^{ch}(q^2)$ have been performed so far [74].

97

Chapter 9

Inelastic Charge Form Factor of ^{4}He

In the energy level diagram of ^{4}He in Fig. 9.1, taken from [75], one can see that this nucleus actually has the ground and first excited states with the required quantum numbers. The $(0^+0)^*$ excited state lies at 20.21 MeV, just above the threshold of the break-up into p+^{3}H at 19.8 MeV. A discussion of the accuracy of the quantum numbers determination for this state is presented in [74, 76]. It is the lowest excited state of ^{4}He, with the next closest resonant level (0^-0) at 21.01 MeV. Thus to detect excitation of the $(0^+0)^*$ level one needs energy resolution better than 0.9 MeV. CEBAF's Hall A detectors will have high momentum resolution of $\delta p/p \simeq 10^{-4}$, thus making detection of the first excited state possible. This state was observed as a narrow Breit-Wigner resonance with $\Gamma \simeq 240$ keV in the inelastic electron scattering experiment in Mainz [74] (see Fig. 9.2). Radiative corrections were subtracted while analyzing the data, and the break-up background was separated by fitting it with a smooth curve. However, the inelastic charge form factor of ^{4}He was measured in this experiment only up to $q^2 < 2.4$ fm^{-2} and experimental errors are large.

98
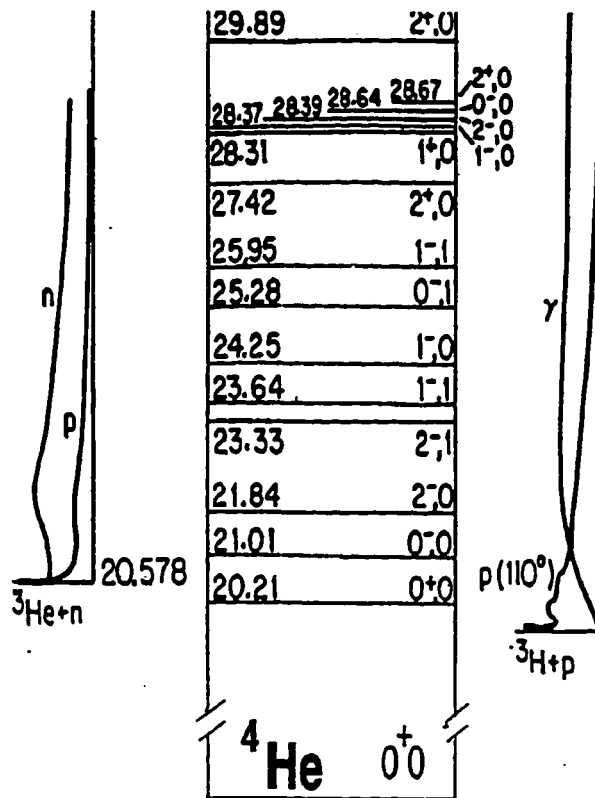
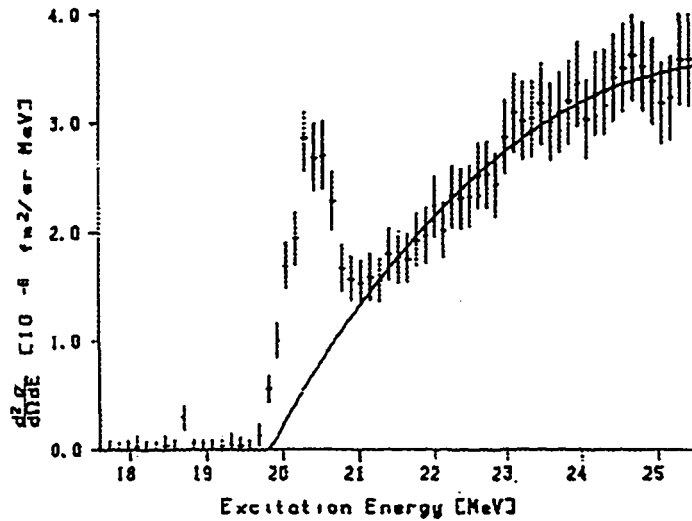Figure 9.1: Energy levels diagram of ^{4}He. J^π, T quantum numbers are shown. All energies are in MeV.

Figure 9.2: Double differential cross section for ^{4}He$(e\,e')^4$He. The solid line represents the break-up background. The (0^+0) excitation at 20.21 MeV is seen as a sharp resonance. Taken from [74].

In the analysis of the $(0^+0)^*$ resonance there arise questions of how well one can take into account the presence of the break-up background, as well as parity and isospin mixing with the neighboring states and the continuum. These questions need to be answered for obtaining quantitative predictions for experiments with the $(0^+0)^*$ state. At the same time, their consideration makes the analysis significantly more difficult. It would seem reasonable to have first an experimental result whether the resonance can be discerned from the background at the q^2 of interest. Since the goal of the present work is to provide a qualitative estimate of what these q^2 are, and whether the $(0^+0)_{gnd} \to (0^+0)^*$ transition can be used in future electroweak experiments, the above mentioned complications will not be considered here. Pure quantum numbers and a resonant character are assumed for the $(0^+0)^*$ state. Just one note can be made here, that an admixture of the (0^-0) state cannot contribute to the inelastic electron scattering cross section or inelastic PV asymmetry because each of them contains a matrix element of the EM current at least once. This current

100

has no multipole capable of connecting the (0^+0) and (0^-0) states. For neutrino scattering, however, there exists a pure axial-current term, and one still faces the question of parity mixing.

Only the Coulomb multipole $\hat{\mathcal{M}}_{0,0}^{coul}$ can contribute to excitation of the $(0^+0)^*$ level in electron scattering, so by measuring a differential cross section (with the break-up background subtracted) one measures the inelastic charge form factor of the transition. To define what exactly is meant here by the charge form factor one can write a fomula for the electron scattering cross section integrated over the resonance (with a break-up background and radiative corrections excluded):

$$\left(\frac{d\sigma}{d\Omega}\right)^{ee'}_{(0^+0)_{gnd} \to (0^+0)^*} = Z^2 \sigma_m \frac{q^4}{\bar{q}^4} |\ F^{ch}_{inel}(q^2)\ |^2 r \qquad (9.1)$$

Here

$$r^{-1} = 1 + \frac{2\epsilon_1}{M_T} \sin^2 \frac{\theta}{2} \qquad (9.2)$$

is a recoil factor and

$$\sigma_M \equiv \frac{\alpha^2 \cos^2(\theta/2)}{4\epsilon_1^2 \sin^2(\theta/2)} \qquad (9.3)$$

is Mott cross section. The first two factors on the right hand side are chosen to normalize the form factor in the same formula for the elastic case to $F^{ch}_{el}(0) = 1$.

The elastic form factor of ^{4}He has been measured up to $q^2 \simeq 45$ fm^{-2} [77]. It was parameterized well analytically in the region below $q^2 \simeq 12$ fm^{-2} by the formula [78]

$$F^{ch}_{el}(q^2) = \left[1 - (a^2 q^2)^6\right] \exp\left(-b^2 q^2\right) \qquad (9.4)$$

where $a = 0.316$ fm and $b = 0.675$ fm. Figure 9.3 shows the existing data on the elastic and inelastic form factors of ^{4}He in this region.

101

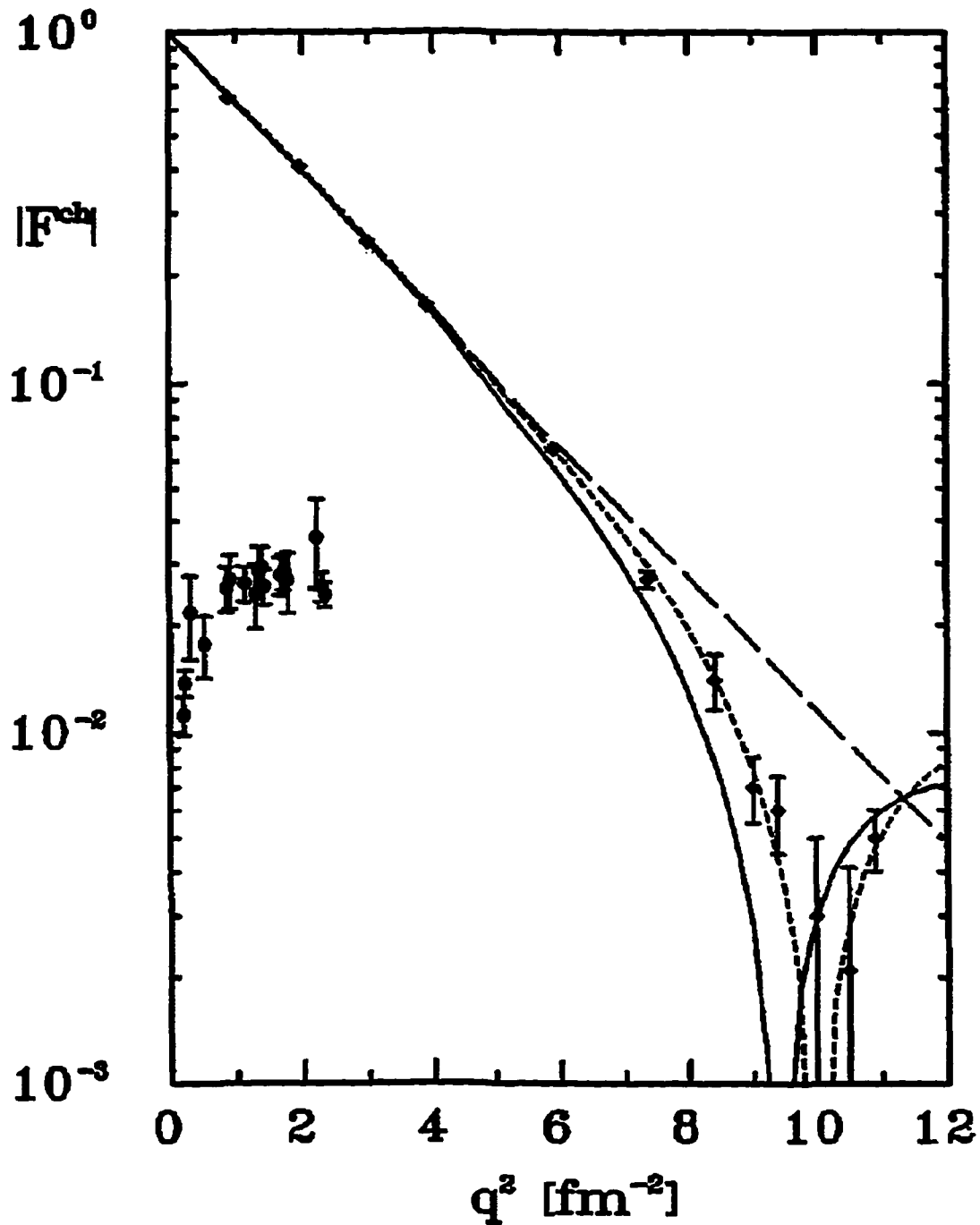Figure 9.3: Experimental data on ^{4}He form factors. Points with circles represent $F^{ch}_{inel}(q^2)$ [74], while points with diamonds represent $F^{ch}_{el}(q^2)$ [78]. Short-dashed line represents the analytical approximation of $F^{ch}_{el}(q^2)$. Long-dashed and solid lines represent the s.h.o. model and the finite square well model fits to $F^{ch}_{el}(q^2)$ correspondingly.

102

Here, an attempt is made to explain the measured low-q^2 data on the inelastic charge form factor, and to predict its behavior at higher q^2, using the following three simple models of the ^{4}He nucleus:

- Collective model of Werntz and Überal [79],

and two shell models with potentials of:

- Simple harmonic oscillator,

- Finite square-well.

Far more sophisticated calculations of the structure of the $(0^+0)^*$ state in ^{4}He have been performed [80, 81]. However, the objectives of the present investigation can be achieved performing the analysis within the mentioned simple models.

9.1 Collective Model ("Breathing Mode")

This model of the (0^+0) excitation of ^{4}He was developed first by Werntz and Überal in 1964 [79]. They approximated the ^{4}He nucleus by a system with a continuous matter distribution $\rho_0(r)$. The first excited $(0^+0)^*$ state is modeled by the system experiencing radial scaling oscillations ("breathing mode"). The scaling factor is assumed to be small and to change harmonically. This breathing mode motion is quantized, and position of the first excitation of the harmonic oscillator is fit to the measured energy of the lowest $(0^+0)^*$ state of ^{4}He. All the parameters of the model are now determined, and one obtains the following formula for the inelastic charge form factor:

$$F_{inel}^{ch}(q^2) = \text{const} \times q \, \frac{dF_{el}^{ch}(q^2)}{dq} \tag{9.5}$$

103

It seems, however, to be an oversimplification to treat ^{4}He, consisting of just four nucleons, as a continuous matter distribution experiencing, as a whole, scaled oscillations. One can leave an overall constant factor to be fit to the existing data for $F_{\text{inel}}^{\text{ch}}(q^2)$ at low q^2 [74]. For $F_{\text{el}}^{\text{ch}}(q^2)$ the analytic expression mentioned in the previous section is used. The data is explained well by const=0.04 with χ^2/N=0.98 if one excludes the first three points with the lowest q^2 (see results in Fig. 9.6). One cannot fit all experimental points within this model. The first three points actually come from a different experiment and, keeping in mind the difficulty of the measurement, this fact can be a possible justification to consider the curve that fits well the rest of the experimental data. This issue will be addressed in greater detail when discussing the finite square-well model.

9.2 Single-Particle Models

9.2.1 General discussion

One can start by considering the $(0^+0)^*$ state of ^{4}He to be discrete, and apply here the general formula for the multipole decomposition of the electron scattering cross section. Only the J=0 Coulomb multipole will contribute to the process investigated. The Coulomb operator is taken to be a single-particle operator, since meson exchange currents are known to make only a minor contribution to electron scattering through the isoscalar charge multipoles, for the intermediate q^2 that are of interest here. Then the Coulomb monopole matrix element is decomposed in a single-particle basis [46]

$$\frac{Z}{\sqrt{4\pi}}F^{\text{ch}}(q^2) \equiv \langle 0^+0; f \parallel \hat{\mathcal{M}}_0^{\text{coul}}(q) \parallel 0^+0; i \rangle$$

$$= \frac{1}{\sqrt{2}}\sum_{a,b}\langle a \parallel \mathcal{M}_0^{(0)}(q) \parallel b \rangle \ \Psi_{00}^{fi}(ab) \qquad (9.6)$$

104

where

$$\mathcal{M}_0^{(0)}(q) = \frac{1}{\sqrt{4\pi}} j_0(qr)$$

is a single-particle Coulomb operator and

$$\Psi_{00}^{fi}(ab) = \langle 0^+0; f \mid c_a^+ c_b \mid 0^+0; i \rangle \tag{9.7}$$

are just numerical coefficients.

For the ground state of ^{4}He a closed-shell configuration with all four nucleons in $(1s)$ state is assumed. Under this assumption the elastic charge form factor is approximated well in the region of interest by both models considered here (see Fig. 9.3). Thus for calculating $F_{el}^{ch}(q^2)$ one considers the filled s-shell, so $\Psi_{00}^{fi} = 2\delta_{ab}$ and

$$F_{el}^{SM}(q^2) = \langle 1s \mid j_0(qr) \mid 1s \rangle \tag{9.8}$$

Let us apply selection rules to the states which the Coulomb monopole operator, as a single-particle operator, will see among those comprising the $(0^+0)^*$ excited state:

$\mid (1s)^{-1}(1p) \rangle$ is ruled out by parity conservation,

$\mid (1s)^{-1}(2s) \rangle$ are allowed (as well as $\mid (1s)^{-1}(ns) \rangle$ in general),

$\mid (1s)^{-1}(1d) \rangle$ and higher l excitations are ruled out since their angular momenta cannot add to produce J=0.

In models with a continuum spectrum, $l = 0$ states from the continuum can also contribute.

For each allowed single-particle contribution to the excited state of ^{4}He there is a particle-hole transition, and for any pure particle-hole transition $\Psi_{00}^{fi}(ab) = \delta_{ar}\delta_{bs}$ in the calculation of $F_{inel}^{ch}(q^2)$. One can use any complete system of states for decomposition of the $(0^+0)^*$ state of ^{4}He, but it would be useful to find a model in which

105

contributions of the few lowest excited states approximate well the inelastic charge form factor.

While comparing form factors calculated in the shell model to experimental results, one has to multiply the former by a single nucleon form factor given by

$$f_{sn}(q^2) = \left[1 + \frac{q^2}{18.84 \text{ fm}^{-2}}\right]^{-2} \tag{9.9}$$

and corrections due to the center-of-mass motion have to be taken into account [46] (see below).

9.2.2 Simple Harmonic Oscillator Model

There are two main reasons to start the analysis by considering a simple harmonic oscillator potential model:

1. The necessary matrix elements are easy to calculate in the closed form.

2. The center-of-mass corrections to the form factor can be treated exactly.

In this model

$$F_{el}^{SM}(q^2) = e^{-y} \tag{9.10}$$

where

$$y = \frac{b_{osc}^2 q^2}{4} \tag{9.11}$$

and b_{osc} is the oscillator parameter of the model. Then

$$F_{el}^{ch}(q^2) = f_{sn} \, F_{CM} \, F_{el}^{SM}(q^2) \tag{9.12}$$

Here $F_{CM} = e^{y/4}$. This is a correction subtracting the spurious effect of the center-of-mass motion.

The oscillator parameter is determined by fitting the experimental $F_{el}^{ch}(q^2)$ for $q^2 < 10 \text{ fm}^{-2}$ (see Fig. 9.3). This is about how far in q^2 the simple harmonic oscillator

106

model can approximate the experimental $F_{el}^{ch}(q^2)$, and thus how far $F_{el}^{ch}(q^2)$ can be predicted in this model. The result of fitting is $b_{osc} = 1.39$ fm. Then for the relative energy of the (2s) state one obtains $E_{exc} = 2\hbar\omega \simeq 43$ MeV. This is about twice the energy of $(0^+0)^*$ in ^{4}He. One can try to model the excited nucleus by considering it to consist of any number of nucleons promoted to the three lowest shell-model states (i.e. 1p, 2s, 1d).

Then, in accord with the general discussion,

$$F_{inel}^{SM}(q^2) = \frac{\alpha}{2}\langle 2s \mid j_0(qr) \mid 1s \rangle \tag{9.13}$$

or upon integration of the matrix element:

$$F_{inel}^{SM}(q^2) = \frac{\alpha}{\sqrt{6}}y\ e^{-y} \tag{9.14}$$

Here α is the probability amplitude for the $(0^+0)^*$ state to be the $\mid (1s)^{-1}, (2s)\rangle$ excitation of the shell model. If the $(0^+0)^*$ state were a pure $\mid (1s)^{-1}, (2s)\rangle$ state of the shell model, α would be equal to 1. Fitting all experimental points excluding the three with the lowest q^2, one determines $\alpha = 0.18$ with $\chi^2/N = 0.92$. Again one cannot fit all the experimental points. One possible reason for that was mentioned in connection with the collective model, another is discussed in the next paragraph. The resulting curve for $F_{inel}^{ch}(q^2)$ is shown in Fig. 9.6. It is seen to follow closely the curve obtained in the "breathing mode" collective model.

There exist reasons to take the results of the simple harmonic oscillator model with a grain of salt. In calculating the charge form factor, the charge density matrix element in the integral is weighted by the square of the radial distance r^2, amplifying the contribution of the tail of the wave function. However, all states in the simple harmonic oscillator potential are bound, while the $(0^+0)^*$ state in ^{4}He lies, in fact, above the threshold of the break-up continuum. The simple harmonic oscillator model makes a poor approximation of the region of large r, which is important in

107

the problem. In momentum space this corresponds to the low-q^2 region, so a failure of an attempt to fit the first three points by a theoretical curve can be attributed to the shortcomings of the model chosen. To improve these results one has to consider the $(0^+0)^*$ state as a resonance, and to choose a shell-model potential that has a continuum spectrum. The shape of the potential that is used for small r is relatively unimportant. To make the formulae treatable, the model potential is chosen to have the shape of a finite square-well.

9.2.3 Finite Square-Well Model

Now the problem is reconsidered on more general grounds, taking into account that the final $(0^+0)^*$ state is actually a resonance in the break-up continuum. The final nuclear state is taken to be $|f\rangle = |p_2 \kappa^{(-)}\rangle$, which is an exact two-particle scattering state of p+^{3}H. All kinematical variables are defined in Fig. 9.4. Then one can follow the analysis of coincidence experiments given in [46]. The general formula for the coincidence cross section can be found there expressed in terms of

$$\mathcal{J}_\mu \equiv \frac{1}{4\pi W}(2\omega_\kappa E_1 E_2 \Omega^3)^{1/2}\langle p_2 \,\kappa^{(-)} \,|\, \int e^{i\vec{q}\cdot\vec{x}} J_\mu(\vec{x})d\vec{x} \,|\, p_1\rangle \qquad (9.15)$$

where W is the final energy of hadrons in the c.m. frame.

On the other hand, from experiment it is known that the scattering is resonant in the $(0^+0)_{\text{gnd}} \to (0^+0)^*$ channel and can be parameterized in the Breit-Wigner form:

$$\left(\frac{d\sigma}{d\Omega d\epsilon_2}\right)^{ee'}_{\text{inel}} = 4\pi\sigma_{\text{m}}\left[\frac{M_{\text{T}}}{W}\frac{\Gamma}{2\pi}\frac{1}{(W-W_{\text{R}})^2+\Gamma^2/4}\right]\frac{q^4}{\vec{q}^4}\,|\,\langle 0 \,\|\, \hat{\mathcal{M}}_0^{\text{coul}}(q) \,\|\, 0\rangle_{\text{res}}\,|^2 \qquad (9.16)$$

After integration over the electron energy, the term in the square brackets gives the recoil factor and the formula (9.1) is reproduced.

The experimental formula (9.16) for the double-differential cross section can be deduced from the general result for the coincidence cross section if one assumes
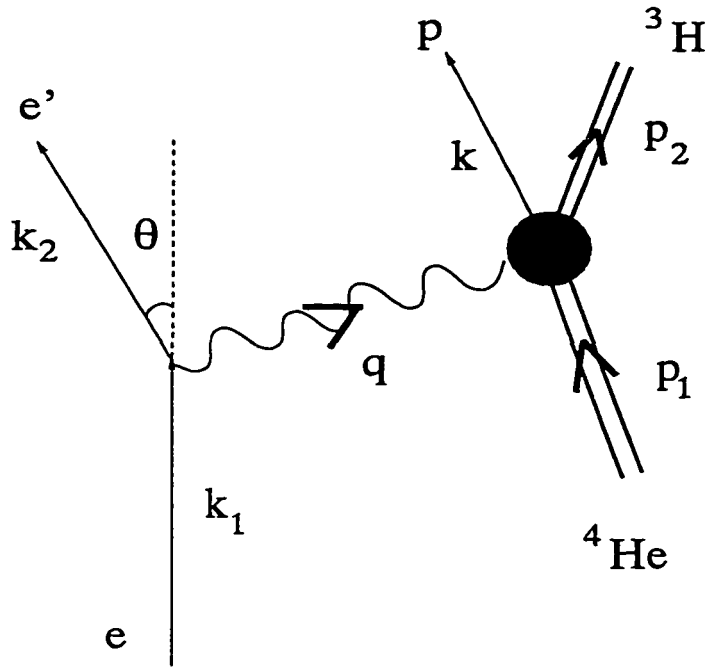
108

Figure 9.4: Diagram for the break-up scattering $^4\mathrm{He}(e\,e'p)^3\mathrm{He}$.

that the hadronic current matrix element has the following form:

$$\left(\frac{\kappa}{\pi}\right)^{1/2}\mathcal{J}_c \;=\; \left(\frac{\Gamma}{2\pi}\right)^{1/2}\frac{1}{W-W_R+i\Gamma/2}\,\langle 0\parallel\hat{\mathcal{M}}_0^{\mathrm{coul}}(q)\parallel 0\rangle_{\mathrm{res}} \tag{9.17}$$

In this formula the q-dependence is separated from the W-dependence, because the matrix element of the Coulomb operator is evaluated at the resonant energy. However, one still does not know the wave functions necessary to evaluate this matrix element.

The question is whether one can convert the general matrix element of the current into this form with the help of the single-particle decomposition of the J=0 Coulomb operator, which is the only operator to contribute to $\mathcal{J}_c$ in the considered process

$$\mathcal{J}_c \;=\; \frac{M_T}{4\pi W}\,(2\omega_\kappa\Omega)^{1/2}\langle 0;f,W\parallel\hat{\mathcal{M}}_0^{\mathrm{coul}}(q)\parallel 0;i\rangle \tag{9.18}$$

where $M_T \simeq \sqrt{E_1 E_2}$. The decomposition of Equation (9.6) is exact for any single-particle operator in any complete single-particle basis.
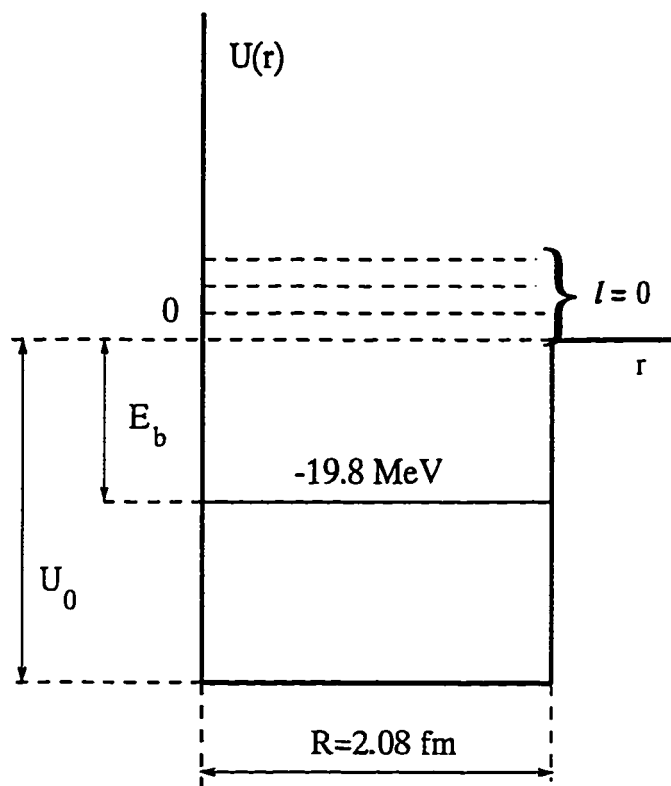
109

Figure 9.5: Potential of the finite square-well model.

110

In this work the finite square-well model potential shown in Fig. 9.5 is considered. The well parameters are adjusted to reproduce the correct single-nucleon binding energy in ^{4}He. One assumes that the $(0^+0)_{\text{gnd}}$ is a closed (1s) shell, and builds the $(0^+0)^*$ state out of the $l = 0$ continuum states. The depth of the well $U_0(R)$ is determined first as a function of R by matching wave functions at the edge of the well. Then one determines $F_{\text{el}}^{\text{SM}}(q^2, R)$ and fits the experimental data on the elastic charge form factor up to $q^2 = 10$ fm^{-2} to determine R (see Fig. 9.3). The value $R = 2.08$ fm approximates the data on $F_{\text{el}}^{\text{ch}}(q^2)$ well. Then U_0 is determined to be $U_0 = 45$ MeV. Coulomb interaction between p and ^{3}H in the final state, which has the potential $U_{\text{coul}}(R) \simeq 0.7$ MeV at the edge of the square-well, is neglected[1].

The Coulomb monopole matrix element of the transition can then be expanded as

$$\langle 0; f, W \mid \hat{\mathcal{M}}_0^{\text{coul}}(q) \mid 0; i \rangle = \int_0^\infty dE \; \mathcal{ME}(q, E) \; \Psi^{fi}(E, W) \qquad (9.19)$$

where

$$\mathcal{ME}(q, E) \equiv \langle l = 0, \; E \mid \mathcal{M}_0(q) \mid 1s \rangle \qquad (9.20)$$

is the single-particle matrix element and

$$\Psi^{fi}(E, W) \equiv \langle 0^+0; f, W \mid c_E^\dagger c_{1s} \mid 0^+0; i \rangle \qquad (9.21)$$

are numerical coefficients.

These relations are exact if the Coulomb monopole is a single-particle operator and if the ground state of ^{4}He is a closed (1s) shell. One remembers that the q-dependence should be separated from the W-dependence in order to cast the matrix element into the form reproducing the cross section of the Breit-Wigner type. This

---

[1] It is assumed here, as in the previous two models, that strong isospin is a good symmetry for the nuclear transition matrix element (even though it is broken by the Coulomb and mass effects in the decay chanels).

111

can be achieved most simply if the single-particle energy E-dependence factors from $\mathcal{ME}(q, E)$. If this separation occurs, the integral over the energy E can be calculated, producing a constant. The shape of the charge form factor of the transition will then coincide with the shape of the single-particle Coulomb monopole matrix element.

Analysis shows that for the single-particle energies up to $E \simeq 10$ MeV and for momentum transfers q^2 ranging from 1 to about 10 fm^{-2}, the E-dependence of the single particle matrix element can be separated, with an accuracy better than 20%, in the following form:

$$\mathcal{ME}(q, E) \simeq \sqrt{\frac{E}{W_R}}\, \mathcal{ME}(q^2, W_R) \tag{9.22}$$

Then if one cuts off the integral over the energy in Equation (9.19) at 10 MeV, the following formula for the charge form factor for transferred momentum below 10 fm^{-2} is obtained

$$F_{inel}^{SM}(q^2) = \text{const} \times \mathcal{ME}(q^2, W_R) \tag{9.23}$$

While comparing this result with the experimental $F_{inel}^{ch}(q^2)$, the c.m. corrections are taken from the simple harmonic oscillator model. Fitting *all* the experimental data on $F_{inel}^{ch}(q^2)$, one obtains const=2.5 with χ^2/N =1.14. Let us consider the first three points of lowest q^2 that troubled the first two models. Even if one forgets about them and fits only the remaining data, the curve that is obtained predicts these points to be where they actually have been measured. This fact adds to the confidence in the model considered. The results are presented in Fig. 9.6.

9.2.4 Numerical results

Figure 9.6 shows how well the inelastic charge form factor curves calculated in the three different models of the ^{4}He nucleus explain experimental results at low q^2.

Predictions for higher q^2 are also projected by these curves. The correct behavior of the form factor at $q^2 \to 0$ is preserved in the single-particle models because the same potential has been used to calculate the ground and excited states of the nucleus. One can see that the best fit to the data is provided by the model with the finite square-well potential. The inelastic charge form factor predicted by this model is seen to be 4 to 10 times smaller than the elastic one in the region of interest around $q^2 \simeq 4 - 7\text{fm}^{-2}$.

To see how useful the $(0^+0)_{\text{gnd}} \to (0^+0)^*$ transition in ^{4}He can be in PV experiments, the corresponding figure-of-merit is discussed here. The figure-of-merit $\mathcal{F}$ is defined as [60]

$$\mathcal{F} \equiv \left(\frac{d\sigma}{d\Omega}\right) A^2 \tag{9.24}$$

It represents a contribution of the internal properties of the target and kinematics of the experiment to the statistical uncertainty in the PV asymmetry measurement. The latter can be calculated as

$$\frac{\delta A}{A} = [\mathcal{F} X_0]^{-1/2}$$
$$X_0 = \mathcal{L} \, \Delta\Omega \, T_0 \tag{9.25}$$

where $\mathcal{L}$ is the luminosity, $\Delta\Omega$ is the detector solid angle, and T_0 is the running time. Estimates for the inelastic PV asymmetry figure-of-merit are shown in Figure 9.7 for $\theta = 10^\circ$. Let us assume the highest CEBAF luminocity for the ^{4}He target of $\mathcal{L} = 5 \times 10^{38}\text{cm}^{-2}\text{s}^{-1}$, $\Delta\Omega = 10\text{msr}$ (angular acceptance of CEBAF Hall A high resolution spectrometer), 1000 hours of running time, and a 100% polarization of the incident electron beam. Then a statistical error of $\delta A/A \simeq 9 - 13\%$ in measuring the PV asymmetry at $\theta = 10^\circ$ can be achieved in an experiment performed at the incident beam energy $E \simeq 1.7 - 2.2$ GeV (which corresponds to $q^2 = 2.2 - 3.7$ fm^{-2}), where the figure-of-merit curve has its maximum, depending on the nuclear state
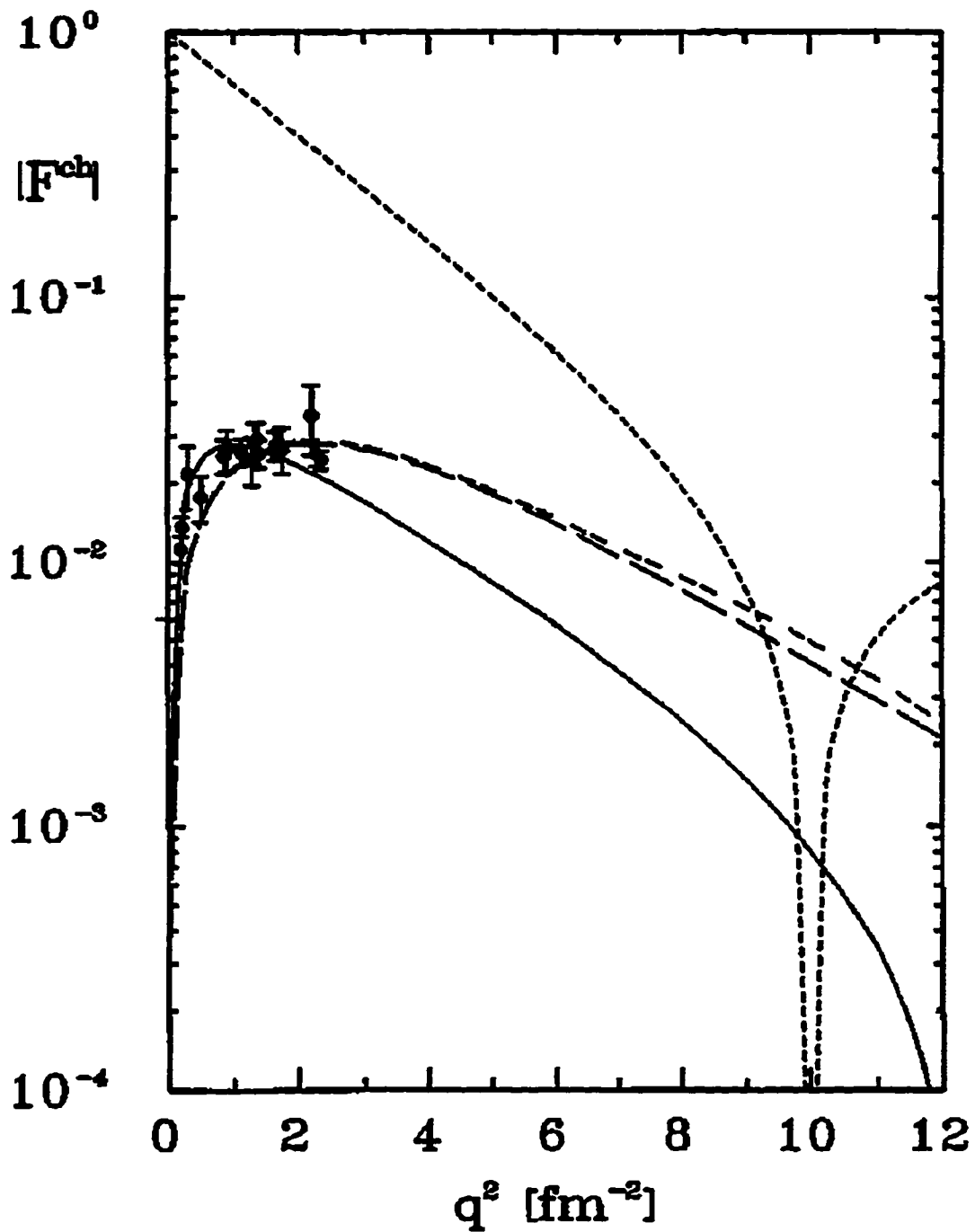
113

Figure 9.6: ⁴He inelastic charge form factor. Light and heavy dashed lines represent the predictions of the collective ("breathing mode") model and the s.h.o. model, correspondingly. Solid line is predicted by the finite square-well model. $F_{el}^{ch}(q^2)$ of ⁴He represented by the short-dashed line is provided for comparison.
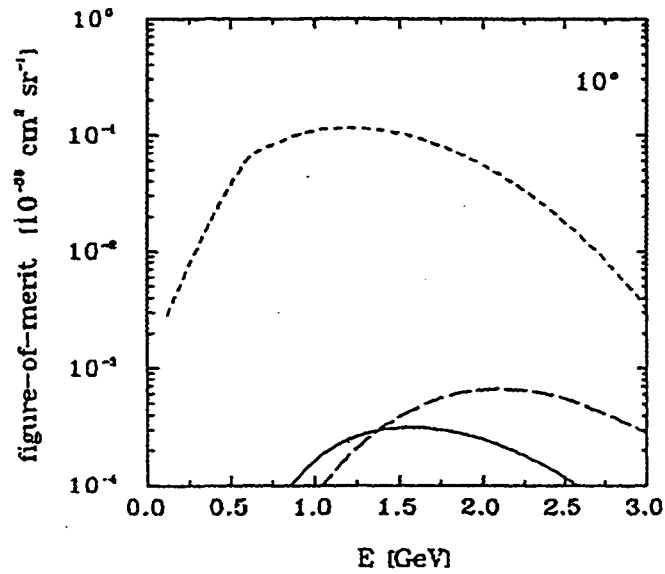
114

Figure 9.7: Figure-of-merit for the PV asymmetry measurements on ^{4}He. The short-dashed line represents the elastic scattering figure-of-merit. The long-dashed and solid curves are predicted by the s.h.o. and finite square-well models for the $(0^+0)_{gnd} \rightarrow (0^+0)^*$ transition in ^{4}He, correspondingly.

model chosen. However, such an experiment on ^{4}He would not be easy to interpret due to the complicated nuclear structure of the $(0^+0)^*$ state.

115

Chapter 10

Conclusions to Part II

1. General relations between PV electron asymmetries and neutrino cross sections for inelastic $(0^+0)_{\text{gnd}} \rightarrow (0^+0)^*$ transitions in nuclei have been obtained. It is shown, for example, that within the single-nucleon picture of the nucleus the inelastic PV asymmetry is identical to that in the elastic scattering. For an isolated nuclear state with pure quantum numbers, deviation of this ratio from one signals the presence of exchange currents.

2. The inelastic neutrino scattering cross section is predicted to be proportional to the inelastic electron scattering cross section. This prediction can in principle be tested experimentally, free of uncertainty in the neutrino flux, if the flux is determined from the corresponding elastic neutrino scattering experiment.

3. The magnitude of the inelastic neutrino scattering charge form factor determines whether such experiments are feasible. The low-q^2 inelastic charge form factor data for the $(0^+0)_{\text{gnd}} \rightarrow (0^+0)^*$ transition in ^{4}He has been explained within three simple models of the excited state. An estimate of this form factor for intermediate transferred momentum (for q^2 from 3 to 10 fm^{-2}) has been made. This estimate can serve as a zeroth-order approximation to the real situation. It is predicted that the

116

inelastic PV asymmetry can be measured with a statistical accuracy of about 9-13%
in the favorable experimental setup considered.

4. Knowledge of the inelastic charge form factor $F^{ch}_{inel}(q^2)$ for ^{4}He is the key
ingredient to all the above predictions. It is important to measure $F^{ch}_{inel}(q^2)$ accurately
to higher momentum transfers. The non-resonant background is expected to increase
with increasing q^2. Can one still see the resonant $(0^+0)^*$ peak at q^2 that would
be used for measuring the PV asymmetry? If electron scattering experiments at
intermediate q^2 give a positive answer, performing state-of-the-art calculation of the
inelastic charge form factor with inclusion of the break-up continuum, wrong parity
and isospin admixtures, and effects of MEC would be in order.

5. To the extent to which radiative corrections and non-resonant background
can be subtracted, and the wrong parity and isospin admixtures taken into account,
measurement of the inelastic PV asymmetry provides determination of a new *nuclear*
transition matrix element of the vector strange current. However, due to the complex
structure of the excited state, and the fact that the transition form factor is much
smaller than the elastic one, the inelastic PV experiment is significantly more difficult
to perform and interpret. Such an experiment will not allow one to gain a better un-
derstanding of the *nucleon* strangeness than can be obtained from the corresponding
elastic experiments.

117

Appendix A

PCAC in the linear realization of the $\sigma - \omega$ model

The objective of this Appendix is to demonstrate that the obtained spatial two-body AXC of order $O(1/M)$ make PCAC satisfied in coordinate space to this order

$$i\left[V(r), \rho_5^{(1)\,(\pm)}\right] + \nabla \cdot \mathbf{J}_5^{(2)\,(\pm)} = O(m_\pi^2) \tag{A.1}$$

for the potentials and AXC corresponding to various exchanged mesons. The analysis in this Appendix is performed for one, "direct", part of the current. The analysis of the other part can be performed identically, by interchanging the roles of the two nucleons involved.

First, consider the σ-model alone. If one does not impose the limit of a very large scalar mass, then there are two types of spatial AXC present: one is due to the simple σ-meson exchange, while the second originates from the diagrams involving the π-production fragments. In momentum space these currents are given by the formulae:

118

$$J_5^{(2)\,(\pm)}(\sigma) \;=\; F_A \frac{g^2}{M}\,\tau_\pm(2)\,\frac{1}{l^2+m_s^2}\,\frac{k}{k^2+m_\pi^2}\,\vec{\sigma}(2)\cdot k \tag{A.2}$$

$$J_5^{(2)\,(\pm)}(\pi) \;=\; F_A \frac{g^2}{M}\,\tau_\pm(2)\,\frac{1}{l^2+m_s^2}\left\{1-q-\frac{k}{k^2+m_\pi^2}\,(l^2+m_\pi^2)\right\} \tag{A.3}$$

for the "sigma" and "pion" currents, accordingly. The corresponding currents in coordinate space are

$$J_5^{(2)\,(\pm)}(\sigma)(x_1\,x_2\,k) = \frac{1}{M}\,\tau_\pm(2)\,e^{ik\cdot x_2}\,\frac{k}{k^2+m_\pi^2}\,\vec{\sigma}(2)\cdot k\;\; V_\sigma(r) \tag{A.4}$$

where $r \equiv x_1 - x_2$ and

$$V_\sigma(r) = \frac{g^2}{4\pi}\,\frac{e^{-m_s r}}{r} \tag{A.5}$$

is the scalar potential calculated within the same σ-model framework; and

$$J_5^{(2)\,(\pm)}(\pi)(x_1\,x_2\,k) = \frac{g^2}{M}\,\tau_\pm(2)\,\vec{\sigma}(2)\cdot(-i\nabla_2)\left\{ -e^{ik\cdot x_1}\frac{k}{k^2+m_\pi^2}\frac{1}{4\pi}\frac{e^{-m_s r}}{r} \right.$$
$$\left. +e^{ik\cdot x_2}\left[-2i\nabla_r+k\left(\frac{m_s^2-m_\pi^2}{k^2+m_\pi^2}-1\right)\right]\frac{1}{8\pi}\,e^{\frac{i}{2}k\cdot r}\underbrace{\int_{-\frac12}^{\frac12} dv\, e^{ivk\cdot r}\,\frac{e^{-L_\sigma r}}{L_\sigma}}_{K} \right\} \tag{A.6}$$

where

$$L_\sigma^2 = k^2(\tfrac{1}{4}-v^2) + m_s^2(\tfrac{1}{2}-v) + m_\pi^2(\tfrac{1}{2}+v) \tag{A.7}$$

Consider the combination $(-ik)\cdot J_5^{(2)\,(\pm)}(\pi)(x_1\,x_2\,k)$ in the limit $m_\pi^2\to 0$. Use

$$(-ik)\cdot\left[-2i\nabla_r+k\left(\frac{m_s^2-m_\pi^2}{k^2+m_\pi^2}-1\right)\right]\left[e^{i(\frac12+v)\,k\cdot r}e^{-L_\sigma r}\right] \;\to\;$$
$$\left[-i(2v\,k^2+m_s^2)+2k\cdot r\frac{L_\sigma}{r}\right]\left[e^{i(\frac12+v)\,k\cdot r}e^{-L_\sigma r}\right] \tag{A.8}$$

Thus, for the last term in the current one obtains after a suitable integration by parts:

$$(-ik)\cdot K \;=\; \frac{1}{8\pi}\,e^{ik\cdot x_2}\left\{ \overbrace{\int_{-\frac12}^{\frac12} dv\left[-i\,(2v\,k^2+m_s^2)\frac{e^{-L_\sigma r}}{L_\sigma}+2i\frac{d}{dv}\left(\frac{e^{-L_\sigma r}}{r}\right)\right]e^{i(\frac12+v)\,k\cdot r}}^{I_1} \right.$$
$$\left. - \underbrace{2i\frac{e^{-L_\sigma r}}{r}\,e^{i(\frac12+v)\,k\cdot r}\Big|_{-\frac12}^{\frac12}}_{I_2} \right\} \tag{A.9}$$

119

$$\frac{d}{dv}\left(\frac{e^{-L_\sigma r}}{r}\right) = -e^{-L_\sigma r}\frac{dL_\sigma}{dv} = \frac{e^{-L_\sigma r}}{2L_\sigma}\left[2v\,\mathbf{k}^2 + m_s^2\right] \tag{A.10}$$

Hence the first term equals zero $I_1 = 0$. To calculate the second term use

$$L_\sigma(v = \tfrac{1}{2}) = 0$$
$$L_\sigma(v = -\tfrac{1}{2}) = m_s \tag{A.11}$$

Then

$$(-i\mathbf{k})\cdot\mathbf{K} = -\frac{i}{r}\frac{1}{4\pi}\left(e^{i\mathbf{k}\cdot\mathbf{x}_1} - e^{-m_s r}e^{i\mathbf{k}\cdot\mathbf{x}_2}\right) \tag{A.12}$$

and the equation for the pion current reduces in the limit $m_\pi \to 0$ to

$$(-i\mathbf{k})\cdot\mathbf{J}_5^{(\pm)}(\pi) = \frac{1}{M}\,\tau_\pm(2)\,\vec{\sigma}(2)\cdot\nabla_2\,[\,\underbrace{\frac{g^2}{4\pi}\frac{e^{-m_s r}}{r}}_{=V_\sigma(r)}\,e^{i\mathbf{k}\cdot\mathbf{x}_2}\,] \tag{A.13}$$

The result for the full current becomes then

$$(-i\mathbf{k})\cdot\left(\mathbf{J}_5^{(\pm)}(\pi) + \mathbf{J}_5^{(\pm)}(\sigma)\right) = \frac{1}{M}\,\tau_\pm(2)\,e^{i\mathbf{k}\cdot\mathbf{x}_2}\,\vec{\sigma}(2)\cdot[\nabla_2\,V_\sigma(r)] \tag{A.14}$$

Recall that

$$i[V_\sigma(r),\,\rho_5^{(1)(\pm)}(\mathbf{x}\,\mathbf{x}_2)] = -\frac{F_A}{M}\,\tau_\pm(2)\,\delta^{(3)}(\mathbf{x} - \mathbf{x}_2)\,\vec{\sigma}(2)\cdot[\nabla_2\,V_\sigma(r)] \tag{A.15}$$

The final result for the axial current of the σ-model shows that PCAC is satisfied to order $O(1/M)$ when the relevant AXC are included in the analysis

$$i\left[V_\sigma(r),\,\rho_5^{(1)\,(\pm)}\right] + \nabla\cdot\mathbf{J}_5^{(2)\,(\pm)}(\pi + \sigma) = 0 \tag{A.16}$$

120

Now, the ω-meson can be introduced in the problem. The PCAC theorem must be satisfied for the full $\sigma - \omega$ model at each order in $1/M$. Since PCAC is satisfied to order $O(1/M)$ by the currents of the σ-model alone, the same must be true separately for the currents originating from the ω-meson exchange (with the corresponding nuclear potential):

$$i\left[V_\omega(r), \rho_5^{(1)\,(\pm)}\right] + \nabla \cdot \mathbf{J}_5^{(2)\,(\pm)}(\omega) = O(m_\pi^2) \tag{A.17}$$

The AXC due to the ω-meson exchange in momentum space is

$$\mathbf{J}_5^{(2)\,(\pm)}(\omega) = F_A \frac{g_v^2}{M} \tau_\pm(2) \frac{\mathbf{k}}{\mathbf{k}^2 + m_\pi^2} \frac{\vec{\sigma}(2) \cdot \mathbf{l}}{\mathbf{l}^2 + m_v^2} \tag{A.18}$$

The corresponding current operator in coordinate space has the form

$$\mathbf{J}_5^{(2)\,(\pm)}(\omega)(\mathbf{x}_1\,\mathbf{x}_2\,\mathbf{k}) = \frac{F_A}{M} \tau_\pm(2)\, e^{i\mathbf{k}\cdot\mathbf{x}_2} \frac{\mathbf{k}}{\mathbf{k}^2 + m_\pi^2}\, i\,\vec{\sigma}(2)\cdot[\nabla_2\, V_v(r)] \tag{A.19}$$

where

$$V_\omega(r) = \frac{g_v^2}{4\pi} \frac{e^{-m_v r}}{r} \tag{A.20}$$

It is easy to calculate the commutator of the single-body axial charge $\rho_5^{(1)\,(\pm)}$ with the ω-exchange potential

$$i[V_\omega(r), \rho_5^{(1)(\pm)}(\mathbf{x}\,\mathbf{x}_2)] = -\frac{F_A}{M} \tau_\pm(2)\, e^{i\mathbf{k}\cdot\mathbf{x}_2}\, i\vec{\sigma}(2)\cdot[\nabla_2\, V_\omega(r)] \tag{A.21}$$

Then the PCAC equation (A.17) is indeed satisfied to order $O(1/M)$.

121

Appendix B

General formulae for the weak cross sections and rates

The results for semileptonic weak rates and cross sections for transitions between discrete nuclear states with pure quantum numbers, which are presented in this Appendix, are taken from the references [7] and [49]. The only additional assumptions made in the derivation there are the existance of a local current density operator $\hat{\mathcal{J}}_\mu(\mathbf{x})$ and sufficient localization of the target in space.

A. Muon capture rate

When the initial nucleus has a nonzero angular momentum $\mathbf{J}_i$, the total angular momentum for a muon−nucleus system $\mathbf{F} = \mathbf{J} + \mathbf{S}$ can take two values $F = J \pm \frac{1}{2}$.

The muon capture rate between two nuclear levels from a given initial hyperfine state:

$$\omega_F(i \to f) = \bar{\omega}(i \to f) + \delta\omega_F(i \to f) \tag{B.1}$$

122

where $\delta\omega_F(i \to f)$ satisfies identically the condition

$$\sum_F (2F + 1)\delta\omega_F(i \to f) = 0 \tag{B.2}$$

Averaging with a statistical operator

$$\rho_F = \frac{2F + 1}{\sum_F(2F + 1)} \tag{B.3}$$

over initial hyperfine states produces immediately

$$\sum_F \rho_F \omega_F(i \to f) = \bar{\omega}_F(i \to f) \tag{B.4}$$

The muon capture rate, statistically averaged over different hyperfine states, is given by

$$\begin{aligned}
\bar{\omega}(i \to f) &= \frac{G^2 \nu^2}{2\pi} |\phi_{1s}|_{av}^2 \frac{4\pi}{2J_i + 1} \left[\sum_{J=0}^{\infty} |\langle J_f \| \hat{\mathcal{M}}_J(\nu) - \hat{\mathcal{L}}_J(\nu) \| J_i \rangle|^2 \right. \\
&\quad \left. + \sum_{J \geq 1}^{\infty} |\langle J_f \| \hat{T}_J^{mag}(\nu) - \hat{T}_J^{el}(\nu) \| J_i \rangle|^2 \right] \mathcal{R}
\end{aligned} \tag{B.5}$$

where the neutrino energy ν is determined from the energy conservation equation: $\nu = m_l - \epsilon_b + E_i - E_f$.

$$|\phi_{1s}|_{av}^2 = R' \frac{(Z\alpha m_l)^3}{\pi} \left(\frac{1}{1 + m_l/M_T} \right)^3 \tag{B.6}$$

where m_l is the lepton mass ($m_\mu = 105.7 \text{MeV}$), M_T and Z are the target nucleus mass and charge, and R' is a reduction factor that accounts for the finite spatial extent of the nuclear charge distribution (for example, $R'(^6\text{Li}) = 0.95$, while $E(^6\text{He}) - E(^6\text{Li}) = 4.021 \text{MeV}$). The recoil factor $\mathcal{R}$ can be calculated for lepton capture according to

$$\mathcal{R} = \left(1 + \frac{\nu}{M_T} \right)^{-1} \tag{B.7}$$

123

Additional contributions to different hyperfine rates are given by

$$\delta\omega_F(i \to f) =$$

$$2\sqrt{2}G^2\nu^2(-1)^{F-J_f+\frac{3}{2}}\begin{Bmatrix} J_i & \frac{1}{2} & F \\ \frac{1}{2} & J_i & 1 \end{Bmatrix} \sum_J \sum_{J'} \sqrt{(2J+1)(2J'+1)}\begin{Bmatrix} J_i & J & J_f \\ J' & J_i & 1 \end{Bmatrix}$$

$$\times \left[i^{J-J'}\langle J_f\|\hat{T}_J^{\text{el}}(\nu) - \hat{T}_J^{\text{mag}}(\nu)\|J_i\rangle \langle J_f\|\hat{T}_{J'}^{\text{el}}(\nu) - \hat{T}_{J'}^{\text{mag}}(\nu)\|J_i\rangle^* \langle J1J'-1|JJ'10\rangle \right.$$

$$+ i^{J-J'}\langle J_f\|\hat{\mathcal{L}}_J(\nu) - \hat{\mathcal{M}}_J(\nu)\|J_i\rangle \langle J_f\|\hat{\mathcal{L}}_{J'}(\nu) - \hat{\mathcal{M}}_{J'}(\nu)\|J_i\rangle^* \langle J0J'0|JJ'10\rangle$$

$$+ 2\sqrt{2}\,\text{Re}\,i^{J-J'}\langle J_f\|\hat{T}_J^{\text{el}}(\nu) - \hat{T}_J^{\text{mag}}(\nu)\|J_i\rangle \langle J_f\|\hat{\mathcal{L}}_{J'}(\nu) - \hat{\mathcal{M}}_{J'}(\nu)\|J_i\rangle^* \langle J1J'0|JJ'11\rangle \Big]$$

$$\times |\phi_{1s}|^2_{\text{av}}\,\mathcal{R} \tag{B.8}$$

B. Beta-decay rate is given by

$$d\omega_{e^-/e^+} = \frac{G^2}{2\pi^3}\,k\epsilon(W_0 - \epsilon)^2 d\epsilon\,\frac{d\Omega_k}{4\pi}\frac{d\Omega_\nu}{4\pi}\frac{4\pi}{2J_i+1}\left\{ \sum_{J=0}^{\infty}\left[(1 + \hat{\nu}\cdot\beta)\,|\langle J_f\|\hat{\mathcal{M}}_J\|J_i\rangle|^2 \right.\right.$$

$$+ (1 - \hat{\nu}\cdot\beta + 2\,\hat{\nu}\cdot\hat{q}\,\hat{q}\cdot\beta)\,|\langle J_f\|\hat{\mathcal{L}}_J\|J_i\rangle|^2$$

$$- \hat{q}\cdot(\hat{\nu} + \beta)\,2\text{Re}\,\langle J_f\|\hat{\mathcal{L}}_J\|J_i\rangle \langle J_f\|\hat{\mathcal{M}}_J\|J_i\rangle|^* \Big]$$

$$+ \sum_{J\geq 1}^{\infty}\left[(1 - \hat{\nu}\cdot\hat{q}\,\hat{q}\cdot\beta)\left(|\langle J_f\|\hat{T}_J^{\text{mag}}\|J_i\rangle|^2 + |\langle J_f\|\hat{T}_J^{\text{el}}\|J_i\rangle|^2\right)\right.$$

$$\pm\,\hat{q}\cdot(\hat{\nu} - \beta)\,2\text{Re}\,\langle J_f\|\hat{T}_J^{\text{mag}}\|J_i\rangle \langle J_f\|\hat{T}_J^{\text{el}}\|J_i\rangle|^* \Big] \left.\right\} F(Z,\epsilon) \tag{B.9}$$

All multipole operators in this equation are evaluated at $\kappa \equiv |\mathbf{q}| = |\mathbf{k}+\nu|$, where q is momentum transferred to *lepton*. The last coefficient $F(Z,\epsilon)$ accounts for the final-state Coulomb interaction. Its approximate magnitude is given by

$$F(Z,\epsilon) \simeq \left|\frac{\phi_\mathbf{k}(0)_{\text{coul}}}{\phi_\mathbf{k}(0)}\right|^2 = \frac{2\pi\eta}{e^{2\pi\eta} - 1} \tag{B.10}$$

where

$$\eta = \frac{zZ\alpha}{\beta}$$

with z - the electron charge, $\alpha = 1/137$ - fine structure constant, and $\vec{\beta} = |\mathbf{k}|/\epsilon$ - the electron velocity.

124

C. Neutrino (antineutrino) charge-changing scattering cross section for the excitation of a discrete target state

$$\left(\frac{d\sigma}{d\Omega}\right)_{\nu/\bar{\nu}} = \frac{G^2 k\epsilon}{4\pi^2} \frac{4\pi}{2J_i+1} \left\{ \sum_{J=0}^{\infty} \left[(1 + \hat{\nu}\cdot\beta) |\langle J_f\|\hat{\mathcal{M}}_J\|J_i\rangle|^2 \right. \right.$$

$$+ (1 - \hat{\nu}\cdot\beta + 2\,\hat{\nu}\cdot\hat{q}\,\,\hat{q}\cdot\beta)\, |\langle J_f\|\hat{\mathcal{L}}_J\|J_i\rangle|^2$$

$$- \hat{q}\cdot(\hat{\nu} + \beta)\, 2\mathrm{Re}\, \langle J_f\|\hat{\mathcal{L}}_J\|J_i\rangle\, \langle J_f\|\hat{\mathcal{M}}_J\|J_i\rangle|^* \Big]$$

$$+ \sum_{J\geq1}^{\infty} \left[(1 - \hat{\nu}\cdot\hat{q}\,\,\hat{q}\cdot\beta) \left(|\langle J_f\|\hat{T}_J^{\mathrm{mag}}\|J_i\rangle|^2 + |\langle J_f\|\hat{T}_J^{\mathrm{el}}\|J_i\rangle|^2 \right) \right.$$

$$\pm\;\; \hat{q}\cdot(\hat{\nu} - \beta)\, 2\mathrm{Re}\, \langle J_f\|\hat{T}_J^{\mathrm{mag}}\|J_i\rangle\, \langle J_f\|\hat{T}_J^{\mathrm{el}}\|J_i\rangle|^* \Big] \left. \right\} \mathcal{R} \qquad (B.11)$$

where $\hat{\nu} \equiv \nu/|\nu|$, $\beta \equiv k/\epsilon$, $\hat{q} \equiv q/|q|$. All multipole operators are evaluated at $\kappa = |q|$, where q is momentum transferred to *lepton*. The recoil factor $\mathcal{R}$ is calculated for the antineutrino scattering cross section according to

$$\mathcal{R} = \left[1 + \frac{\nu}{M_T} \left(1 - \frac{\epsilon}{k}\cos\theta\right)\right]^{-1} \qquad (B.12)$$

125

Appendix C

Reduction of a three-body matrix element of a two-body operator

The objective of this Appendix is to reduce matrix elements of a two-body operator between the ^{3}H$-^3$He three-particle nuclear states to a combination of individual two-body matrix elements. One can perform this reduction, utilizing the general matrix element reduction formulae given in Appendix I.B of [6]. For the ^{3}H$-^3$He nuclear system

$$
\langle \left(\frac{1}{2}\right)^3; \frac{1}{2} {}^+ \frac{1}{2} :: \hat{T}_{JT}(2) :: \left(\frac{1}{2}\right)^3; \frac{1}{2} {}^+ \frac{1}{2} \rangle = 3 \cdot 2^4 \begin{Bmatrix} \frac{1}{2} & \frac{1}{2} & J \\ \frac{1}{2} & \frac{1}{2} & 0 \end{Bmatrix} \begin{Bmatrix} \frac{1}{2} & \frac{1}{2} & T \\ \frac{1}{2} & \frac{1}{2} & 0 \end{Bmatrix} \sum_{J_{22}T_{22},J'_{22}T'_{22}}
$$

$$
\left[\left(\frac{1}{2}\right)^3 \left(\frac{1}{2} {}^+ \frac{1}{2}\right) \left\{ \left| \frac{1}{2} \left(\frac{1}{2}\right)^2 (J_{22}T_{22}) \right] \right. \left[\left(\frac{1}{2}\right)^3 \left(\frac{1}{2} {}^+ \frac{1}{2}\right) \left\{ \left| \frac{1}{2} \left(\frac{1}{2}\right)^2 (J'_{22}T'_{22}) \right] \times \right. \right.
$$

$$
(-1)^{J'_{22}+T'_{22}} \begin{Bmatrix} J_{22} & J'_{22} & J \\ \frac{1}{2} & \frac{1}{2} & \frac{1}{2} \end{Bmatrix} \begin{Bmatrix} T_{22} & T'_{22} & T \\ \frac{1}{2} & \frac{1}{2} & \frac{1}{2} \end{Bmatrix} \langle \left(\frac{1}{2}\right)^2; J_{22}T_{22} :: \hat{T}_{JT}(2) :: \left(\frac{1}{2}\right)^2; J'_{22}T''_{22} \rangle \quad (C.1)
$$

Now consider that only $(J_{22}\, T_{22}) = (0\,1)$ or $(1\,0)$ intermediate two-particle states are allowed due to required antisymmetry of states obtained by angular momentum and

isospin coupling. Then, calculating the encountered 6-j symbols, one obtains

$$\langle \left(\tfrac{1}{2}\right)^3; \tfrac{1}{2}\,\tfrac{+1}{2} :: \hat{T}_{JT}(2) :: \left(\tfrac{1}{2}\right)^3; \tfrac{1}{2}\,\tfrac{+1}{2} \rangle = -3 \cdot 2^2\,(-1)^{J+T} \times$$

$$\left\{ \left[\left(\tfrac{1}{2}\right)^3 \left(\tfrac{1}{2}\,\tfrac{+1}{2}\right) \left\{ \left| \tfrac{1}{2} \left(\tfrac{1}{2}\right)^2 (01) \right] \right.\right]^2 \times \right.$$

$$\frac{-1}{\sqrt{2}}\, \delta_{J0} \left(\frac{1}{\sqrt{6}}\,\delta_{T0} - \frac{1}{\sqrt{3}}\,\delta_{T1} \right) \langle \left(\tfrac{1}{2}\right)^2; 01 :: \hat{T}_{JT}(2) :: \left(\tfrac{1}{2}\right)^2; 01 \rangle +$$

$$\left[\left(\tfrac{1}{2}\right)^3 \left(\tfrac{1}{2}\,\tfrac{+1}{2}\right) \left\{ \left| \tfrac{1}{2} \left(\tfrac{1}{2}\right)^2 (01) \right] \right. \left[\left(\tfrac{1}{2}\right)^3 \left(\tfrac{1}{2}\,\tfrac{+1}{2}\right) \left\{ \left| \tfrac{1}{2} \left(\tfrac{1}{2}\right)^2 (10) \right] \times \right.\right.$$

$$\frac{1}{6} \left(\langle \left(\tfrac{1}{2}\right)^2; 01 :: \hat{T}_{JT}(2) :: \left(\tfrac{1}{2}\right)^2; 10 \rangle + \langle \left(\tfrac{1}{2}\right)^2; 10 :: \hat{T}_{JT}(2) :: \left(\tfrac{1}{2}\right)^2; 01 \rangle \right) +$$

$$\left[\left(\tfrac{1}{2}\right)^3 \left(\tfrac{1}{2}\,\tfrac{+1}{2}\right) \left\{ \left| \tfrac{1}{2} \left(\tfrac{1}{2}\right)^2 (10) \right] \right.\right]^2 \times$$

$$\left. \frac{-1}{\sqrt{2}}\, \delta_{T0} \left(\frac{1}{\sqrt{6}}\,\delta_{J0} - \frac{1}{\sqrt{3}}\,\delta_{J1} \right) \langle \left(\tfrac{1}{2}\right)^2; 10 :: \hat{T}_{JT}(2) :: \left(\tfrac{1}{2}\right)^2; 10 \rangle \right\} \qquad (C.2)$$

The axial charge exchange operator is an isovector $T = 1$ operator. Angular and parity selection rules for the $(\tfrac{1}{2}\,\tfrac{+1}{2}) \to (\tfrac{1}{2}\,\tfrac{+1}{2})$ transition determine that only $J = 1$ Coulomb multipole contribution must be considered. For this operator the first and the last terms in the previous equation disappear because of the Kroneker delta-symbols involved, and the result takes the form:

$$\langle \left(\tfrac{1}{2}\right)^3; \tfrac{1}{2}\,\tfrac{+1}{2} :: \hat{M}_{11}^5(2) :: \left(\tfrac{1}{2}\right)^3; \tfrac{1}{2}\,\tfrac{+1}{2} \rangle =$$

$$-2 \left[\left(\tfrac{1}{2}\right)^3 \left(\tfrac{1}{2}\,\tfrac{+1}{2}\right) \left\{ \left| \tfrac{1}{2} \left(\tfrac{1}{2}\right)^2 (01) \right] \right. \left[\left(\tfrac{1}{2}\right)^3 \left(\tfrac{1}{2}\,\tfrac{+1}{2}\right) \left\{ \left| \tfrac{1}{2} \left(\tfrac{1}{2}\right)^2 (10) \right] \times \right.\right.$$

$$\left\{ \langle \left(\tfrac{1}{2}\right)^2; 01 :: \hat{M}_{11}^5(2) :: \left(\tfrac{1}{2}\right)^2; 10 \rangle + \langle \left(\tfrac{1}{2}\right)^2; 10 :: \hat{M}_{11}^5(2) :: \left(\tfrac{1}{2}\right)^2; 01 \rangle \right\} \qquad (C.3)$$

Bibliography

[1] K. Kubodera, *Hyperfine Interactions* **78**, 3 (1993).

[2] J. D. Walecka, *Theoretical Nuclear and Subnuclear Physics* (Oxford Univ. Press, 1995).

[3] D. O. Riska and G. E. Brown, *Phys. Lett.* **38B**, 193 (1972).

[4] D. O. Riska, *Phys. Rep.* **181**, 207 (1989).

[5] eds. M. Rho and D. Wilkinson, *Mesons in Nuclei* (North-Holland Publishing Company, 1979).

[6] J. D. Dubach, J. H. Koch, and T. W. Donnelly, *Nucl. Phys.* **A271**, 279 (1976).

[7] J. D. Walecka, in *Muon Physics Vol. II, eds. V. W. Hughes and C.S. Wu* (Academic Press, New York, 1975).

[8] M. Chemtob and M. Rho, *Nucl. Phys.* **A163**, 1 (1971).

[9] K. Kubodera, J. Delorme, and M. Rho, *Phys. Rev. Lett.* **40**, 755 (1978).

[10] M. Rho and G. E. Brown, *Comments Part. Nucl. Phys.* **10**, 201 (1981).

[11] K. Kubodera and M. Rho, *Phys. Rev. Lett.* **67**, 3479 (1991).

[12] M. B. Barbaro, A. D. Pace, T. W. Donnelly, and A. Molinari, *Nucl. Phys.* **A569**, 701 (1994).

[13] M. J. Musolf and T. W. Donnelly, *Phys. Lett.* **B318**, 263 (1993).

[14] Y. Umino, J. M. Udias, and P. J. Mulders, *Phys. Rev. Lett.* **74**, 4993 (1995).

[15] G. Barenboim, A. O. Gattone, and E. D. Izquierdo, *Phys. Rev.* **C48**, 2537 (1993).

[16] M. Kirchbach, D. O. Riska, and K. Tsushima, *Nucl. Phys.* **A542**, 616 (1992).

[17] D. O. Riska, *Phys. Rep.* **242**, 345 (1994).

[18] M. J. Kirchbach and D. O. Riska, *Nucl. Phys.* **A578**, 511 (1994).

[19] E. Ivanov and E. Truhlik, *Nucl. Phys.* **A316**, 437 (1979).

[20] I. S. Towner, *Nucl. Phys.* **A542**, 631 (1992).

[21] J. G. Congleton and E. Truhlik, *Phys. Rev.* **C53**, 956 (1996).

[22] T. S. Park, I. S. Towner, and K. Kubodera, *Nucl. Phys.* **A579**, 381 (1994).

[23] T. S. Park, D. P. Min, and M. Rho, *Phys. Rep.* **233**, 341 (1993).

[24] M. Rho, *Phys. Rev. Lett.* **66**, 1275 (1991).

[25] T. S. Park, D. P. Min, and M. Rho, *Nucl. Phys.* **515**, A596 (1996).

[26] P. G. Blunden and D. O. Riska, *Nucl. Phys.* **A536**, 697 (1992).

[27] R. Machleidt, in *Advances in Nuclear Physics, v. 19, eds. J. W. Negele and E. Vogt* (Plenum Press, New York, 1989).

[28] T. S. Lee and D. O. Riska, *Phys. Rev. Lett.* **70**, 2237 (1993).

[29] H. Leutwyler, Lectures on "Hadrons 1994" workshop, BUTP-94/13, 1994.

[30] S. Weinberg, *Phys. Lett.* **B251**, 288 (1990).

[31] S. Weinberg, *Phys. Rev.* **166**, 1568 (1968).

[32] B. D. Serot and J. D. Walecka, in *Advances in Nuclear Physics, v. 16, eds. J. W. Negele and E. Vogt* (Plenum Press, New York, 1986).

[33] C. J. Horowitz and B. D. Serot, *Nucl. Phys.* **A368**, 503 (1981).

[34] R. J. Furnstahl, *Phys. Lett.* **152B**, 313 (1985).

[35] M. Gell-Mann and M. Levy, *Nuovo Cimento* **16**, 705 (1960).

[36] S. Weinberg, *Phys. Rev. Lett.* **18**, 188 (1967).

[37] W. Lin and B. D. Serot, *Nucl. Phys.* **A512**, 637 (1990).

[38] D. O. Riska, Lecture notes, "HUGS at CEBAF" summer workshop, 1995.

[39] S. L. Adler and Y. Dothan, *Phys. Rev.* **151**, 1267 (1966).

[40] I. S. Towner and J. C. Hardy, in *Symmetries and Fundamental Interactions in Nuclei, eds. W. C. Haxton and E. M. Henley* (World Scientific, 1995).

[41] T. W. Donnelly and J. D. Walecka, *Nucl. Phys.* **A274**, 368 (1976).

[42] R. Schiavilla, J. Carlson, and R. B. Wiringa, AIP Conf. Proc., no. 334 p. 79, Few-Body Problems in Physics, 1995.

[43] J. C. McCarthy, I. Sick, R. R. Whitney, and M. R. Yearian, *Phys. Rev. Lett.* **25**, 884 (1970).

[44] H. Collard *et al.*, *Phys. Rev.* **138**, B57 (1965).

[45] B. T. Chertock, E. C. Jones, W. L. Bendel, and L. W. Fagg, *Phys. Rev. Lett.* **23**, 34 (1969).

[46] J. D. Walecka, *Electron Scattering (Lecture Notes)* (Argonne National Laboratory, ANL-83-50, 1983).

[47] A. de Shalit and I. Talmi, *Nuclear Shell Theory* (Academic Press, New York, 1963).

[48] J. D. Dubach, Ph.D. thesis, Stanford University, 1975.

[49] J. D. Walecka, *Nucl. Phys.* **A258**, 367 (1976).

[50] S. Fiarman and S. S. Hanna, *Nucl. Phys.* **A251**, 1 (1975).

[51] L. B. Auerbach *et al.*, *Phys. Rev.* **138**, B127 (1965).

[52] T. W. Donnelly and J. D. Walecka, *Phys. Lett.* **B44**, 330 (1973).

[53] T. Lauritsen and F. Ajzenberg-Selove, *Nucl. Phys.* **78**, 1 (1966).

[54] J. P. Deutsch *et al.*, *Phys. Lett.* **B26**, 315 (1968).

[55] S. M. Ananyan, *Acta Physica Polonica* **B26**, 1751 (1995).

[56] E. K. Warburton, *Phys. Rev.* **C44**, 233 (1991).

[57] T. A. Brody and M. Moshinsky, *Tables of Transformation Brackets* (Monographias del Instituto de Fisica, Universidad Nacional de Mexico, 1960).

[58] A. R. Edmonds, *Angular Momentum in Quantum Mechanics* (Princeton University Press, 1960).

[59] D. B. Kaplan and A. Manohar, *Nucl. Phys.* **B310**, 537 (1988).

[60] M. J. Musolf *et al.*, *Phys. Rep.* **239**, 1 (1994).

[61] C. J. Horowitz, H. Kim, D. P. Murdock, and S. Pollock, *Phys. Rev.* **C48**, 3078 (1993).

[62] G. T. Garvey, S. Krewald, E. Kolbe, and K. Langanke, *Phys. Lett.* **B289**, 249 (1992).

[63] E. M. Henley, G. Krein, S. J. Pollock, and A. G. Williams, *Phys. Lett.* **B269**, 31 (1991).

[64] T. Suzuki, *Nucl. Phys.* **A515**, 609 (1990).

[65] D. H. Beck, *Phys. Rev.* **D39**, 3248 (1989).

[66] T. W. Donnelly, J. Dubach, and I. Sick, *Nucl. Phys.* **A503**, 589 (1989).

[67] E. Beise, spokesperson, CEBAF proposal PR-91-004, 1991.

[68] J. M. Finn and P. A. Souder, spokespersons, CEBAF proposal PR-91-010, 1991.

[69] L. A. Ahrens *et al.*, *Phys. Rev.* **D35**, 785 (1987).

[70] T. W. Donnelly and R. D. Peccei, *Phys. Rep.* **50**, 1 (1979).

[71] M. J. Musolf, R. Schiavilla, and T. W. Donnelly, *Phys. Rev.* **C50**, 2173 (1994).

[72] P. A. Souder *et al.*, *Phys. Rev. Lett.* **65**, 694 (1990).

[73] R. Lanou, private communication.

[74] G. Köbshall *et al.*, *Nucl. Phys.* **A405**, 648 (1983).

[75] D. R. Tilley, H. R. Weller, and G. M. Hale, *Nucl. Phys.* **A541**, 1 (1992).

[76] S. Fiarman and W. E. Meyerhof, *Nucl. Phys.* **A206**, 1 (1973).

[77] R. G. Arnold *et al.*, *Phys. Rev. Lett.* **40**, 1429 (1978).

[78] R. F. Frosh, J. C. McCarthy, R. E. Rand, and M. R. Yearian, *Phys. Rev.* **160**, 874 (1967).

[79] C. Werntz and H. Überall, *Phys. Rev.* **149**, 762 (1966).

[80] V. S. Vasilevski and I. Y. Rybkin, *Sov. J. Nucl. Phys.* **46**, 220 (1987).

[81] J. Carlson and R. Wiringa, private communication.

Vita

Sergei Ananyan was born in Moscow, Russia, July 26, 1966. Graduated from the secondary school number 4 in that city in June 1983, received B.S. from Department of Physics of Moscow State University in 1989. In September 1991, the author entered the College of William and Mary as a graduate student in the Department of Physics.